

Testing Multivariate Conditional Independence Using Exchangeable Sampling and Sufficient Statistics

Xiaotong Lin¹, Jie Xie¹, Fangqiao Tian², and Dongming Huang¹

¹Department of Statistics and Data Science, National University of Singapore

²Department of Mathematics, National University of Singapore

Abstract

We consider testing multivariate conditional independence between a response Y and a covariate vector X given additional variables Z . We introduce the Multivariate Sufficient Statistic Conditional Randomization Test (MS-CRT), which generates exchangeable copies of X by conditioning on sufficient statistics of $\mathbb{P}(X | Z)$. MS-CRT requires no modeling assumption on Y and accommodates any test statistics, including those derived from complex predictive models. It relaxes the assumptions of standard conditional randomization tests by allowing more unknown parameters in $\mathbb{P}(X | Z)$ than the sample size. MS-CRT avoids multiplicity corrections and effectively detects joint signals, even when individual components of X have only weak effects on Y . Our method extends to group selection with false discovery rate control. We develop efficient implementations for two important cases where $\mathbb{P}(X, Z)$ is either multivariate normal or belongs to a graphical model. For normal models, we establish the minimax rate optimality. For graphical models, we demonstrate the superior performance of our method compared to existing methods through comprehensive simulations and real-data examples.

Keywords: conditional independence, conditional randomization test, model-X framework, high-dimensional inference, minimax hypothesis testing, graphical model.

1 Introduction

The question of whether a specific set of variables influences a response of interest, after accounting for other observed variables, is important in many modern research areas, such as economics, finance, and biology. For example, in genomic studies, researchers aim to identify genes associated with a particular disease, while in financial econometrics, analysts seek to determine which market indicators drive investment returns. In high-dimensional settings where the number of covariates is comparable to or exceeds the sample size, this question becomes particularly challenging as classical inference methods often become unreliable. This motivates the development of new statistical methods.

To be concrete, we consider the problem of testing *multivariate conditional independence* (MCI). Let Y denote the response variable and X be a p -dimensional covariate vector. Suppose X is divided into two sub-vectors, $X_{\mathcal{T}}$ and $X_{\mathcal{S}}$, where \mathcal{T} is a group of covariates of interest and $\mathcal{S} = \mathcal{T}^c$ is the remaining variables. The MCI null hypothesis is stated as

$$H_0 : Y \perp\!\!\!\perp X_{\mathcal{T}} \mid X_{\mathcal{S}} \quad (1.1)$$

which asserts that the dependence between Y and X is fully through $X_{\mathcal{S}}$, thereby $X_{\mathcal{T}}$ is unimportant for Y . We focus on the case where $|\mathcal{T}| > 1$, i.e., multiple covariates are jointly tested for conditional independence with the response. Examples of applications are discussed in Section 1.2. In problems like these examples, three major challenges arise:

1. In the high-dimensional setting, the sample size is often too small to guarantee the asymptotic validity of classical testing procedures.
2. In practice, the dependence of Y on $(X_{\mathcal{T}}, X_{\mathcal{S}})$ can be so complicated that no theoretically solid inference method exists.
3. When \mathcal{T} contains many variables, their collective influence may be substantial, yet each individual effect can be too weak to detect using any method.

While the conditional randomization test (CRT) is proven valuable in addressing the first two challenges (Candès et al., 2018), its direct application to testing MCI encounters significant limitations. First, the original CRT requires either full knowledge or an accurate estimation of the conditional distribution $P(X_{\mathcal{T}} \mid X_{\mathcal{S}})$, which is rarely satisfied in practice. Second, most existing CRT implementations focus on univariate $X_{\mathcal{T}}$, and their direct extension to the multivariate settings requires multiple testing adjustments, which can result in a substantial loss of power. For example, in the low-dimensional linear regression experiment of Section 6, with $|T| = 8$, the F-test achieves over 60% power at a certain signal strength, whereas the CRT with Bonferroni adjustment yields below 15% power. This stark contrast highlights the pressing need for more efficient strategies to test MCI.

1.1 Our contributions

To overcome the limitations of classical CRTs in testing MCI, we propose the multivariate sufficient statistic CRT (MS-CRT). By conditioning on sufficient statistics, the MS-CRT relaxes the requirement for precise knowledge of the conditional distribution $\mathcal{P}(X_{\mathcal{T}} \mid X_{\mathcal{S}})$. Furthermore, it bypasses the need for multiple testing adjustments and achieves high power by capturing joint signals. The MS-CRT imposes no modelling assumptions on the response Y and is particularly well-suited to cases where the joint distribution of the covariates lies in a parametric model.

While the idea of the MS-CRT is straightforward, its implementation demands model-specific derivations, which are highly nontrivial. We develop efficient algorithms to generate exchangeable samples of $X_{\mathcal{T}}$ in two important cases:

1. For X following a normal distribution, we introduce the Multivariate Normal CRT (MVN-CRT) and establish its minimax rate optimality.

2. For X following a graphical model, we develop the graphical conditional randomization test (G -CRT) and empirically demonstrate its superior performance compared to existing methods in numerical studies.

To the best of our knowledge, our work is the first to develop a CRT method tailored for multivariate $X_{\mathcal{T}}$, accompanied by a power analysis demonstrating optimality. When variables are grouped, our methods extend to *group selection*, where the goal is to identify important groups while controlling false discovery rate.

This paper is organized as follows. Section 2 reviews the CRT method and introduces our general method.

In Section 3, we detail the implementation of MVN-CRT for multivariate normal covariates and establish the minimax rate optimality. In Section 4, we detail the implementation of G -CRT for high-dimensional graphical models. Section 5 considers group selection. Section 6 demonstrates the effectiveness of our methods in simulation studies under various settings. We exemplify the usefulness of our method through applications to real-world datasets in Section 7. Section 8 concludes with a discussion and future directions. Details of literature reviews, proofs, auxiliary algorithms, numerical studies, and real-data applications are provided in the supplementary material.

1.2 Related literature

Testing MCI is important in many applications, such as the following:

1. Model simplification. In many studies, \mathcal{S} is pre-selected as potentially containing all important variables that influence Y . Verifying $X_{\mathcal{T}} \perp\!\!\!\perp Y \mid X_{\mathcal{S}}$ can justify excluding $X_{\mathcal{T}}$ from subsequent modelling and inference.
2. Testing multivariate treatment effects. In observational studies, the primary goal is to determine whether a set of treatment (or intervention) variables $X_{\mathcal{T}}$ has a causal effect on Y after controlling for observed confounders $X_{\mathcal{S}}$; see Imai and Van Dyk (2004) for a detailed discussion on causal inference with general treatment regimes.
3. Group-level inference. In many applications, variables are organized into predefined groups based on prior knowledge or natural clustering. For instance, genes are often grouped into gene sets based on biological knowledge (Goeman et al., 2004), while economic indicators can be grouped by market sectors (Dose and Cincotti, 2005). Testing the joint effect of a group, rather than individual variables, can increase power.

Testing conditional independence is an important topic in statistics. As shown by Shah and Peters (2020), achieving valid conditional independence tests with nontrivial power necessarily requires assumptions on the null distribution class. Existing methods can thus be categorized according to their respective assumptions.

Our work belongs to the “model- X ” framework, which assumes F_X the distribution of X is known or satisfies some assumptions but makes no assumptions on $F_{Y|X}$ the conditional distribution of Y given X . The seminal work by Candès et al. (2018) introduced the conditional randomization test (CRT) and model- X knockoffs within this framework. The CRT

has attracted significant attention and has been extended in various directions (Bates et al., 2020; Shaer et al., 2023; Tansey et al., 2022; Liu et al., 2022; Niu et al., 2024a).

The original CRT faces practical limitations when applied to MCI testing, particularly in high-dimensional settings. A key challenge is the requirement of knowing the true conditional distribution $P(X|Z)$, which is rarely satisfied in practice. While several advancements have been made to address the issue of inexact $P(X|Z)$ (Bellot and van der Schaar, 2019; Berrett et al., 2020; Niu et al., 2024b; Li and Liu, 2023; Barber and Janson, 2022), the asymptotic guarantees of these methods are tied to the estimation error and may be questionable in finite samples. Moreover, most CRT variants focus on univariate conditional independence, and extending them to multivariate $X_{\mathcal{T}}$ using multiple testing corrections can lead to a substantial loss of power.

Several related works have theoretically investigate the power of CRTs in high-dimensional models. Wang and Janson (2022) focuses on the univariate CRT in linear regression, while Katsevich and Ramdas (2022) consider a semiparametric setting where the dimension of $X_{\mathcal{T}}$ is fixed and Y is normal with mean $\beta^{\top} X_{\mathcal{T}} + g(X_{\mathcal{S}})$. These results are different from ours, since we allow the dimension of $X_{\mathcal{T}}$ to grow as fast as linear with n and provide a matched minimax lower bound.

Beyond the model-X framework, there are other methods for conditional independence testing, including non-parametric kernel-based methods, correlation-based measures, and regression-based methods in the “fixed-X” framework. Appendix A provides a detailed review of the related literature.

1.3 Notation

The cardinality of any set U is denoted as $|U|$. Define $[p] := \{1, \dots, p\}$ for any positive integer p . For $\mathcal{T} \subseteq [p]$ and a vector X , let $X_{\mathcal{T}}$ be the sub-vector $(X_j)_{j \in \mathcal{T}}$; and for a matrix \mathbf{X} , let \mathbf{X}_j be the j th column and $\mathbf{X}_{\mathcal{T}}$ the submatrix formed by the columns corresponding to \mathcal{T} . Also, let $X_{-\mathcal{T}} := (X_j)_{j \notin \mathcal{T}}$ and $\mathbf{X}_{-\mathcal{T}} := \mathbf{X}_{\mathcal{T}^c}$. For any $q \geq 1$, let $\|\cdot\|_q$ be the standard ℓ_q norm. For a square matrix \mathbf{A} , $\text{diag}(\mathbf{A})$ is the diagonal matrix with the same diagonal entries as \mathbf{A} . We write $\mathbf{A} \succ \mathbf{0}$ if \mathbf{A} is positive definite. $\mathbf{N}_p(\boldsymbol{\mu}, \boldsymbol{\Sigma})$ denotes the p -variate normal distribution with mean $\boldsymbol{\mu}$ and covariance matrix $\boldsymbol{\Sigma}$. Let $\boldsymbol{\Omega} := \boldsymbol{\Sigma}^{-1} = (\omega_{ij})$ be the precision matrix. For any random vectors Y , X , and Z , denote by $\mathbf{P}(X | Y)$ the conditional distribution of X given Y , write $X \perp\!\!\!\perp Y$ if X and Y are independent and write $X \perp\!\!\!\perp Y | Z$ if X and Y are conditionally independent given Z . Write $X \stackrel{d}{=} Y$ if X and Y have the same distribution. Denote by $\tilde{\mathbf{X}}^{(m)}$ the m -th copy of the observed data \mathbf{X} .

2 CRT for Multivariate Conditional Independence

We first introduce CRTs and elucidate their limitations for MCI testing. We then propose our method and discuss the construction of test statistics.

2.1 Conditional Randomization Test

The Conditional Randomization Test (CRT) was introduced by Candès et al. (2018) and is closely related to the concept of propensity scores (Rosenbaum and Rubin, 1983). It provides a flexible way to test whether a variable $X_{\mathcal{T}}$ (here $|\mathcal{T}| = 1$) is independent of a response Y given other covariates $X_{\mathcal{S}}$. The CRT requires no assumptions about the conditional distribution of $Y \mid (X_{\mathcal{T}}, X_{\mathcal{S}})$. Instead, it assumes the distribution of $X_{\mathcal{T}} \mid X_{\mathcal{S}}$ is known. This approach is often called the *model-X framework* because it shifts the modelling focus from $Y \mid (X_{\mathcal{T}}, X_{\mathcal{S}})$ to $X_{\mathcal{T}} \mid X_{\mathcal{S}}$. This shift is especially useful when researchers have more knowledge of how $X_{\mathcal{T}}$ depends on $X_{\mathcal{S}}$ than of how Y depends on both.

The univariate CRT operates as follows. Suppose $\{(Y_i, X_i) : i = 1, \dots, n\}$ are independent and identically distributed copies of (Y, X) . Let \mathbf{Y} be the vector of responses $\{Y_i\}$, \mathbf{x} be the vector of $\{X_{i,\mathcal{T}}\}$, and \mathbf{Z} be the matrix of observations $\{X_{i,\mathcal{S}}\}$. Given a known distribution for $\mathbf{x} \mid \mathbf{Z}$, a test statistic function $T(\cdot)$, and an integer M , the CRT generates M independent samples $\mathbf{x}^{(1)}, \dots, \mathbf{x}^{(M)}$ from $\mathbf{x} \mid \mathbf{Z}$, each drawn conditionally independently of the original data (\mathbf{Y}, \mathbf{x}) . The CRT p-value is then computed as

$$\text{pVal} = \frac{1}{M+1} \left(1 + \sum_{m=1}^M \mathbf{1} \{T(\mathbf{Y}, \mathbf{x}^{(m)}, \mathbf{Z}) \geq T(\mathbf{Y}, \mathbf{x}, \mathbf{Z})\} \right).$$

Under the null hypothesis that $X_{\mathcal{T}} \perp Y \mid X_{\mathcal{S}}$, this construction guarantees exact type I error control, i.e., $\mathbb{P}(\text{pVal} \leq \alpha) \leq \alpha$ for any significance level $\alpha \in [0, 1]$. The choice of T is flexible and can reflect prior knowledge or use complex machine-learning algorithms, which makes the CRT adaptable and powerful. The generation of the M copies and the computation of the M test statistics can be paralleled to reduce computation time.

2.2 Limitations of CRT applied to MCI

While the CRT is powerful and flexible for testing conditional independence, it encounters significant difficulties when applied to testing MCI.

The first challenge comes from the multiplicity of the set \mathcal{T} . Much of the literature on CRT focuses on the univariate case where \mathcal{T} has only a single variable. For the multivariate case where \mathcal{T} has many variables, a natural extension is to apply CRTs to each variable in \mathcal{T} separately and then adjust for multiple testing. However, this approach is inefficient, since the conservativeness introduced by multiplicity adjustments leads to a substantial loss of power. Moreover, testing each variable separately fails to capture joint dependence: although $X_{\mathcal{T}}$ as a whole might strongly influence Y , the contribution of each individual variable may be too weak to detect through separate univariate tests.

A second challenge arises from the requirement that the conditional distribution $\mathcal{P}(X_{\mathcal{T}} \mid X_{\mathcal{S}})$ is exactly known. This condition is rarely met in practice, especially when \mathcal{T} is large. For example, if X follows a multivariate normal distribution with an unknown covariance matrix, $\mathcal{P}(X_{\mathcal{T}} \mid X_{\mathcal{S}})$ will involve the unknown covariance parameters. Estimation of such parameters can inflate the type I error rate, which undermines the reliability of the test.

2.3 Multivariate sufficient statistic CRT

We propose the *multivariate sufficient statistic CRT (MS-CRT)* to address the limitations of the original CRT in testing MCI. Instead of assuming that $\mathcal{P}(X_{\mathcal{T}} | X_S)$ is fully known, we assume it lies in a parametric model that admits a sufficient statistic. Under this assumption, we generate copies of $X_{\mathcal{T}}$ that remain exchangeable with the observed data.

Suppose that \mathbf{X} is an $n \times p$ matrix of covariate observations and that the conditional distribution of $\mathbf{X}_{\mathcal{T}}$ given \mathbf{X}_S lies in a model with sufficient statistic $\Phi = \phi(\mathbf{X}_{\mathcal{T}}; \mathbf{X}_S)$. Without looking at \mathbf{Y} the vector of responses, we draw M copies $\tilde{\mathbf{X}}_{\mathcal{T}}^{(m)}$ of $\mathbf{X}_{\mathcal{T}}$ such that $(\mathbf{X}_{\mathcal{T}}, \tilde{\mathbf{X}}_{\mathcal{T}}^{(1)}, \dots, \tilde{\mathbf{X}}_{\mathcal{T}}^{(M)})$ are exchangeable given (\mathbf{X}_S, Φ) . Let $T(\mathbf{y}, \mathbf{x}_{\mathcal{T}}, \mathbf{x}_S)$ be a statistic whose larger (positive) values indicate stronger evidence against the null. With $T_0 := T(\mathbf{Y}, \mathbf{X}_{\mathcal{T}}, \mathbf{X}_S)$ and $T_m := T(\mathbf{Y}, \tilde{\mathbf{X}}_{\mathcal{T}}^{(m)}, \mathbf{X}_S)$ for $m \in [M]$, the p-value is given by

$$\text{pVal}_T = \frac{1}{M+1} \left(1 + \sum_{m=1}^M \mathbb{1}\{T_m \geq T_0\} \right), \quad (2.1)$$

which controls the finite-sample type I error as summarized in Proposition 1.

Proposition 1. *Suppose the copies $\tilde{\mathbf{X}}_{\mathcal{T}}^{(m)}$ are generated without looking at \mathbf{Y} . If conditional on (\mathbf{X}_S, Φ) , the sequence $(\mathbf{X}_{\mathcal{T}}, \tilde{\mathbf{X}}_{\mathcal{T}}^{(1)}, \dots, \tilde{\mathbf{X}}_{\mathcal{T}}^{(M)})$ is exchangeable, then under the null hypothesis that $\mathbf{Y} \perp\!\!\!\perp \mathbf{X}_{\mathcal{T}} | \mathbf{X}_S$, we have $\mathbf{P}(\text{pVal}_T \leq \alpha) \leq \alpha$ for any significance level $\alpha \in (0, 1)$.*

By conditioning on a sufficient statistic, the MS-CRT relaxes the requirement of the original CRT that $\mathbb{P}(X_{\mathcal{T}} | X_S)$ must be fully known or accurately estimated.

Some previous work has used sufficient statistics to relax assumptions in the model-X framework. Huang and Janson (2020) explore this idea for constructing a model-X knock-off, which is a single copy $\bar{\mathbf{X}}$ of the observed \mathbf{X} such that swapping any column of $\bar{\mathbf{X}}$ with the same column of \mathbf{X} leaves the joint distribution of $(\mathbf{X}, \bar{\mathbf{X}})$ unchanged. Despite the similarity in leveraging sufficient statistics, knockoff construction differs fundamentally from exchangeable sampling. In particular, if one generates M knockoffs $\bar{\mathbf{X}}^{(m)}$ of \mathbf{X} , the collection $(\mathbf{X}_{\mathcal{T}}, \bar{\mathbf{X}}_{\mathcal{T}}^{(1)}, \dots, \bar{\mathbf{X}}_{\mathcal{T}}^{(M)})$ is generally not exchangeable; for instance, the pair $(\bar{\mathbf{X}}_{\mathcal{T}}^{(2)}, \bar{\mathbf{X}}_{\mathcal{T}}^{(1)})$ does not have the same distribution as $(\mathbf{X}_{\mathcal{T}}, \bar{\mathbf{X}}_{\mathcal{T}}^{(1)})$ (see Appendix A.4 for more details). Wang and Janson (2022) study the power properties of the CRT when conditioning on a sufficient statistic, but their analysis is limited to the univariate CRT under normal distributions. To our knowledge, we are the first to explore the idea of conditioning on sufficient statistics for testing MCI.

Additionally, MS-CRT avoids multiple testing adjustments when $|\mathcal{T}| > 1$ by treating $\mathbf{X}_{\mathcal{T}}$ as a whole. This is an advantage in contrast with the univariate CRT, which requires conservative Bonferroni correction for testing $H_{0,i} : \mathbf{Y} \perp\!\!\!\perp \mathbf{X}_i | \mathbf{X}_{-i}$ for each $i \in \mathcal{T}$ separately. By directly testing the joint hypothesis $H_0 : \mathbf{Y} \perp\!\!\!\perp \mathbf{X}_{\mathcal{T}} | \mathbf{X}_S$, effectively captures joint signals and achieves higher power, especially when T is large and individual effects are weak.

The MS-CRT controls Type I error in finite samples for any dimension p without assumptions on $Y | X$, making it applicable even when $p \gg n$ or Y is difficult to model. It also maintains CRT's flexibility to employ any test statistic T , which can incorporate advanced models, predictive algorithms, or domain-specific knowledge. These features make the MS-CRT a promising tool for testing MCI in complex and high-dimensional problems.

While the general principle behind MS-CRT is conceptually straightforward, implementing it for testing MCI demands substantial innovations. First, it can be challenging to sample correctly from $\mathbb{P}(\mathbf{X}_{\mathcal{T}} \mid \mathbf{X}_{\mathcal{S}}, \Phi)$, especially in high-dimensional settings. Second, it is nontrivial to design test statistics that are effective in capturing joint signals in high-dimensional MCI testing. These issues will be addressed in the following sections.

Remark 1. *The p -value computed in (2.1) is valid but can be improved by randomization. By randomly breaking ties, we redefine the p -value as*

$$pVal_T = \frac{1}{M} (A + B), \text{ where } A = \sum_{i=1}^M 1_{\tilde{T}_i > T_0}, B \sim \text{Unif}(0, S), \text{ and } S = 1 + \sum_{i=1}^M 1_{\tilde{T}_i = T_0}. \quad (2.2)$$

When $(T_0, \tilde{T}_1, \dots, \tilde{T}_M)$ is exchangeable, this p -value distributed uniformly on $(0, 1)$.

2.4 Test statistics for MCI

The effectiveness of MS-CRT depends on the choice of test statistic $T(\cdot)$, which is designed to capture potential dependence between Y and $X_{\mathcal{T}}$. While univariate CRTs typically use variable-specific importance measures (e.g., regression coefficients), MS-CRT requires statistics that reflect the joint importance of $X_{\mathcal{T}}$, ideally by aggregating the importance of individual variables. We outline three approaches for constructing such statistics, each offering distinct advantages.

Approach 1: Direct Aggregation. This approach first fits a regression of Y on X and then aggregates dependence measures for $X_{\mathcal{T}}$. Approach 1 is straightforward and forms the basis for the other approaches. Below are four examples:

- **LM-SST:** Fit a linear regression and sum the squared t-statistics for $X_{\mathcal{T}}$.
- **GLM-Dev:** Fit a generalized linear model (GLM) and compute the deviance. For a linear model, this coincides with the sum of squared residuals (**LM-SSR**).
- **MaxCor:** Maximum absolute sample correlation between Y and X_j for all $j \in \mathcal{T}$.
- **RF:** Train a random forest and sum the importance scores for variables in \mathcal{T} . An example of importance score is the mean decrease in accuracy (MDA). Similar strategies can be applied using another machine learning method and its importance measures.

Approach 2: Distillation with augmented predictors. For high-dimensional covariates, distillation improves computational efficiency and signal extraction (Liu et al., 2022). We first extract (distill) the information about Y contained by the non-randomized component $X_{\mathcal{S}}$ and then use the distilled information together with the randomized component $X_{\mathcal{T}}$ to define the statistic. Concretely, this approach comprises two steps:

- **Step 1: Distill $X_{\mathcal{S}}$.** Regress Y on $X_{\mathcal{S}}$ to obtain fitted values $\hat{\mathbf{Y}}_0$;
- **Step 2: Augment predictors.** Construct a test statistic using Approach 1 with \mathbf{Y} and the augmented predictors $[\hat{\mathbf{Y}}_0, \mathbf{X}_{\mathcal{T}}]$.

Below are two examples:

- **GLM-L1-D:** First distill using ℓ_1 -penalized GLM (Step 1) and then compute **GLM-Dev** with augmented predictors (Step 2). The distillation offers sparsity.
- **RF-D:** First distill using Random Forest (Step 1) and then compute **RF** with augmented predictors (Step 2). The distillation offers nonparametric flexibility.

Approach 3: Distilled Residuals. This approach shares the same first step as the Approach 2. In the second step, however, we apply Approach 1 directly to the distilled residual $\mathbf{Y} - \hat{\mathbf{Y}}_0$ on $\mathbf{X}_{\mathcal{T}}$.

Below are three examples:

- **GLM-L1-R-SST:** First distill using ℓ_1 -penalized GLM (Step 1) and then compute **LM-SST** on residuals and $X_{\mathcal{T}}$ (Step 2).
- **LM-L1-R-SSR:** First distill using ℓ_1 -penalized LM (Step 1) and then compute **LM-SSR** on residuals and $X_{\mathcal{T}}$ (Step 2).
- **RF-RR:** First treat the response as a numeric variable and distill using random forest regression (Step 1), and then compute **RF** on residuals and $X_{\mathcal{T}}$ (Step 2).

Both Approaches 2 and 3 improve computational efficiency by avoiding repeated fitting of complex models using the common component $X_{\mathcal{S}}$. They are also preferred in high-dimensional problems where Approach 1 does not apply.

In summary, each proposed statistic targets a unique aspect of dependence between Y and $X_{\mathcal{T}}$. For well-specified models, model-based statistics (e.g., **LM-SST** and **GLM-Dev**) are more efficient. For complex dependence, machine learning-based statistics (e.g., **RF**) offer greater flexibility. When prior knowledge suggests that signals are spread out, a dense-targeting statistic such as **LM-SSR** is preferable. In contrast, if only a few large signals are expected, a sparse-targeting statistic like **MaxCor** is more powerful. In our asymptotic power analysis in Section 3.2, we employ **LM-SSR** for dense alternatives and **MaxCor** for sparse alternatives. The numerical performance of the other statistics are examined in Section 6.1. Choosing an effective statistic depends on the anticipated dependence structure and domain knowledge. Our examples are not exhaustive but serve as adaptable templates to guide the tailored construction.

3 Multivariate Normal Models

This section studies the implementation of MS-CRT for multivariate normal distributions and study its theoretical power property.

3.1 Multivariate Normal CRT

Suppose $X \sim N_p(0, \Sigma)$ for some covariance matrix $\Sigma \in \mathbb{R}^{p \times p}$ (see Remark 2 for the extension to unknown means). We use $\mathbf{Y} \in \mathbb{R}^n$ and $\mathbf{X} \in \mathbb{R}^{n \times p}$ to denote the stack of n i.i.d. realizations of Y and X .

Let $t = |\mathcal{T}|$ and $s = |\mathcal{S}| = p - t$.

Suppose $n > s$. To introduce the sampling algorithm, we use the following notations: let $\mathbf{P}_{\mathcal{R}} \in \mathbb{R}^{(n-s) \times n}$ be a matrix whose rows formed an orthonormal set orthogonal to the columns of $\mathbf{X}_{\mathcal{S}}$ so that

$$\mathbf{P}_{\mathcal{R}} \mathbf{P}_{\mathcal{R}}^{\top} = \mathbf{I}_{n-s} \quad \text{and} \quad \mathbf{P}_{\mathcal{R}}^{\top} \mathbf{P}_{\mathcal{R}} = \mathbf{I}_n - \mathbf{X}_{\mathcal{S}} (\mathbf{X}_{\mathcal{S}}^{\top} \mathbf{X}_{\mathcal{S}})^{-1} \mathbf{X}_{\mathcal{S}}^{\top}. \quad (3.1)$$

Let $r = \min\{n - s, t\}$, and define the matrix $\mathbf{Q} \in \mathbb{R}^{r \times t}$ as

$$\mathbf{Q} = \begin{cases} (\mathbf{X}_{\mathcal{T}}^{\top} \mathbf{P}_{\mathcal{R}}^{\top} \mathbf{P}_{\mathcal{R}} \mathbf{X}_{\mathcal{T}})^{1/2} & n - s > t, \\ \mathbf{P}_{\mathcal{R}} \mathbf{X}_{\mathcal{T}} & n - s \leq t. \end{cases} \quad (3.2)$$

Given that $(\mathbf{X}_{\mathcal{T}}, \mathbf{X}_{\mathcal{S}})$ is jointly normal, we propose Algorithm 1, named *Multivariate Normal CRT (MVN-CRT)*, to generate copies $\tilde{\mathbf{X}}_{\mathcal{T}}^{(m)}$ ($m \in [M]$) that are conditionally exchangeable with $\mathbf{X}_{\mathcal{T}}$ given $\mathbf{X}_{\mathcal{S}}$. Proposition 2 summarizes the desired properties of Algorithm 1.

Algorithm 1 Multivariate Normal CRT (MVN-CRT)

- **Input:** n -vector of response \mathbf{Y} , $n \times p$ matrix of covariates \mathbf{X} , partition $\mathcal{T} \cup \mathcal{S} = [p]$, test statistic function $T(\cdot)$, number of randomizations M . Suppose $n > s$, where $s = |\mathcal{S}|$.
 - **Step 1:** For each $j \in [M]$, define $U^{(j)} \in \mathbb{R}^{n-s, r}$ as follows. Sample r independent vectors $\{\mathbf{v}_1^j, \dots, \mathbf{v}_r^j\}$ from the standard $(n - s)$ -dimensional normal distribution and apply the Gram-Schmidt process to obtain the columns of $U^{(j)}$.
 - **Step 2:** For each $j \in [M]$, define $\tilde{\mathbf{X}}_{\mathcal{T}}^{(j)} = \mathbf{X}_{\mathcal{S}} (\mathbf{X}_{\mathcal{S}}^{\top} \mathbf{X}_{\mathcal{S}})^{-1} \mathbf{X}_{\mathcal{S}}^{\top} \mathbf{X}_{\mathcal{T}} + \mathbf{P}_{\mathcal{R}}^{\top} U^{(j)} \mathbf{Q}$, where $\mathbf{P}_{\mathcal{R}}$ is defined in (3.1) and \mathbf{Q} in (3.2).
 - **Step 3:** Compute and output the p-value pVal_T defined in (2.1).
-

Proposition 2. Suppose the rows of \mathbf{X} are i.i.d. observations sampled from (3.3). For the copies $\tilde{\mathbf{X}}_{\mathcal{T}}^{(j)}, j = 1, \dots, M$ generated from Algorithm 1, the followings hold:

1. $\mathbf{X}_{\mathcal{T}}^{\top} \mathbf{X}_{\mathcal{S}} = \left(\tilde{\mathbf{X}}_{\mathcal{T}}^{(j)} \right)^{\top} \mathbf{X}_{\mathcal{S}}, \mathbf{X}_{\mathcal{T}}^{\top} \mathbf{X}_{\mathcal{T}} = \left(\tilde{\mathbf{X}}_{\mathcal{T}}^{(j)} \right)^{\top} \tilde{\mathbf{X}}_{\mathcal{T}}^{(j)}, j = 1, \dots, M$
2. Under the null hypothesis that $\mathbf{Y} \perp \mathbf{X}_{\mathcal{T}} \mid \mathbf{X}_{\mathcal{S}}$, we have $\mathbf{P}(\text{pVal}_T \leq \alpha) \leq \alpha$ for any significance level $\alpha \in (0, 1)$.

Proposition 2 establishes the validity of the MVN-CRT. As previously argued, this validity does not depend on the model for $Y \mid X$ or the choice of statistic $T(\cdot)$.

Remark 2. We have assumed the mean of X is zero to simplify the exposition. If the mean of X is unknown, we augment \mathcal{S} with a dummy element 0 and augment $\mathbf{X}_{\mathcal{S}}$ with the vector $\mathbf{1}_n$. The rest of our method remains the same.

3.2 Power analysis and optimality of multi CRT

We study the power optimality of the MVN-CRT (Algorithm 1).

Given a test statistic T and level α , denote the corresponding test as $\phi_{T,\alpha}$.

By partitioning the covariance matrix Σ according to \mathcal{T} and \mathcal{S} as

$$\Sigma = \begin{bmatrix} \Sigma_{\mathcal{T}\mathcal{T}} & \Sigma_{\mathcal{T}\mathcal{S}} \\ \Sigma_{\mathcal{S}\mathcal{T}} & \Sigma_{\mathcal{S}\mathcal{S}} \end{bmatrix},$$

we can rewrite the distribution as

$$X_{\mathcal{S}} \sim N_s(0, \Sigma_{\mathcal{S}\mathcal{S}}) \quad \text{and} \quad X_{\mathcal{T}} | Z_{\mathcal{S}} \sim N_t(\xi X_{\mathcal{S}}, \Sigma_{\mathcal{T}|\mathcal{S}}), \quad (3.3)$$

where $\xi = \Sigma_{\mathcal{T}\mathcal{S}}\Sigma_{\mathcal{S}\mathcal{S}}^{-1} \in \mathbb{R}^{t \times s}$, and $\Sigma_{\mathcal{T}|\mathcal{S}} = \Sigma_{\mathcal{T}\mathcal{T}} - \Sigma_{\mathcal{T}\mathcal{S}}\Sigma_{\mathcal{S}\mathcal{S}}^{-1}\Sigma_{\mathcal{S}\mathcal{T}}$. Although CRTs operate with no assumption on Y , for tractable power analysis, we consider the linear regression model that assumes

$$Y | X \sim N(X_{\mathcal{T}}^{\top}\beta_{\mathcal{T}} + X_{\mathcal{S}}^{\top}\beta_{\mathcal{S}}, \sigma^2), \quad (3.4)$$

where $\beta_{\mathcal{S}} \in \mathbb{R}^t$, $\beta_{\mathcal{S}} \in \mathbb{R}^s$, and $\sigma > 0$. For the model in (3.4), testing (1.1) is equivalent to testing $H_0 : \beta_{\mathcal{T}} = \mathbf{0}$. We use θ to denote all the parameters $(\beta_{\mathcal{T}}, \beta_{\mathcal{S}}, \Sigma, \sigma)$. The parameter space is defined as:

$$\Theta = \left\{ \theta = (\beta_{\mathcal{T}}, \beta_{\mathcal{S}}, \Sigma, \sigma) : \beta_{\mathcal{T}} \in \mathbb{R}^t, \beta_{\mathcal{S}} \in \mathbb{R}^s, M_0^{-1} \leq \lambda_{\min}(\Sigma) \leq \lambda_{\max}(\Sigma) \leq M_0, \right. \\ \left. 0 < \sigma \leq M_1, \text{ and } \|\beta_{\mathcal{T}}\|_2^2 + \|\beta_{\mathcal{S}}\|_2^2 \leq M_2 \right\},$$

where $M_0 > 1$ and $M_1, M_2 > 0$ are universal constants. The null parameter subspace is $\Theta_0 = \{\theta = (\beta_{\mathcal{T}}, \beta_{\mathcal{S}}, \Sigma, \sigma) \in \Theta : \beta_{\mathcal{T}} = \mathbf{0}\}$. Here, the conditions $M_0^{-1} \leq \lambda_{\min}(\Sigma) \leq \lambda_{\max}(\Sigma) \leq M_0$ and $0 < \sigma \leq M_2$ are two mild regularity assumptions on the design and noise level that have been employed by related works (Cai and Guo, 2017, 2018). Let $\beta = (\beta_{\mathcal{T}}^{\top}, \beta_{\mathcal{S}}^{\top})^{\top} \in \mathbb{R}^{p \times 1}$. Since $\text{Var}(Y_i) = \sigma^2 + \beta^{\top}\Sigma\beta$, the bound on the norm of β can be interpreted as a constraint on the variance of Y_i , which is a common assumption.

The distribution of X in (3.3) and the conditional distribution of Y in (3.4) imply that

$$\mathbb{E}_{\theta}((X_{\mathcal{T}} - \mathbb{E}_{\theta}(X_{\mathcal{T}} | X_{\mathcal{S}}))(Y - \mathbb{E}_{\theta}(Y | X_{\mathcal{S}})) | X_{\mathcal{S}}) = \Sigma_{\mathcal{T}|\mathcal{S}}\beta_{\mathcal{T}}.$$

This suggests a straightforward test statistic and characterizations of alternative populations via the magnitude of $\Sigma_{\mathcal{T}|\mathcal{S}}\beta_{\mathcal{T}}$. In particular, we consider two different types of alternatives.

Dense alternatives. We consider the ℓ_2 -norm and define the alternative space as

$$\Theta_{\text{dense}}(h) = \left\{ \theta = (\beta_{\mathcal{T}}, \beta_{\mathcal{S}}, \Sigma, \sigma) \in \Theta : \|\Sigma_{\mathcal{T}|\mathcal{S}}\beta_{\mathcal{T}}\|_2 \geq h \right\}.$$

For dense alternatives, we suppose $n > s + t$ so that the classical F-test can be implemented. We consider the test statistic defined as

$$T_{\text{dense}}(\mathbf{Y}, \mathbf{X}_{\mathcal{T}}, \mathbf{X}_{\mathcal{S}}) = \left\| (\mathbf{Y}^{\top} \mathbf{P}_{\mathcal{R}}^{\top} \mathbf{P}_{\mathcal{R}} \mathbf{Y})^{-1/2} \mathbf{Y}^{\top} \mathbf{P}_{\mathcal{R}}^{\top} \mathbf{P}_{\mathcal{R}} \mathbf{X}_{\mathcal{T}} (\mathbf{X}_{\mathcal{T}}^{\top} \mathbf{P}_{\mathcal{R}}^{\top} \mathbf{P}_{\mathcal{R}} \mathbf{X}_{\mathcal{T}})^{-1/2} \right\|_2^2.$$

To understand this statistic, consider regressing Y and each element of $X_{\mathcal{T}}$ on $X_{\mathcal{S}}$ separately, where the residuals are $\mathbf{P}_{\mathcal{R}}^{\top} \mathbf{P}_{\mathcal{R}} Y$ and $\mathbf{P}_{\mathcal{R}}^{\top} \mathbf{P}_{\mathcal{R}} \mathbf{X}_{\mathcal{T}}$ respectively. Consequently, T_{dense} equals to the R^2 statistic computed based on regressing the residual of Y on the residual of $X_{\mathcal{T}}$. Using this statistic is equivalent to using the **LM-SSR** statistic.

Sparse alternative. We consider the ℓ_{∞} -norm and define the alternative space as

$$\Theta_{\text{sparse}}(h) = \left\{ \theta = (\beta_{\mathcal{T}}, \beta_{\mathcal{S}}, \Sigma, \sigma) \in \Theta : \|\Sigma_{\mathcal{T}|\mathcal{S}} \beta_{\mathcal{T}}\|_{\infty} \geq h \right\}.$$

For sparse alternatives, we consider the test statistic defined as

$$T_{\text{sparse}}(\mathbf{Y}, \mathbf{X}_{\mathcal{T}}, \mathbf{X}_{\mathcal{S}}) = \max_{j \in \mathcal{T}} \left| \frac{\mathbf{Y}^{\top} \mathbf{P}_{\mathcal{R}}^{\top} \mathbf{P}_{\mathcal{R}} \mathbf{X}_j}{\|\mathbf{P}_{\mathcal{R}} \mathbf{Y}\| \|\mathbf{P}_{\mathcal{R}} \mathbf{X}_j\|} \right|,$$

which is the maximum (absolute) correlation (i.e., **MaxCor**) between the residual $\mathbf{P}_{\mathcal{R}}^{\top} \mathbf{P}_{\mathcal{R}} \mathbf{Y}$ and the residual $\mathbf{P}_{\mathcal{R}}^{\top} \mathbf{P}_{\mathcal{R}} \mathbf{X}_j$ among $j \in \mathcal{T}$.

We consider this asymptotic setting: as the sample size n increases, the dimensions s and t increase while the separation $h = h_n$ vanishes. Theorem 1 characterizes the asymptotic power of the MVN-CRT with appropriate test statistics.

Theorem 1. *Fixed $0 < \alpha < \beta < 1$ and $s \leq c_1 n$ for some positive constant $c_1 \in (0, 1)$. Suppose $M \geq \max(2\alpha^{-1}, \log(2(1 - \beta)^{-1}))$.*

1. (**Dense alternative**) Suppose $t \leq c_2 n$ for some positive constant $c_2 < 1 - c_1$. With test statistics T_{dense} , we have

$$\liminf_{n \rightarrow \infty} \inf_{\theta \in \Theta_{\text{dense}}(h_{1,n})} \mathbb{E}_{\theta} \phi_{T_{\text{dense}}, \alpha} \geq \beta,$$

where $h_{1,n} = C_1 t^{1/4} / \sqrt{n}$ for some constant $C_1 > 0$.

2. (**Sparse alternative**) Suppose $\log t = o(n)$. With test statistics T_{sparse} , we have

$$\liminf_{n \rightarrow \infty} \inf_{\theta \in \Theta_{\text{sparse}}(h_{2,n})} \mathbb{E}_{\theta} \phi_{T_{\text{sparse}}, \alpha} \geq \beta$$

where $h_{2,n} = C_2 \sqrt{\log(et)/n}$ for some constant $C_2 > 0$.

Theorem 1 implies that the power of the MVN-CRT converges to 1 for (1) dense alternatives with $\|\Sigma_{\mathcal{T}|\mathcal{S}} \beta_{\mathcal{T}}\|_2 \gg t^{1/4} / \sqrt{n}$, and (2) sparse alternatives with $\|\Sigma_{\mathcal{T}|\mathcal{S}} \beta_{\mathcal{T}}\|_{\infty} \gg \sqrt{\log(et)/n}$. The next theorem shows that the separation rate required in Theorem 1 is optimal and cannot be improved by any method. For $0 < \alpha < 1$ and a given parameter space Θ , let the set of all tests of level α w.r.t. the null space Θ_0 be

$$\Phi_{\alpha}(\Theta_0) = \left\{ \psi : (\mathbf{Y}, \mathbf{X}) \rightarrow [0, 1] \mid \sup_{\theta \in \Theta_0} \mathbb{E}_{\theta}[\psi] \leq \alpha \right\}.$$

Theorem 2. *Fix $0 < \alpha < \beta < 1$. (1). Suppose $t \leq C_1 n^2$ for some constant $C_1 > 0$, then we have*

$$\limsup_{n \rightarrow \infty} \sup_{\psi \in \Phi_{\alpha}(\Theta_0)} \inf_{\theta \in \Theta_{\text{dense}}(h_{3,n})} \mathbb{E}_{\theta} \psi \leq \beta,$$

where $h_{3,n} = c_3 t^{1/4} / \sqrt{n}$ for some constant $c_3 > 0$.

(2). Suppose $\log t \leq C_2 n$ for some constant $C_2 > 0$, then we have

$$\limsup_{n \rightarrow \infty} \sup_{\psi \in \Phi_\alpha(\Theta_0)} \inf_{\theta \in \Theta_{\text{sparse}}(h_{4,n})} \mathbb{E}_\theta \psi \leq \beta,$$

where $h_{4,n} = c_4 \sqrt{\log t / n}$ for some constant $c_4 > 0$.

Theorem 2 and Theorem 1 together establish the rate optimality of the MVN-CRT under both the dense alternative and the sparse alternative.

When \mathcal{T} is a singleton $\{i\}$, the problem reduces to testing whether $\beta_i = 0$, which has recently attracted much attention (Bradic et al., 2022; Wen et al., 2022; Celentano and Montanari, 2024; Gao and Wang, 2022).

When $t > 1$, our result is, to the best of our knowledge, the first one on the separation rate for testing $\beta_{\mathcal{T}} = \mathbf{0}$ against the dense alternative in moderately high dimensions. Two closely related works are discussed as follows. Verzelen and Villers (2010) considered goodness-of-fit tests based on F-statistics and derived power guarantees that are similar to ours. However, their lower bound is about testing $\beta_{1:p} = \mathbf{0}$ rather than $\beta_{\mathcal{T}} = \mathbf{0}$. Gao and Wang (2022) studied two-sample testing of high-dimensional linear regression coefficients. Their approach transforms the problem into a one-sample test, whose null is of the form $\beta_{1:p} = \mathbf{0}$. This aligns with a special case of our setting where $s = 0$, but their method and analysis do not extend to testing MCI. Furthermore, when $t \asymp n$, their power guarantee under the dense alternative requires the ℓ_2 -norm to be at least of order $\sqrt{\log n / n}$, which is suboptimal compared to the minimax rate $\sqrt{1/n}$.

4 Graphical Models

This section studies the implementation of MS-CRT for graphical models. Let $G = (\mathcal{V}, \mathcal{E})$ be a graph with vertex set $\mathcal{V} = [p]$, and let N_i be the neighborhood of node i . Let \mathcal{M}_G be a family of distributions of X that satisfy the *local Markov property* for each $i \in \mathcal{T}$, which means that $X_i \perp\!\!\!\perp X_{-(N_i \cup \{i\})} \mid X_{N_i}$. This property implies $\mathbf{P}(X_i \mid X_{-i}) = \mathbf{P}(X_i \mid X_{N_i})$. If each conditional distribution $\mathbf{P}(X_i \mid X_{N_i})$ admits a sufficient statistic, we can efficiently construct exchangeable copies.

Specifically, suppose the rows of \mathbf{X} are i.i.d. samples from a distribution in \mathcal{M}_G . Our goal is to generate copies $\tilde{\mathbf{X}}_{\mathcal{T}}^{(m)}$ ($m \in [M]$) such that $(\mathbf{X}_{\mathcal{T}}, \tilde{\mathbf{X}}_{\mathcal{T}}^{(1)}, \dots, \tilde{\mathbf{X}}_{\mathcal{T}}^{(M)})$ is exchangeable conditional on $\mathbf{X}_{\mathcal{S}}$. The sampling method proceeds in two layers:

1. For each variable $i \in \mathcal{T}$, we use a local update that replaces \mathbf{X}_i with a new column $\bar{\mathbf{X}}_i$ generated using only \mathbf{X}_{N_i} and a sufficient statistic $\Psi_i = \Psi_i(\mathbf{X}_i; \mathbf{X}_{N_i})$.
2. Let \mathcal{I} be a permutation of \mathcal{T} . We generate Markov chains by incorporating the local updates of columns sequentially. Starting from \mathbf{X} , a forward sweep along \mathcal{I} yields an intermediate hub $\mathbf{X}^{(hub)}$. Then starting from $\mathbf{X}^{(hub)}$, multiple copies are generated independently by performing reverse sweeps (using reversed \mathcal{I}).

Algorithm 2 Sampling exchangeable copies for graphical models

Input: $n \times p$ data matrix \mathbf{X} , graph G (or neighborhood N_i of each $i \in [p]$), number of copies M , number of iterations L (set to 1 by default), permutation \mathcal{I} of a subset $\mathcal{T} \subset [p]$.

Step 1: Start from \mathbf{X} and apply local updates according to the order \mathcal{I} for L times to generate $\mathbf{X}^{(hub)}$.

Step 2: For $m = 1, 2, \dots, M$, independently start from $\mathbf{X}^{(hub)}$ and apply local updates according to the reversed order of \mathcal{I} for L times to generate $\tilde{\mathbf{X}}^{(m)}$.

Output: $\tilde{\mathbf{X}}^{(1)}, \dots, \tilde{\mathbf{X}}^{(M)}$.

We present the complete sampling procedure as Algorithm 2 and we refer to the resulting CRT as the *graphical conditional randomization test*, or G -CRT to emphasize the reliance on the graph. To ensure the validity of G -CRT, we impose the following assumption on the local update mechanism.

Condition 1. For each $i \in \mathcal{T}$, let $\bar{\mathbf{X}}_i$ be the new column yielded by the local update with index i . Then, (1) $\Psi_i(\bar{\mathbf{X}}_i; \mathbf{X}_{N_i}) = \Psi_i(\mathbf{X}_i; \mathbf{X}_{N_i}) = \Psi_i$, and (2) either $\mathbf{X}_i = \bar{\mathbf{X}}_i$, or $\bar{\mathbf{X}}_i$ and \mathbf{X}_i are i.i.d. conditional $(\mathbf{X}_{N_i}, \Psi_i)$.

Proposition 3. Suppose \mathbf{X} is a $n \times p$ matrix and G is a graph on $[p]$. Let $\{\tilde{\mathbf{X}}^{(m)}\}_{m=1}^M$ be the output of Algorithm 2. If Assumption 1 holds, then $\tilde{\mathbf{X}}_{-\mathcal{T}}^{(m)} = \mathbf{X}_{-\mathcal{T}}$ for all $m \in [M]$ and $\mathbf{X}_{\mathcal{T}}, \tilde{\mathbf{X}}_{\mathcal{T}}^{(1)}, \dots, \tilde{\mathbf{X}}_{\mathcal{T}}^{(M)}$ are conditionally exchangeable given $\mathbf{X}_{-\mathcal{T}}$.

Condition 1 ensures the detailed balance for each update of the generated Markov chains, under which Propositions 3 and 1 together ensure the validity of G -CRT. Notably, we can implement G -CRT with no constraints on the dimension p , even when p is arbitrarily larger than n .

Though general, deriving a local update mechanism based on conditional distributions given sufficient statistics is nontrivial. Below, we consider two examples of graphical models where we have local update mechanisms that satisfy Condition 1.

4.1 Gaussian Graphical Models

Suppose $X \sim \mathbf{N}_p(\boldsymbol{\mu}, \boldsymbol{\Sigma})$ with mean $\boldsymbol{\mu} \in \mathbb{R}^p$ and covariance matrix $\boldsymbol{\Sigma} \succ \mathbf{0}$. Let $\boldsymbol{\Omega} = \boldsymbol{\Sigma}^{-1}$ be the precision matrix (Dempster, 1972). A key property of the precision matrix is that an off-diagonal entry ω_{ij} equals zero if and only if X_i and X_j are conditionally independent given the remaining variables. The Gaussian graphical model (GGM) with respect to G is defined as

$$\mathcal{M}_G = \{\mathbf{N}_p(\boldsymbol{\mu}, \boldsymbol{\Omega}^{-1}) : \boldsymbol{\mu} \in \mathbb{R}^p, \boldsymbol{\Omega} \succ \mathbf{0}, \omega_{ij} = 0 \text{ if } (i, j) \notin \mathcal{E}\}. \quad (4.1)$$

For GGMs, Lin et al. (2025) proposed the *residual rotation* update for each variable: decompose \mathbf{X}_i into its projection on the column span of \mathbf{X}_{N_i} plus a residual, then replace the residual with a randomly rotated copy. This update satisfies Condition 1 (see Appendix B.1 for details).

4.2 Discrete Graphical Models

Suppose \mathcal{M}_G is a discrete graphical model and each variable X_i takes values in $\{1, 2, \dots, K_i\}$. The sufficient statistic for $\mathbf{P}(X_i | X_{N_i})$ is the count of each possible value of X_i within subgroups defined by the configuration of its neighbors. Specifically, for any fixed configuration v of X_{N_i} , define

$$\mathcal{H}_v = \{j \in [n] : \mathbf{X}_{j,N_i} = v\} \quad \text{and} \quad n_{v,k} = \sum_{j \in \mathcal{H}_v} \mathbb{I}\{\mathbf{X}_{ji} = k\}, \quad k \in [K_i].$$

The collection $\Psi_i = \{n_{v,k} : k \in [K_i], \forall v\}$ forms a sufficient statistic for $\mathbf{P}(\mathbf{X}_i | \mathbf{X}_{N_i})$. Conditional on $(\mathbf{X}_{N_i}, \Psi_i)$, the values of $\mathbf{X}_{\mathcal{H}_v,i}$ across different v are independent, and within each \mathcal{H}_v , all locations of $\mathbf{X}_{j,i}$ that preserve the counts $\{n_{v,k} : k \in [K_i]\}$ are equally likely. Consequently, a local update satisfying Condition 1 is to permute the observed values of X_i within each \mathcal{H}_v separately. This approach is efficient if the sample size is sufficiently larger than the number of possible neighbor configurations $\{v\}$. Otherwise, the permutation within each \mathcal{H}_v often remains identical, which makes the resulting test powerless.

4.3 On the graphical modeling assumption for X

Our G -CRT only requires that the local Markov property w.r.t. G holds for \mathcal{T} , which is a relatively mild condition. Suppose G_* is the exact graph *faithful* to $\mathbf{P}(X)$, meaning that for $i \neq j$, X_i and X_j are conditionally independent if and only if (i, j) is not an edge in G_* . The G -CRT is valid as long as $G_* \subset G$, that is, G can contain possibly more edges than G_* . Appendix E.1 numerically demonstrates that using moderately oversized super graphs only induces a slight loss in power.

Finding a supergraph G of the exact graph G_* is often achievable in practice. For GGMs with $p < n$, G can be chosen conveniently as the complete graph. When $p > n$, a suitable G can often be derived from temporal or spatial data structures, domain knowledge, or large historical datasets. Real-world examples include time series with autoregressive structures, spatial air quality measurements, financial stock prices with cross-sectional dependence, and gene expression data with gene regulatory networks verified in related studies.

If G has to be selected based on data, the selection should use an independent dataset (or via appropriate data-splitting) to maintain Type I error control of the test. When unlabeled observations (covariates without responses) are available as in semi-supervised learning, they can be used in the selection. An investigation into optimal strategies is left for future research.

Given the supergraph G , the G -CRT provides finite-sample Type I error control for testing MCI even with more unknown parameters than the sample size. In GGMs, for instance, if $|\mathcal{T}|$ scales with p and the node degrees of G scale with n , then the number of unknown parameters grows at the order of pn , which is far larger than n , but the G -CRT remains valid since it avoids explicit parameter estimation.

5 Group Selection using MS-CRT

In many applications, variables are naturally grouped. The goal of a *group selection* method is to uncover which groups are important for Y , rather than selecting individual

variables, while controlling the error rates.

Suppose the p covariates are partitioned into g disjoint groups, $\mathcal{T}_1, \dots, \mathcal{T}_g$. For each group \mathcal{T}_j , we test the null hypothesis of group-wise conditional independence $H_0^{(j)} : Y \perp\!\!\!\perp X_{\mathcal{T}_j} \mid X_{\mathcal{T}_j^c}$. Rejecting $H_0^{(j)}$ indicates that group \mathcal{T}_j provides information about Y beyond what is already captured by the other groups. For each group \mathcal{T}_j , we apply MS-CRT to obtain a group-specific p-value, pVal_j , which quantifies the evidence against $H_0^{(j)}$. Since we conduct g such tests simultaneously, we use multiple testing corrections—specifically the BH or BY procedures (Benjamini and Hochberg, 1995; Benjamini and Yekutieli, 2001), or the more recent e-BH approach (Wang and Ramdas, 2022)—to control the false discovery rate (FDR). Let $\mathcal{D} \subset [g]$ be the index set of rejected (discovered) groups, and let \mathcal{N} be the indices where the null holds. The FDR is defined as $\mathbb{E}[|\mathcal{D} \cap \mathcal{N}| / \max(|\mathcal{D}|, 1)]$. Implementation details for BH, BY, and e-BH are provided in Appendix B.2. To apply the e-BH procedure, we compute the randomized p-values in (2.2) and transform them to boost e-values using Algorithm 3, whose validity follows from Proposition 4.

Algorithm 3 Transforming p-values to boosted e-values

Input: p-values $\{\text{pVal}_1, \dots, \text{pVal}_g\}$, FDR level α .

Step 1: For $i \in [g]$, define $\delta_i = \frac{\alpha}{g(1+i)}$ and calculate $b_i = \sum_{k=1}^i \delta_k$.

Step 2: For each p-value pVal_j , determine the index $i = \sum_{k=1}^g \mathbb{I}(\text{pVal}_j > b_k)$ and transform it into a boosted e-value using $E_j = \frac{g}{\alpha(i+1)}$

Output: Boosted e-values $\{E_1, E_2, \dots, E_g\}$.

Proposition 4. Define $T(z) = \frac{g}{\lceil g/z \rceil} 1_{\{z \geq 1\}}$ and fix $\alpha \in (0, 1)$. If an input p_j of Algorithm 3 follows $\text{Unif}(0, 1)$, then the output E_j satisfies $\mathbb{E}[T(\alpha E_j)] \leq \alpha$.

Proposition 4 implies that for randomized p-values, Algorithm 3 outputs boosted e-values (see Equation (11) in Section 4.2 of Wang and Ramdas (2022)). Consequently, the selection using the BH procedure applied to $\{1/E_j\}_{j=1}^g$ controls the FDR at level α . This guarantee follows Theorem 3 of Wang and Ramdas (2022) and our model-X assumption.

6 Simulation Studies

We conduct extensive simulation experiments to evaluate the numerical performance of G -CRT for MCI testing and group selection under various settings. Code can be found on GitHub (<https://github.com/xiaotong0201/CSS-GGM.git>).

6.1 Multivariate Conditional Independence Testing

We evaluate the power of the G -CRT with several test statistics (Section 2.4) for testing MCI. We highlight the key findings to demonstrate the effectiveness of the G -CRT. Additional details on simulation setups, method implementation, and comprehensive comparisons are provided in Appendix D.

We examine four data-generating models for Y : linear regression, nonlinear regression, logistic regression, and nonlinear binary regression. The covariate vector X is sampled from a normal distribution, where the graph G is obtained by randomly permuting the nodes of a band graph with bandwidth 6. We use a constant factor θ to control the magnitude of the dependence of Y on X . The null hypothesis is $H_0 : Y \perp\!\!\!\perp X_{\mathcal{T}} \mid X_{-\mathcal{T}}$ with $\mathcal{T} = \{1, 2, \dots, 8\}$; note that \mathcal{T} is not particular to the band graph structure because the nodes of G have been permuted. Our G -CRT uses graph G but does not use the precision matrix or the mean.

For each model, we consider both low-dimensional ($p = 20, n = 50$) and high-dimensional ($p = 120, n = 80$) settings, and we compare our method with several existing tests. In each figure, power is estimated as the fraction of rejections at level $\alpha = 0.05$ across at least 400 repetitions and error bars represent one standard error.

Gaussian linear regression. Figure 6 presents power curves for Gaussian linear regressions as a function of θ . In the low-dimensional setting (Figure 6a), the G -CRT with either LM-SST or LM-SSR statistic achieves remarkable performance: it outperforms the Bonferroni-adjusted dCRT and matches the power of the F-test. This is notable since the F-test is the UMPI test in low-dimensional linear regression, which suggests the G -CRT can match optimal tests when they are applicable. Turning to the high-dimensional setting (Figure 6b), G -CRT with either L1-R-SSR or L1-R-SST statistic consistently achieves substantially higher power than the Bonferroni-adjusted dCRT (Liu et al., 2022) and de-sparsified Lasso (De-Lasso) (van de Geer et al., 2014).

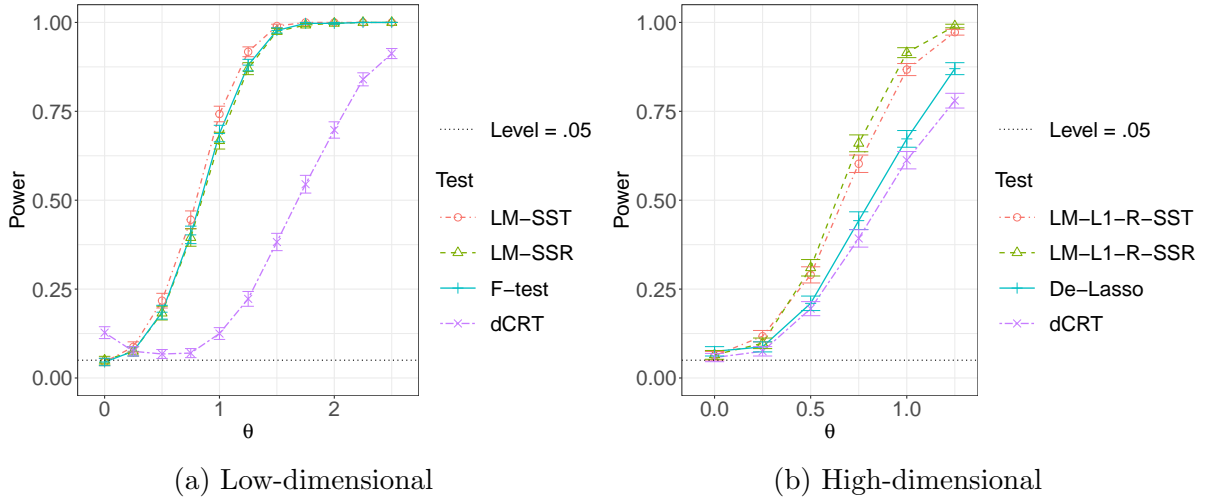


Figure 1: Power comparison in linear regressions. The first two tests are the G -CRT with different statistics, and the other two are existing methods.

Nonlinear regression. Figure 7 presents power curves for nonlinear regressions, where we focus on machine learning-based statistics. In both low-dimensional (Figure 7a) and high-dimensional (Figure 7b) settings, G -CRT with either RF-D or RF-RR statistic achieves substantially higher power than the F-test (low-dimensional), the Bonferroni-adjusted de-sparsified Lasso (high-dimensional), and dCRT (with random forests). The direct RF statistic is comparable to the two distillation-based statistics in the low-dimensional case, but the advantage of distillation is evident in the high-dimensional case.

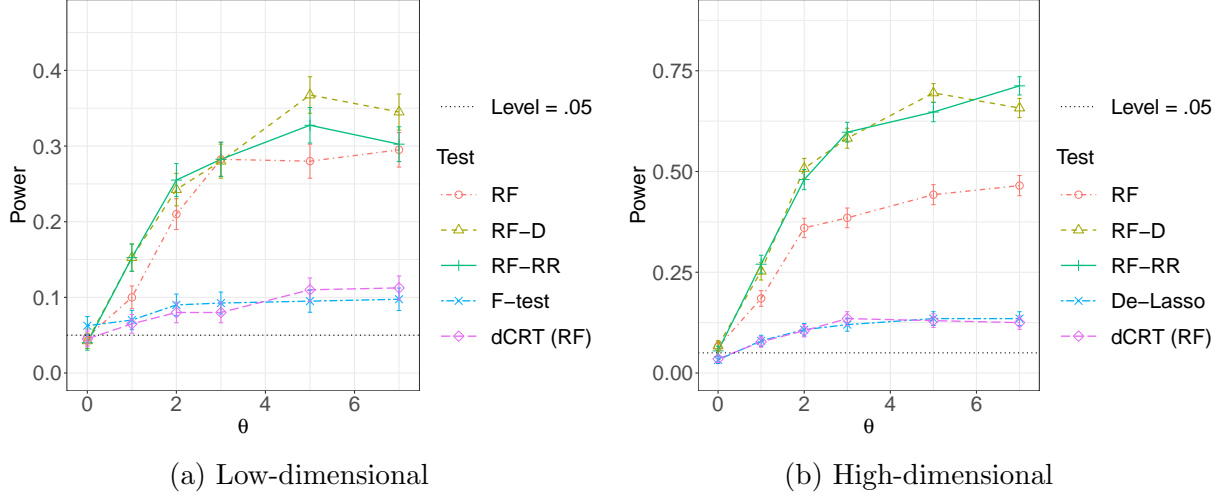


Figure 2: Power comparison in nonlinear regressions. The first three tests are the G -CRT with different statistics, and the other two are existing methods.

Logistic regression Figure 8 presents power curves for logistic regressions. In the low-dimensional case (Figure 8a), G -CRT with the GLM-Dev statistic outperforms the Bonferroni-adjusted dCART, while the classical Chi-squared test fails to control Type I error. In the high-dimensional case (Figure 8b), G -CRT with L1-D or L1-R-SST statistic performs significantly better than both the Bonferroni-adjusted dCART and the bias-correction method CGM Cai et al. (2023).

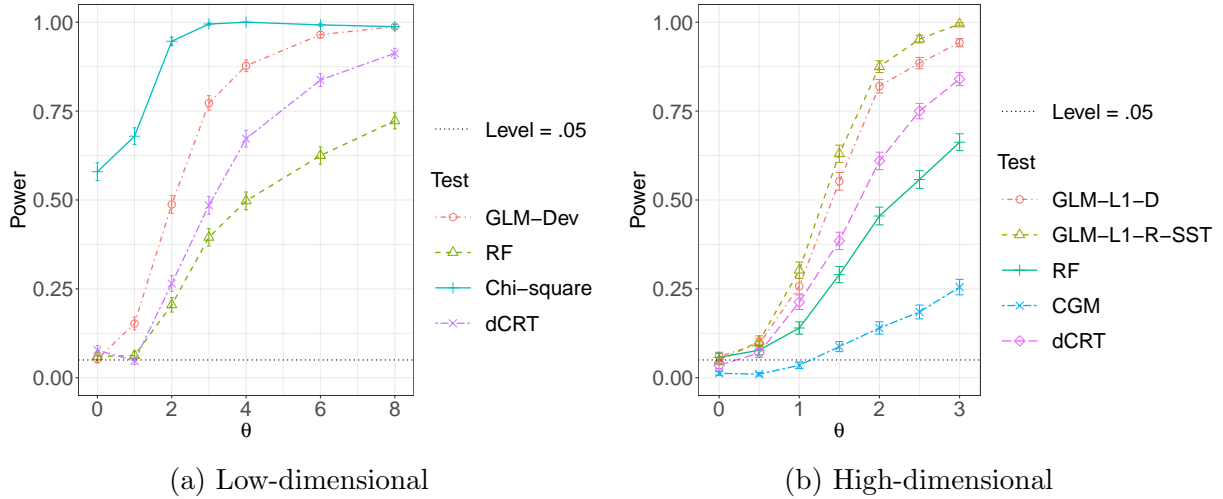


Figure 3: Power comparison in logistic regressions. The first two low-dimensional tests and the first three high-dimensional tests are the G -CRT with different statistics, and the other two are existing methods.

Nonlinear binary regression Figure 9 presents power curves for nonlinear binary regressions, where we focus on machine learning-based statistics. The findings parallel those in Figure 7, but the Bonferroni-adjusted dCART is nearly powerless in both low- and high-

dimensional settings. Besides, the classical Chi-square test fails to control the Type I error in low dimensions, and CGM is powerless in high dimensions.

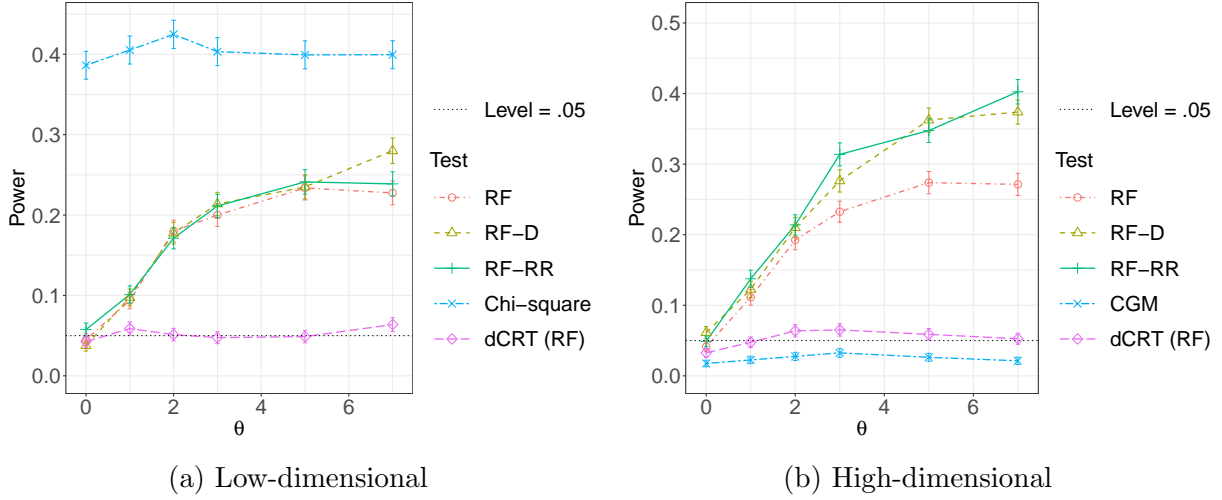


Figure 4: Power comparison in nonlinear binary regressions. The first three tests are the G -CRT with different statistics, and the other two are existing methods.

Across all figures, the G -CRT controls the Type I error and significantly outperforms Bonferroni-adjusted tests by effectively capturing the joint signal.

Additional experiments are provided in the supplementary material to investigate other aspects of the G -CRT. Key findings are summarized as follows:

- (1) Appendix E.1 studies the power when a moderately oversized supergraph is used in the G -CRT, which induces only a slight loss in power compared to the true graph;
- (2) Appendix E.2 examines the case where $X_{\mathcal{T}}$ is univariate and shows that the G -CRT remains comparable to the competitors;
- (3) Appendix E.3 studies the performance under violations of the Gaussian assumption and we observe that the G -CRT is robust to moderate violations.

6.2 Group Selection

To evaluate the group selection method using G -CRT, we modified the high-dimensional linear regression experiment by partitioning covariates into 15 groups (each of size 8), with 20 true signals distributed among three groups. Other settings remain unchanged, and the magnitude of signals is controlled by θ . For comparison, we included another model-X method, the group knockoff filter proposed by Chu et al. (2024), implemented with the true distribution of X to ensure a strong benchmark. Each experiment is repeated 400 times at a nominal FDR level of 0.1.

Figure 5 summarizes the results. Our method, combined with appropriate FDR control procedures (BH, BY, or eBH), provides effective FDR control and achieves high power. Notably, the eBH procedure balances power and theoretical FDR guarantees; BH has high power but lacks a FDR guarantee, while BY has a theoretical guarantee but is too conservative. The group knockoff filter performs poorly here, mainly because it is designed for

scenarios with hundreds of groups while the number of groups is small (15) in this experiment. These findings suggest that using the eBH procedure with G -CRT is effective for group selection when the number of groups is moderate.

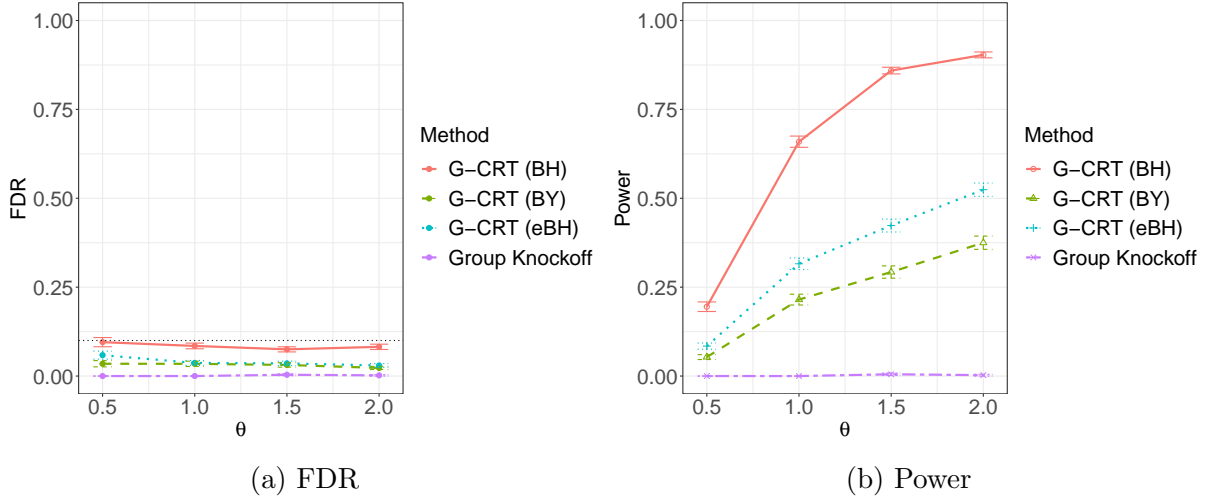


Figure 5: Performance of group selection methods in linear regression with $(n, p) = (80, 120)$. There are 15 groups of size 8, and three groups are important. FDR level= 10%.

7 Real-World Examples

This section examines the effectiveness of our proposed methods in real datasets.

7.1 Dependence of fund return

In finance, delayed disclosure of portfolio holdings in hedge funds and mutual funds presents challenges and opportunities in financial markets (Agarwal et al., 2013).

In this example, we illustrate how to infer whether a fund’s return Y depend on certain stocks. Specifically, we want to test if Y depends on a subset of stocks $X_{\mathcal{T}}$, after adjusting for other stocks $X_{-\mathcal{T}}$, i.e., $Y \perp\!\!\!\perp X_{\mathcal{T}} \mid X_{-\mathcal{T}}$. We employ a fund with disclosed holdings to establish a ground truth, but the strategy here can guide investors in future analysis on funds with undisclosed holdings.

In our example, Y is the weekly average return of the SPDR Dow Jones Industrial Average ETF Trust (DIA) and X are the weekly average returns of 103 large stocks. We consider the period from September 1st, 2020 to Jun 30th, 2022, which results in a dataset with $n = 92$ and $p = 103$. Details about the dataset can be found in Appendix F.1.1.

We consider two examples of set \mathcal{T} :

1. $\mathcal{T}_1 = \{\text{CAT, DOW, HON, MMM, PG}\}$: five stocks from traditional sectors such as materials and manufacturing with small or moderate stock prices during the period.
2. $\mathcal{T}_2 = \{\text{AMGN, CRM, MSFT, UNH}\}$: stocks from biotechnology, technology, and healthcare sectors with relatively large stock prices during the period.

Table 1: p-values of MCI tests with different \mathcal{T} on the DIA returns.

\mathcal{T}	LM-L1-R-SSR	RF-RR	dCRT (L1)	dCRT (RF)
\mathcal{T}_1	0.043	0.048	0.070	0.285
\mathcal{T}_2	0.001	0.007	0.000	0.107

Since the holdings of the fund DIA are disclosed and both \mathcal{T}_1 and \mathcal{T}_2 have a real influence on Y , we can compare different tests by their abilities to reject the null hypothesis.

We consider the G -CRT with the statistics L1-R-SSR and RF-RR, and compare it with the de-sparsified Lasso and the dCRT with either Gaussian Lasso models (L1) or random forests (RF). In Appendix F.1.2, we build a GGM for X and conduct a simulation study to show that the four CRTs control the Type-I error while the de-sparsified Lasso does not.

We conduct our G -CRTs and the dCRTs on the DIA returns with \mathcal{T}_1 and \mathcal{T}_2 , and summarize their p-values in Table 1. For \mathcal{T}_1 , both G -CRTs reject the null hypothesis at the level $\alpha = 0.05$, while the dCRTs accept the null hypothesis. In this example, each of the five stocks in \mathcal{T}_1 has a relatively small influence on the fund return, but they together as a whole are influential, whose signal can be detected by the G -CRTs.

For \mathcal{T}_2 , all the considered tests yield small p-values. We subsequently consider a situation where the response variables are contaminated by additive noises and thus the “signal-to-noise” ratio becomes smaller. The details of this experiment can be found in Appendix F.1.3, where the G -CRT with the LM-L1-R-SSR statistic has uniformly higher rejection rates and exhibits robustness to additive noises.

In conclusion, the G -CRT is shown powerful in detecting weak joint dependence and robust to noise. Its superior performance suggests its potential in financial application.

7.2 Breast Cancer Relapse

We illustrate the application of the G -CRT in a situation where the classical likelihood ratio test is not applicable. The breast cancer relapse (BCR) dataset is collected by Wang et al. (2005) for identifying genes associated with metastasis (data accessible at NCBI GEO database (Barrett et al., 2012), accession GSE2034). We focus on a subgroup of 209 patients and analyze the 60 genes identified for this subgroup by the original study.

In our experiment, we consider a response variable Y with three categories: (1) no relapse, (2) relapsed without metastases, and (3) relapsed with metastases, each considered within four years. X is the expression level of 60 genes. A preliminary analysis using different variable selection methods results in two nested sets of important variables: \mathcal{S} and $\mathcal{S} \cup \mathcal{T}$. We consider testing for the null hypothesis that $H_0 : Y \perp\!\!\!\perp X_{\mathcal{T}} \mid X_{\mathcal{S}}$ using the likelihood ratio test for multinomial logistic regression, the G -CRT with the RF statistic, and the Bonferroni-adjusted dCRT with either Gaussian Lasso models or random forests. Details of this example can be found in Appendix F.2.

Our findings are: (1) in simulations, the classical asymptotic likelihood ratio test cannot control the Type-I error while the G -CRTs and the dCRTs can; (2) when applied to the BCR dataset, the two dCRTs yield p-values larger than 0.2, while the G -CRT with the statistic RF rejects the null with a p-value of 0.002. This example illustrates the efficiency and applicability of our method when classical methods fail.

8 Discussion

This study proposes the multivariate sufficient statistic conditional randomization test (MS-CRT) for testing multivariate conditional independence (MCI) under model-X framework. By conditioning on sufficient statistics rather than estimating model parameters, MS-CRT maintains finite-sample Type I error control while greatly relaxing the restrictive assumption of the original CRT. A key advantage over univariate methods is that MS-CRT captures joint effects, and consequently, it circumvents the need for multiple testing adjustments and remains powerful in settings where joint effects are strong but individual effects are too weak to be detected separately.

We develop efficient implementations of MS-CRT for two important classes of models of X : (1) MVN-CRT for multivariate normal models and (2) G -CRT for high-dimensional graphical models. For MVN-CRT, we study its asymptotic power in linear regression and establish its minimax rate optimality when the alternative is either dense or sparse. For G -CRT, we numerically demonstrate its superior power performance compared to Bonferroni-adjusted univariate CRTs and fixed- X methods, through both extensive simulation studies and real-world data analyses.

Our work opens several future research directions. First, more efforts are needed in designing test statistics to capture joint effects in specific applications. Second, extending G -CRT to a wider range of Markov random fields, such as *exponential family graphical models* (Wainwright et al., 2008), could broaden its applicability. Lastly, it remains open to study theoretical power guarantees for G -CRT, where the main difficulty lies in characterizing the distribution of copies generated from Markov chains when the graph structure is complicated.

Acknowledgements

D. Huang was partially supported by NUS Start-up Grant A-0004824-00-0.

References

- Emmanuel Candès, Yingying Fan, Lucas Janson, and Jinchi Lv. Panning for gold: ‘model-X’ knockoffs for high dimensional controlled variable selection. *Journal of the Royal Statistical Society Series B: Statistical Methodology*, 80(3):551–577, 01 2018.
- Kosuke Imai and David A Van Dyk. Causal inference with general treatment regimes: Generalizing the propensity score. *Journal of the American Statistical Association*, 99(467):854–866, 2004.
- Jelle J. Goeman, Sara A. van de Geer, Floor de Kort, and Hans C. van Houwelingen. A global test for groups of genes: Testing association with a clinical outcome. *Bioinformatics*, 20(1):93–99, January 2004.
- Christian Dose and Silvano Cincotti. Clustering of financial time series with application to index and enhanced index tracking portfolio. *Physica A: Statistical Mechanics and its Applications*, 355(1):145–151, 2005.

- Rajen D. Shah and Jonas Peters. The hardness of conditional independence testing and the generalised covariance measure. *The Annals of Statistics*, 48(3):1514 – 1538, 2020. doi: 10.1214/19-AOS1857.
- Stephen Bates, Matteo Sesia, Chiara Sabatti, and Emmanuel Candès. Causal inference in genetic trio studies. *Proceedings of the National Academy of Sciences*, 117(39):24117–24126, 2020.
- Shalev Shaer, Gal Maman, and Yaniv Romano. Model-X Sequential Testing for Conditional Independence via Testing by Betting. In *Proceedings of The 26th International Conference on Artificial Intelligence and Statistics*, pages 2054–2086. PMLR, April 2023. URL <https://proceedings.mlr.press/v206/shaer23a.html>.
- Wesley Tansey, Victor Veitch, Haoran Zhang, Raul Rabadan, and David M. Blei. The holdout randomization test for feature selection in black box models. *Journal of Computational and Graphical Statistics*, 31(1):151–162, 2022.
- Molei Liu, Eugene Katsevich, Lucas Janson, and Aaditya Ramdas. Fast and powerful conditional randomization testing via distillation. *Biometrika*, 109(2):277–293, 2022.
- Ziang Niu, Jyotishka Ray Choudhury, and Eugene Katsevich. Computationally efficient and statistically accurate conditional independence testing with spacrt. *arXiv preprint arXiv:2407.08911*, 2024a.
- Alexis Bellot and Mihaela van der Schaar. Conditional Independence Testing using Generative Adversarial Networks. In *Advances in Neural Information Processing Systems*, volume 32. Curran Associates, Inc., 2019. URL https://papers.nips.cc/paper_files/paper/2019/hash/dc87c13749315c7217cdc4ac692e704c-Abstract.html.
- Thomas B. Berrett, Yi Wang, Rina Foygel Barber, and Richard J. Samworth. The conditional permutation test for independence while controlling for confounders. *Journal of the Royal Statistical Society Series B: Statistical Methodology*, 82(1):175–197, 2020.
- Ziang Niu, Abhinav Chakraborty, Oliver Dukes, and Eugene Katsevich. Reconciling model-X and doubly robust approaches to conditional independence testing. *The Annals of Statistics*, 52(3):895–921, June 2024b. ISSN 0090-5364, 2168-8966. doi: 10.1214/24-AOS2372. URL <https://projecteuclid.org/journals/annals-of-statistics/volume-52/issue-3/Reconciling-model-X-and-doubly-robust-approaches-to-conditional-independence/10.1214/24-AOS2372.full>.
- Shuangning Li and Molei Liu. Maxway CRT: improving the robustness of the model-X inference. *Journal of the Royal Statistical Society Series B: Statistical Methodology*, page qkad081, 08 2023.
- Rina Foygel Barber and Lucas Janson. Testing goodness-of-fit and conditional independence with approximate co-sufficient sampling. *The Annals of Statistics*, 50(5):2514 – 2544, 2022.

- Wenshuo Wang and Lucas Janson. A high-dimensional power analysis of the conditional randomization test and knockoffs. *Biometrika*, 109(3):631–645, 2022.
- Eugene Katsevich and Aaditya Ramdas. On the power of conditional independence testing under model-X. *Electronic Journal of Statistics*, 16(2):6348–6394, January 2022. ISSN 1935-7524, 1935-7524. doi: 10.1214/22-EJS2085. URL <https://projecteuclid.org/journals/electronic-journal-of-statistics/volume-16/issue-2/On-the-power-of-conditional-independence-testing-under-model-X/10.1214/22-EJS2085.full>.
- Paul R. Rosenbaum and Donald B. Rubin. The central role of the propensity score in observational studies for causal effects. *Biometrika*, 70(1):41–55, 1983.
- Dongming Huang and Lucas Janson. Relaxing the assumptions of knockoffs by conditioning. *The Annals of Statistics*, 48(5):3021–3042, 2020.
- T. Tony Cai and Zijian Guo. Confidence intervals for high-dimensional linear regression: Minimax rates and adaptivity. *The Annals of Statistics*, 45(2):615 – 646, 2017. doi: 10.1214/16-AOS1461. URL <https://doi.org/10.1214/16-AOS1461>.
- T. Tony Cai and Zijian Guo. Accuracy assessment for high-dimensional linear regression. *The Annals of Statistics*, 46(4):1807 – 1836, 2018. doi: 10.1214/17-AOS1604. URL <https://doi.org/10.1214/17-AOS1604>.
- Jelena Bradic, Jianqing Fan, and Yinchu Zhu. Testability of high-dimensional linear models with nonsparse structures. *Annals of statistics*, 50(2):615, 2022.
- Kaiyue Wen, Tengyao Wang, and Yuhao Wang. Residual permutation test for high-dimensional regression coefficient testing. *arXiv preprint arXiv:2211.16182*, 2022.
- Michael Celentano and Andrea Montanari. Correlation adjusted debiased lasso: debiasing the lasso with inaccurate covariate model. *Journal of the Royal Statistical Society Series B: Statistical Methodology*, 86(5):1455–1482, 06 2024. ISSN 1369-7412. doi: 10.1093/jrssb/qkae039. URL <https://doi.org/10.1093/jrssb/qkae039>.
- Fengnan Gao and Tengyao Wang. Two-sample testing of high-dimensional linear regression coefficients via complementary sketching. *The Annals of Statistics*, 50(5):2950 – 2972, 2022. doi: 10.1214/22-AOS2216. URL <https://doi.org/10.1214/22-AOS2216>.
- Nicolas Verzelen and Fanny Villers. Goodness-of-fit tests for high-dimensional gaussian linear models. *The Annals of Statistics*, 38(2):704–752, 2010.
- Arthur P. Dempster. Covariance selection. *Biometrics*, 28(1):157–175, 1972.
- Xiaotong Lin, Weihao Li, Fangqiao Tian, and Dongming Huang. Goodness-of-fit tests for high-dimensional gaussian graphical models via exchangeable sampling, 2025. URL <https://arxiv.org/abs/2312.01815>.

- Yoav Benjamini and Yosef Hochberg. Controlling the false discovery rate: a practical and powerful approach to multiple testing. *Journal of the Royal statistical society: series B (Methodological)*, 57(1):289–300, 1995.
- Yoav Benjamini and Daniel Yekutieli. The control of the false discovery rate in multiple testing under dependency. *The Annals of Statistics*, 29(4):1165 – 1188, 2001. doi: 10.1214/aos/1013699998.
- Ruodu Wang and Aaditya Ramdas. False discovery rate control with e-values. *Journal of the Royal Statistical Society: Series B (Statistical Methodology)*, 84(3):822–852, 2022. ISSN 1467-9868. doi: 10.1111/rssb.12489. URL <https://onlinelibrary.wiley.com/doi/abs/10.1111/rssb.12489>.
- Sara van de Geer, Peter Bühlmann, Ya’acov Ritov, and Ruben Dezeure. On asymptotically optimal confidence regions and tests for high-dimensional models. *The Annals of Statistics*, 42(3):1166 – 1202, 2014.
- T Tony Cai, Zijian Guo, and Rong Ma. Statistical inference for high-dimensional generalized linear models with binary outcomes. *Journal of the American Statistical Association*, 118(542):1319–1332, 2023.
- Benjamin B. Chu, Jiaqi Gu, Zhaomeng Chen, Tim Morrison, Emmanuel Candes, Zihuai He, and Chiara Sabatti. Second-order group knockoffs with applications to GWAS, March 2024. URL <http://arxiv.org/abs/2310.15069>. arXiv:2310.15069 [q-bio, stat].
- Vikas Agarwal, Wei Jiang, Yuehua Tang, and Baozhong Yang. Uncovering hedge fund skill from the portfolio holdings they hide. *The Journal of Finance*, 68(2):739–783, 2013.
- Yixin Wang, Jan G. M. Klijn, Yi Zhang, Anieta M. Sieuwerts, Maxime P. Look, Fei Yang, Dmitri Talantov, Mieke Timmermans, Marion E. Meijer-van Gelder, Jack Yu, Tim Jatkoe, Els M. J. J. Berns, David Atkins, and John A. Foekens. Gene-expression profiles to predict distant metastasis of lymph-node-negative primary breast cancer. *Lancet (London, England)*, 365(9460):671–679, 2005.
- Tanya Barrett, Stephen E Wilhite, Pierre Ledoux, Carlos Evangelista, Irene F Kim, Maxim Tomashevsky, Kimberly A Marshall, Katherine H Phillippy, Patti M Sherman, Michelle Holko, et al. NCBI GEO: archive for functional genomics data sets—update. *Nucleic acids research*, 41(D1):D991–D995, 2012.
- Martin J Wainwright, Michael I Jordan, et al. Graphical models, exponential families, and variational inference. *Foundations and Trends® in Machine Learning*, 1(1–2):1–305, 2008.
- Dae Woong Ham, Kosuke Imai, and Lucas Janson. Using machine learning to test causal hypotheses in conjoint analysis. *arXiv.org*, 2022.
- Cun-Hui Zhang and Stephanie Zhang. Confidence intervals for low dimensional parameters in high dimensional linear models. *Journal of the Royal Statistical Society Series B: Statistical Methodology*, 76(1):217–242, 2014.

- Adel Javanmard and Andrea Montanari. Confidence intervals and hypothesis testing for high-dimensional regression. *Journal of Machine Learning Research*, 15(82):2869–2909, 2014a.
- Cyrus J DiCiccio and Joseph P Romano. Robust permutation tests for correlation and regression coefficients. *Journal of the American Statistical Association*, 112(519):1211–1220, 2017. doi: 10.1080/01621459.2016.1202117.
- Lihua Lei and Peter J Bickel. An assumption-free exact test for fixed-design linear models with exchangeable errors. *Biometrika*, 108(2):397–412, 2021. doi: 10.1093/biomet/asaa079.
- Kaiyue Wen, Tengyao Wang, and Yuhao Wang. Residual permutation test for regression coefficient testing. *arXiv.org*, December 2024. URL <https://www.proquest.com/publiccontent/docview/2742868090?pq-origsite=summon&sourcetype=Working%20Papers>.
- Yinchu Zhu and Jelena Bradic. Linear hypothesis testing in dense high-dimensional linear models. *Journal of the American Statistical Association*, 113(524):1583–1600, 2018.
- Kenji Fukumizu, Arthur Gretton, Xiaohui Sun, and Bernhard Schölkopf. Kernel measures of conditional dependence. In *Advances in Neural Information Processing Systems 20 (NIPS)*, pages 489–496, Vancouver, Canada, 2007. Curran Associates, Inc. URL <https://papers.nips.cc/paper/3340-kernel-measures-of-conditional-dependence>.
- Kun Zhang, Jonas Peters, Dominik Janzing, and Bernhard Schölkopf. Kernel-based conditional independence test and application in causal discovery. In *Proceedings of the 27th Conference on Uncertainty in Artificial Intelligence (UAI)*, pages 804–813, Barcelona, Spain, 2011. AUAI Press. URL <https://dl.acm.org/doi/10.5555/3020548.3020641>.
- George Doran, David Liang, Tim Rogers, and Daniel L. Rubin. Permutation-based kernel conditional independence test. In *Proceedings of the 30th Conference on Uncertainty in Artificial Intelligence (UAI)*, pages 132–141, Quebec City, Canada, 2014. AUAI Press. URL <https://dl.acm.org/doi/10.5555/3020751.3020766>.
- Eric V Strobl, Kun Zhang, and Shyam Visweswaran. Approximate kernel-based conditional independence tests for fast non-parametric causal discovery. *Journal of Causal Inference*, 7(1):20180017, 2019.
- Meyer Scetbon, Laurent Meunier, and Yaniv Romano. An asymptotic test for conditional independence using analytic kernel embeddings. In *International Conference on Machine Learning*, pages 19328–19346. PMLR, 2022.
- Dino Sejdinovic, Bharath K. Sriperumbudur, Arthur Gretton, and Kenji Fukumizu. Equivalence of distance-based and rkhs-based statistics in hypothesis testing. *The Annals of Statistics*, 41(5):2263–2291, 2013. URL <https://projecteuclid.org/euclid.aos/1386857414>.

- Xueqin Wang, Wenliang Pan, Wenhao Hu, Yuan Tian, and Heping Zhang. Conditional distance correlation. *Journal of the American Statistical Association*, 110(512):1726–1734, 2015. URL <https://www.tandfonline.com/doi/full/10.1080/01621459.2014.993081>.
- Mariusz Kubkowski, Jan Miłniczuk, and Paweł Teisseyre. How to gain on power: novel conditional independence tests based on short expansion of conditional mutual information. *Journal of Machine Learning Research*, 22(62):1–57, 2021.
- Jakob Runge. Conditional independence testing based on a nearest-neighbor estimator of conditional mutual information. In *Proceedings of the Twenty-First International Conference on Artificial Intelligence and Statistics*, pages 938–947. PMLR, March 2018. URL <https://proceedings.mlr.press/v84/runge18a.html>.
- Rajat Sen, Ananda Theertha Suresh, Karthikeyan Shanmugam, Alexandros G. Dimakis, and Sanjay Shakkettai. Model-powered Conditional Independence test. In *Proceedings of the 31st International Conference on Neural Information Processing Systems, NIPS’17*, pages 2955–2965, Red Hook, NY, USA, 2017. Curran Associates Inc. ISBN 9781510860964.
- Sandeep S. Dave, George Wright, Bruce Tan, Andreas Rosenwald, Randy D. Gascoyne, Wing C. Chan, Richard I. Fisher, Rita M. Brazier, Lisa M. Rimsza, Thomas M. Grogan, Thomas P. Miller, Michael LeBlanc, Timothy C. Greiner, Dennis D. Weisenburger, James C. Lynch, Julie Vose, James O. Armitage, Erlend B. Smeland, Stein Kvaloy, Harald Holte, Jan Delabie, Joseph M. Connors, Peter M. Lansdorp, Qin Ouyang, T. Andrew Lister, Andrew J. Davies, Andrew J. Norton, H. Konrad Muller-Hermelink, German Ott, Elias Campo, Emilio Montserrat, Wyndham H. Wilson, Elaine S. Jaffe, Richard Simon, Liming Yang, John Powell, Hong Zhao, Neta Goldschmidt, Michael Chiorazzi, and Louis M. Staudt. Prediction of survival in follicular lymphoma based on molecular features of tumor-infiltrating immune cells. *The New England Journal of Medicine*, 351(21):2159–2169, November 2004. ISSN 1533-4406. doi: 10.1056/NEJMoa041869.
- Shuangge Ma, Xiao Song, and Jian Huang. Supervised group lasso with applications to microarray data analysis. *BMC bioinformatics*, 8(60):1–17, 2007.
- Ming Yuan and Yi Lin. Model selection and estimation in regression with grouped variables. *Journal of the Royal Statistical Society. Series B. Statistical Methodology*, 68(1):49–67, January 2006.
- Lukas Meier, Sara van de Geer, and Peter Bühlmann. The group Lasso for logistic regression. *Journal of the Royal Statistical Society. Series B. Statistical Methodology*, 70(1):53–71, February 2008.
- Ran Dai and Rina Barber. The knockoff filter for fdr control in group-sparse and multitask regression. In *International conference on machine learning*, pages 1851–1859. PMLR, 2016.
- Asher Spector and Lucas Janson. Powerful knockoffs via minimizing reconstructability. *The Annals of Statistics*, 50(1):252–276, 2022.

- Rina Foygel Barber and Emmanuel J. Candès. Controlling the false discovery rate via knockoffs. *The Annals of Statistics*, 43(5), October 2015. ISSN 0090-5364. doi: 10.1214/15-AOS1337. URL <http://arxiv.org/abs/1404.5609>. arXiv:1404.5609 [math, stat].
- Morris L. Eaton. *Multivariate statistics: a vector space approach*. Wiley, New York, 1983. ISBN 0471027766;9780471027768;.
- Michel Ledoux. *The Concentration of Measure Phenomenon*, volume 89 of *Mathematical Surveys and Monographs*. American Mathematical Society, Providence, RI, 2001. ISBN 978-0-8218-3792-4. URL <https://bookstore.ams.org/surv-89-s>.
- Friedrich Götze and Holger Sambale. Higher order concentration on Stiefel and Grassmann manifolds. *Electronic Journal of Probability*, 28(none):1 – 30, 2023. doi: 10.1214/23-EJP966. URL <https://doi.org/10.1214/23-EJP966>.
- Lucien Birgé. An alternative point of view on lepsi’s method. *Lecture Notes-Monograph Series*, pages 113–133, 2001.
- Jun Shao. *Mathematical Statistics*. Springer Texts in Statistics. Springer, New York, NY, 2003.
- Adel Javanmard and Andrea Montanari. Confidence intervals and hypothesis testing for high-dimensional regression. *The Journal of Machine Learning Research*, 15(1):2869–2909, 2014b.
- Peter Bühlmann. Statistical significance in high-dimensional linear models. *Bernoulli*, 19(4):1212 – 1242, 2013.
- Peter McCullagh and John A Nelder. *Generalized Linear Models*, volume 37 of *Monographs of Statistics and Applied Probability*. CRC Press, 2 edition, 1989.
- Trevor J Hastie and Daryl Pregibon. Generalized linear models. In *Statistical models in S*, pages 195–247. Routledge, 2017.
- Shantaram P. Hegde and John B. McDermott. The market liquidity of DIAMONDS, Q’s, and their underlying stocks. *Journal of Banking & Finance*, 28(5):1043–1067, 2004.
- Ronald Aylmer Fisher and Frank Yates. *Statistical tables for biological, agricultural, and medical research*. Hafner Publishing Company, 1953.
- T Mark Beasley, Stephen Erickson, and David B Allison. Rank-based inverse normal transformations are increasingly used, but are they merited? *Behavior genetics*, 39:580–595, 2009.
- Zachary R McCaw, Jacqueline M Lane, Richa Saxena, Susan Redline, and Xihong Lin. Operating characteristics of the rank-based inverse normal transformation for quantitative trait analysis in genome-wide association studies. *Biometrics*, 76(4):1262–1272, 2020.

Jerome H. Friedman, Trevor Hastie, and Robert Tibshirani. Regularization paths for generalized linear models via coordinate descent. *Journal of Statistical Software*, 33(1):1–22, 2010.

Trevor Hastie, Robert Tibshirani, Jerome H Friedman, and Jerome H Friedman. *The elements of statistical learning: data mining, inference, and prediction*. Springer, 2 edition, 2009.

Appendix

Appendix A provides a more detailed and complete version of the literature review discussed in the main text. Appendix B includes algorithms of residual rotation for GGMs and procedures for controlling FDR in group selection. Appendix C contains the omitted proofs for the theoretical results in the main paper. Appendix D presents additional details for the simulation studies in Section 6 in the main text. Appendix E provides additional simulation studies to examine several aspects of the G -CRT. Appendix F shows detailed information about the applications of our testing methods to real-world datasets in Section 7 in the main text. Code for reproducing our experiments is maintained on GitHub (<https://github.com/xiaotong0201/CSS-GGM.git>).

A Literature Review

This appendix provides a more detailed and complete version of the literature review discussed in the main text.

Testing conditional independence that $X_{\mathcal{T}} \perp\!\!\!\perp Y \mid X_{\mathcal{S}}$ is a central problem in statistics with wide-ranging applications in graphical modelling, causal inference, and variable selection. First of all, the necessity of modelling assumptions for testing conditional independence has been theoretically justified in the literature (Shah and Peters, 2020), which implies that with no assumption on the joint distribution of (X, Y, Z) , a valid test for $X \perp\!\!\!\perp Y \mid Z$ is powerless against any alternative. This means that some assumptions must be made to the class of null distributions to have some power.

A.1 Model-X inference

The “model-X” framework assumes F_X the distribution of X is known or satisfies some assumptions, while making no assumptions on $F_{Y|X}$ the conditional distribution of Y given X . Candès et al. (2018) introduced the conditional randomization test (CRT) and model-X knockoffs under this framework. The CRT has been extended and developed in various directions in recent years. Bates et al. (2020) applied the idea of the CRT to develop a method for causal inferences using genetic datasets that include parents and offspring. Shaer et al. (2023) extended CRT to streaming data under arbitrary dependency structures. To accelerate the computation of test statistics, Tansey et al. (2022) proposed the holdout randomization test, while Liu et al. (2022) introduced the distilled CRT (dCRT). Recently, Niu et al. (2024a) leverages a saddlepoint approximation to dCRT to achieve similar statistical performance with significantly reduced computational demands.

The original CRT requires sampling from the true conditional distribution of $X \mid Z$, which may be impractical. To adjust errors arising from imperfectly modelled $P(X \mid Z)$, several refinements have been proposed. Bellot and van der Schaar (2019) proposed to use generative adversarial networks to approximate the conditional distribution. Berrett et al. (2020) proposed permuting the observed value non-uniformly and they developed an error bound on the inflation of the Type I error. Niu et al. (2024b) studied the double robustness of the dCRT, and Li and Liu (2023) proposed using the conditional distribution of $Y \mid Z$ to calibrate the resampling distribution. The aCSS method proposed by Barber and Janson (2022) can also be applied to implementing a CRT. These methods provide asymptotic validity guarantees that are contingent on estimation error of $P(X \mid Z)$. In contrast, our proposed MS-CRT provide exact finite-sample error control. To the best of our knowledge, nearly all CRT methods have been developed for univariate X . The only exception is Ham et al. (2022), who studied the significance of a multidimensional factor in conjoint analysis.

Regarding the power of CRT-based tests, Wang and Janson (2022) derived explicit expressions of the asymptotic power of the CRT in high-dimensional linear regression. (Katsevich and Ramdas, 2022) used the Neyman–Pearson lemma to identify the most powerful CRT statistic and derive its asymptotic power in semiparametric models. Our power analysis, to the best of our knowledge, is the first to investigate the power optimality of testing MCI within the model-X framework.

A.2 Other methods for testing conditional independence

Beyond the Model-X framework, other approaches exist for testing MCI. These can broadly be categorized into “fixed-X” regression-based methods and non-parametric methods.

In the “fixed-X” framework, it is assumed that the conditional distribution $F_{Y|X}$ belongs to a specific parametric (or semiparametric) regression model, where testing conditional independence reduces to testing whether the corresponding regression coefficients are zero. In this framework, high-dimensional inference methods focus on confidence interval construction and hypothesis testing for low-dimensional parameters within regression models. Along this line, Zhang and Zhang (2014) developed a bias correction method for constructing confidence intervals for low-dimensional linear combinations of the regression coefficients in high-dimensional linear models. van de Geer et al. (2014) and Javanmard and Montanari (2014a) further developed various debiasing methods based on Lasso to achieve optimality. Recently, Cai et al. (2023) extended the debiasing method to high-dimensional generalized linear models (GLMs) with binary outcomes. These debiasing methods typically rely on the ultra-sparsity assumption on the regression coefficients that the number of true nonzero coefficients is of order $o(\sqrt{n/\log p})$, which may be restricted in practice. Recently, inference methods that do not require sparsity assumptions have been developed based on different statistical principles: some are based on permutation (DiCiccio and Romano, 2017; Lei and Bickel, 2021; Wen et al., 2024), some on Fisher statistics (Verzelen and Villers, 2010), and others on Neyman orthogonalization principles (Zhu and Bradic, 2018; Bradic et al., 2022). All these methods are primarily developed for linear models.

Apart from the model-X and fixed-X frameworks, there exists a substantial body of work on nonparametric CI testing using kernel methods (Fukumizu et al., 2007; Zhang et al., 2011;

Doran et al., 2014; Strobl et al., 2019; Scetbon et al., 2022), correlation measures (Sejdinovic et al., 2013; Wang et al., 2015; Kubkowski et al., 2021), and nearest-neighbor methods (Runge, 2018; Sen et al., 2017). These nonparametric methods often have less stringent assumptions, but they are often developed and analyzed in settings where the number of variables is smaller than the sample size $p < n$ and where the tested set \mathcal{T} is univariate.

A.3 Group selection

In many applications, variables are naturally structured into pre-defined groups (Goeman et al., 2004), which group selection is a relevant task. The goal is to identify important groups of variables rather than selecting individual variables (Dave et al., 2004; Ma et al., 2007). Parametric methods for group selection often employ penalties such as group Lasso in regression models (Yuan and Lin, 2006; Meier et al., 2008). Dai and Barber (2016) proposed a fixed-X knockoff method for FDR-controlled group selection in Gaussian linear regression, but this requires the sample size $n \geq p$ and is not directly applicable to high-dimensional settings. The model-X knockoff method can be extended to perform group selection (Spector and Janson, 2022; Chu et al., 2024). However, similar to the original CRT, the theoretical validity of group knockoffs relies on knowing the exact distribution of X .

A.4 Comparison between knockoffs and exchangeable copies

This subsection compares the exchangeable sampling and knockoff constructions. A similar discussion has appeared in the appendix of our related work Lin et al. (2025), but we include it here for completeness.

The validity of the p-value defined in (2.1) requires that $\{\mathbf{X}_{\mathcal{T}}, \tilde{\mathbf{X}}_{\mathcal{T}}^{(1)}, \dots, \tilde{\mathbf{X}}_{\mathcal{T}}^{(M)}\}$ are exchangeable conditional on $(\mathbf{X}_{\mathcal{S}}, \mathbf{Y})$, that is, the conditional distribution is invariant to permuting any subset of these datasets. Sampling these copies $\tilde{\mathbf{X}}_{\mathcal{T}}^{(m)}$ may appear similar to the knockoff construction (Barber and Candès, 2015; Candès et al., 2018), but there is a crucial difference. We use the model-X knockoff framework proposed in Candès et al. (2018) as an example, and the discussion below easily extends to the fixed-X knockoff framework used in Barber and Candès (2015).

For knockoff filters, a single dataset $\bar{\mathbf{X}}$ is constructed to replicate the dependencies in the original dataset \mathbf{X} . The key property of the knockoff construction, known as the swap invariance property, requires that for each variable j , swapping the j -th column of \mathbf{X} with the corresponding column of $\bar{\mathbf{X}}$ leaves their joint distribution unchanged. Formally, for any $j \in \{1, 2, \dots, p\}$, we have the distributional equivalence

$$[\mathbf{X}, \bar{\mathbf{X}}]_{\text{swap}(j)} \stackrel{d}{=} [\mathbf{X}, \bar{\mathbf{X}}].$$

The swap invariance property is the foundation of the FDR control of the knockoff filter in variable selection.

To connect with the focus of the current paper, the swap invariance property also guarantees that the original and knockoff datasets, as a pair, are exchangeable. However, when multiple knockoffs $\{\bar{\mathbf{X}}^{(1)}, \dots, \bar{\mathbf{X}}^{(M)}\}$ are generated, the pairwise exchangeability does not automatically extend to the joint exchangeability. Since each knockoff dataset is generated

by conditioning on the observed data \mathbf{X} , \mathbf{X} plays a distinguished role that the knockoffs do not share. This distinction is critical: while the swap invariance property ensures pairwise exchangeability between \mathbf{X} and $\bar{\mathbf{X}}^{(m)}$, it does not guarantee joint exchangeability across multiple knockoffs (e.g., $\bar{\mathbf{X}}^{(1)}$ and $\bar{\mathbf{X}}^{(2)}$) and \mathbf{X} together.

In fact, exchanging the position of \mathbf{X} with any of the knockoffs $\bar{\mathbf{X}}^{(m)}$ will change the joint distribution. For instance,

$$[\mathbf{X}, \bar{\mathbf{X}}^{(1)}, \dots, \bar{\mathbf{X}}^{(M)}] \text{ and } [\bar{\mathbf{X}}^{(1)}, \mathbf{X}, \dots, \bar{\mathbf{X}}^{(M)}]$$

do not follow the same distribution in general. We therefore note that knockoff construction methods do not naturally extend to exchangeable sampling, and vice versa.

B Algorithms

B.1 Residual rotation for GGMs

Suppose the rows of the observed data \mathbf{X} are independent and identically distributed (i.i.d.) samples from some population P in a GGM \mathcal{M}_G . Lin et al. (2025) introduce an algorithm that can efficiently generate copies $\tilde{\mathbf{X}}^{(m)}$ ($m = 1, \dots, M$) so that $\mathbf{X}, \tilde{\mathbf{X}}^{(1)}, \dots, \tilde{\mathbf{X}}^{(M)}$ are exchangeable. The first step of their algorithm is the so-called *residual rotation*, which is outlined in Algorithm 4. Proposition 5 guarantees that it satisfies Assumption 1 and Theorem 3 guarantees the exchangeability. Both results are proved by Lin et al. (2025).

Algorithm 4 Sampling one column via residual rotation

Input: $n \times p$ data matrix \mathbf{X} , index i of the variable to sample, neighborhood N_i of i
If $n \leq |N_i| + 1$, set $\tilde{\mathbf{X}}_i = \mathbf{X}_i$; otherwise, proceed to the following steps.

Step 1: Apply least squares linear regression to \mathbf{X}_i on $[\mathbf{1}_n, \mathbf{X}_{N_i}]$

Step 2: Obtain the fitted vector \mathbf{F} and the residual vector \mathbf{R} from the regression

Step 3: Draw a standard normal n -vector \mathbf{E} . Apply least squares linear regression to \mathbf{E} on $[\mathbf{1}_n, \mathbf{X}_{N_i}]$, and obtain the residual $\tilde{\mathbf{R}}$

Step 4: Compute $\tilde{\mathbf{X}}_i = \mathbf{F} + \tilde{\mathbf{R}} \frac{\|\mathbf{R}\|}{\|\tilde{\mathbf{R}}\|}$

Output: $\tilde{\mathbf{X}}_i$

Proposition 5. Suppose the rows of \mathbf{X} are i.i.d. samples from a distribution in \mathcal{M}_G . Let $\tilde{\mathbf{X}}_i$ be the output of Algorithm 4 with index i , N_i be its neighborhood, and $\tilde{\mathbf{X}}$ be a matrix formed by replacing the i -th column of \mathbf{X} with $\tilde{\mathbf{X}}_i$. Then, $\psi_G(\mathbf{X}) = \psi_G(\tilde{\mathbf{X}})$ and the conditional distribution of $\tilde{\mathbf{X}}$ given $\mathbf{X} = \mathbf{x}$ is the same as that of \mathbf{X} for almost every $\mathbf{x} \in \mathbb{R}^{n \times p}$. Furthermore, if $n \geq 3 + |N_i|$, then $\tilde{\mathbf{X}}_i \neq \mathbf{X}_i$, a.s.

Theorem 3. Suppose \mathbf{X} is a $n \times p$ matrix and G is a graph whose node set is $[p]$. Let $\{\tilde{\mathbf{X}}^{(m)}\}_{m=1}^M$ be the output of Algorithm 2 with local update using Algorithm 5. If the rows of \mathbf{X} are i.i.d. samples from a distribution in \mathcal{M}_G as defined in (4.1), then $\mathbf{X}, \tilde{\mathbf{X}}^{(1)}, \dots, \tilde{\mathbf{X}}^{(M)}$ are exchangeable. Furthermore, if the elements of \mathcal{I} form a subset of $[p]$, denoted by \mathcal{T} , then

$\tilde{\mathbf{X}}_{-\mathcal{T}}^{(m)} = \mathbf{X}_{-\mathcal{T}}$ for all $m \in [M]$ and $\mathbf{X}_{\mathcal{T}}, \tilde{\mathbf{X}}_{\mathcal{T}}^{(1)}, \dots, \tilde{\mathbf{X}}_{\mathcal{T}}^{(M)}$ are conditionally exchangeable given $\mathbf{X}_{-\mathcal{T}}$.

An application of Algorithm 2 is the *Monte Carlo goodness-of-fit* (MC-GoF) test for the null hypothesis that the distribution of \mathbf{X} belongs to \mathcal{M}_G . The procedure of the MC-GoF test is outlined in Algorithm 5. The function $T(\cdot)$ can be any test statistic function such that larger values are regarded as evidence against the null hypothesis. Lin et al. (2025) proposed some promising choices such as PRC, ERC, F_{Σ} , and $\text{GLR-}\ell_1$. Theoretical analyses showed that the MC-GoF test can achieve minimax rate optimal power in some high-dimensional settings.

Algorithm 5 Monte Carlo goodness-of-fit (MC-GoF) test for GGMs

Input: $n \times p$ data matrix \mathbf{X} , graph G , test statistic function $T(\cdot)$, number of copies M
Require: $n - 1 >$ maximum degree of G
Step 1: Apply Algorithm 2 with $\mathcal{I} = (1, 2, \dots, p)$ to obtain $\tilde{\mathbf{X}}^{(1)}, \dots, \tilde{\mathbf{X}}^{(M)}$
Step 2: Calculate the statistics $T(\mathbf{X}), T(\tilde{\mathbf{X}}^{(1)}), T(\tilde{\mathbf{X}}^{(2)}), \dots, T(\tilde{\mathbf{X}}^{(M)})$
Step 3: Compute the (one-sided) p-value

$$\text{pVal}_T = \frac{1}{M+1} \left(1 + \sum_{m=1}^M \mathbb{1} \left\{ T(\tilde{\mathbf{X}}^{(m)}) \geq T(\mathbf{X}) \right\} \right)$$

Output: pVal_T

B.2 Procedures for controlling FDR in group selection

This appendix outlines the multiple testing correction procedures employed in the CRT-Based group selection procedure to address the issue of multiplicity in Section 5. In addition to the classical Benjamini-Hochberg (BH) procedure (Benjamini and Hochberg, 1995) and Benjamini-Yekutieli (BY) procedure (Benjamini and Yekutieli, 2001), we also consider the e-BH procedure based on e-values, which have emerged from recent advancements in multiple testing theory (Wang and Ramdas, 2022).

The following algorithms detail the BH procedure and e-BH procedure as applied to the context of group selection. The BY procedure is the same as the BH procedure but with α replaced by α/c_g where $c_g = \sum_{i=1}^g 1/i$.

Algorithm 6 Benjamini-Hochberg (BH) Procedure for Group Selection

Input: p-values from group-wise MS-CRTs: $\{\text{pVal}_1, \dots, \text{pVal}_g\}$, FDR level α .
1: Sort p-values in ascending order: $\text{pVal}_{(1)} \leq \text{pVal}_{(2)} \leq \dots \leq \text{pVal}_{(g)}$.
2: Find the largest index k such that $\text{pVal}_{(k)} \leq \frac{k}{g}\alpha$.
3: **Output:** Set of rejected groups $\{j : \text{pVal}_{(j)} \leq \text{pVal}_{(k)}\}$.

Algorithm 7 e-BH Procedure for Group Selection

Input: p-values from group-wise MS-CRTs: $\{\text{pVal}_1, \dots, \text{pVal}_g\}$, FDR level α .

- 1: Use Algorithm 3 to transform p-values to boosted e-values, denoted by $\{E_1, E_2, \dots, E_g\}$.
 - 2: Apply BH procedure (Algorithm 6) to $\{1/E_1, 1/E_2, \dots, 1/E_g\}$.
 - 3: **Output:** Set of rejected groups by BH.
-

To prove Proposition 4, we first introduce a lemma.

Lemma 1. *Given a sequence of $\{\delta_k\}_{k=1}^g$ and $\{\ell_k\}_{k=1}^g$. Define the partition points by*

$$b_0 = 0 \quad \text{and} \quad b_k = b_{k-1} + \frac{q}{g} \delta_k, \quad k \geq 1.$$

For $x \in (b_{k-1}, b_k]$, define $Y(x) = \frac{q}{q\ell_k}$; for $x > b_g$, define $Y(x) = 1/(2q)$. Suppose $X \sim \text{Unif}(0, 1)$. If

$$\sum_{k: \ell_k \leq g} \frac{\delta_k}{\lceil \ell_k \rceil} \leq 1,$$

then $Y(X)$ is a boosted e-variable satisfying that

$$\mathbb{E}[T(qY(X))] \leq q.$$

Proof of Lemma 1. If $x > b_g$, then $qY(x) < 1$. Therefore,

$$qY(x) \geq 1 \iff \ell_k \leq g, \text{ and } x \in (b_{k-1}, b_k].$$

Note that

$$\mathbb{P}(X \in (b_{k-1}, b_k]) = b_k - b_{k-1} = \frac{q}{g} \delta_k.$$

For $x \in (b_{k-1}, b_k]$ with $\ell_k \leq g$, we have

$$\frac{q}{qY(x)} = \ell_k \quad \text{and} \quad T(qY(x)) = \frac{q}{\lceil \ell_k \rceil}.$$

Therefore,

$$\mathbb{E}[T(qY(X))] = \sum_{k: \ell_k \leq g} \frac{q}{g} \delta_k \frac{q}{\lceil \ell_k \rceil} = \sum_{k: \ell_k \leq g} \frac{q \delta_k}{\lceil \ell_k \rceil} \leq q.$$

□

We can now prove Proposition 4.

Proof of Proposition 4. Define

$$\begin{aligned} q &= \alpha, \quad \delta_k = \frac{1}{1+k}, \quad b_k = b_{k-1} + \frac{q}{g(k+1)}, \\ \ell_k &= k, \quad \text{for } k = 1, \dots, g. \end{aligned}$$

For $x \in (b_{k-1}, b_k]$, define

$$Y(x) = \frac{g}{qk},$$

and $Y(x) = q/2$ for $x > b_g$. It is clear from Algorithm 3 that the output $E_j = Y(p_j)$ for the input p_j . Since $\sum_{k=1}^g \frac{1}{k(k+1)} = \sum_{k=1}^g \left(\frac{1}{k} - \frac{1}{k+1} \right) = 1 - \frac{1}{g+1} \leq 1$, we can apply Lemma 1 to see that if $X \sim \text{Unif}(0, 1)$, then $\mathbb{E}[T(qY(X))] = q(1 - \frac{1}{g+1}) \leq q$. □

C Proofs of Main Results

This section provides the omitted proofs for the theoretical results in the main paper.

In the proof of Sections C.2 and C.3, we make use of the following notions. For $n \geq k$, the Stiefel manifold $W_{n,k} = \{V \in \mathbb{R}^{n \times k} \mid V^T V = \mathbf{I}_k\}$. In the special case where $n = k$, $W_{n,n}$ reduces to the orthogonal group $O(n) = \{V \in \mathbb{R}^{n \times n} \mid V^T V = V V^T = \mathbf{I}_n\}$. Let $\mu_{n,d}$ denote the unique Haar (invariant) measure on $W_{n,d}$.

C.1 Proof of Proposition 1

Recall that

1. $\mathbf{X}_{\mathcal{T}}, \tilde{\mathbf{X}}_{\mathcal{T}}^{(1)}, \dots, \tilde{\mathbf{X}}_{\mathcal{T}}^{(M)}$ are conditionally exchangeable given $\mathbf{X}_{-\mathcal{T}}$, and
2. under the null hypothesis, \mathbf{Y} and $\mathbf{X}_{\mathcal{T}}$ are conditionally independent given $\mathbf{X}_{-\mathcal{T}}$.

Therefore, under the null hypothesis, it holds that \mathbf{Y} and $(\mathbf{X}_{\mathcal{T}}, \tilde{\mathbf{X}}_{\mathcal{T}}^{(1)}, \dots, \tilde{\mathbf{X}}_{\mathcal{T}}^{(M)})$ are conditionally independent given $\mathbf{X}_{-\mathcal{T}}$. This implies that $\mathbf{X}_{\mathcal{T}}, \tilde{\mathbf{X}}_{\mathcal{T}}^{(1)}, \dots, \tilde{\mathbf{X}}_{\mathcal{T}}^{(M)}$ are conditionally exchangeable given $(\mathbf{X}_{-\mathcal{T}}, \mathbf{Y})$.

By definition of $\tilde{\mathbf{X}}^{(j)}$, we have $\mathbf{X}, \tilde{\mathbf{X}}^{(1)}, \dots, \tilde{\mathbf{X}}^{(M)}$ are conditionally exchangeable given \mathbf{Y} . As a result, we conclude that T_0, T_1, \dots, T_M are conditionally exchangeable given \mathbf{Y} . Hence, for any $\alpha \in (0, 1)$, $\mathbf{P}(\text{pval}_T \leq \alpha \mid \mathbf{Y}) \leq \alpha$, which implies that $\mathbf{P}(\text{pval}_T \leq \alpha) \leq \alpha$.

C.2 Proof of Proposition 2

Let $\tilde{\mathbf{X}}_{\mathcal{T}}$ be a copy generated from Algorithm 1.

We only need to prove

$$\mathbf{X}_{\mathcal{T}}^T \mathbf{X}_{\mathcal{S}} = \tilde{\mathbf{X}}_{\mathcal{T}}^T \mathbf{X}_{\mathcal{S}}, \mathbf{X}^T \mathbf{X}_{\mathcal{T}} = \tilde{\mathbf{X}}_{\mathcal{T}}^T \tilde{\mathbf{X}}_{\mathcal{T}} \quad (\text{C.1})$$

and given $\mathbf{X}_{\mathcal{S}}$

$$(\mathbf{X}_{\mathcal{T}}, \tilde{\mathbf{X}}_{\mathcal{T}}) \stackrel{d}{=} (\tilde{\mathbf{X}}_{\mathcal{T}}, \mathbf{X}_{\mathcal{T}}). \quad (\text{C.2})$$

Proof of (C.1) Note that

$$\tilde{\mathbf{X}}_{\mathcal{T}} = \mathbf{X}_{\mathcal{S}} (\mathbf{X}_{\mathcal{S}}^T \mathbf{X}_{\mathcal{S}})^{-1} \mathbf{X}_{\mathcal{S}}^T \mathbf{X}_{\mathcal{T}} + \mathbf{P}_{\mathcal{R}}^T U \mathbf{Q},$$

where U follows $\mu_{n-s,r}$ on $W_{n-s,r}$ with respect to the Haar measure (see Proposition 7.2 in Eaton (1983)). By (3.1) and (3.2), we have

$$\mathbf{P}_{\mathcal{R}} \mathbf{X}_{\mathcal{S}} = \mathbf{0}, \quad \text{and} \quad \mathbf{Q}^T \mathbf{Q} = \mathbf{X}_{\mathcal{T}}^T \mathbf{P}_{\mathcal{R}}^T \mathbf{P}_{\mathcal{R}} \mathbf{X}_{\mathcal{T}} = \mathbf{X}_{\mathcal{T}}^T \mathbf{X}_{\mathcal{T}} - \mathbf{X}_{\mathcal{T}}^T \mathbf{X}_{\mathcal{S}} (\mathbf{X}_{\mathcal{S}}^T \mathbf{X}_{\mathcal{S}})^{-1} \mathbf{X}_{\mathcal{S}}^T \mathbf{X}_{\mathcal{T}}.$$

Therefore,

$$\begin{aligned} \tilde{\mathbf{X}}_{\mathcal{T}}^T \mathbf{X}_{\mathcal{S}} &= \mathbf{X}_{\mathcal{T}}^T \mathbf{X}_{\mathcal{S}} (\mathbf{X}_{\mathcal{S}}^T \mathbf{X}_{\mathcal{S}})^{-1} \mathbf{X}_{\mathcal{S}}^T \mathbf{X}_{\mathcal{S}} = \mathbf{X}_{\mathcal{T}}^T \mathbf{X}_{\mathcal{S}} \\ \tilde{\mathbf{X}}_{\mathcal{T}}^T \tilde{\mathbf{X}}_{\mathcal{T}} &= \mathbf{X}_{\mathcal{T}}^T \mathbf{X}_{\mathcal{S}} (\mathbf{X}_{\mathcal{S}}^T \mathbf{X}_{\mathcal{S}})^{-1} \mathbf{X}_{\mathcal{S}}^T \mathbf{X}_{\mathcal{S}} (\mathbf{X}_{\mathcal{S}}^T \mathbf{X}_{\mathcal{S}})^{-1} \mathbf{X}_{\mathcal{S}}^T \mathbf{X}_{\mathcal{T}} + \mathbf{Q}^T U^T \mathbf{P}_{\mathcal{R}} \mathbf{P}_{\mathcal{R}}^T U \mathbf{Q} \\ &= \mathbf{X}_{\mathcal{T}}^T \mathbf{X}_{\mathcal{S}} (\mathbf{X}_{\mathcal{S}}^T \mathbf{X}_{\mathcal{S}})^{-1} \mathbf{X}_{\mathcal{S}}^T \mathbf{X}_{\mathcal{T}} + \mathbf{Q}^T \mathbf{Q} \\ &= \mathbf{X}_{\mathcal{T}}^T \mathbf{X}_{\mathcal{T}}. \end{aligned}$$

Proof of (C.2) Part 1. When $n-s > t$, we only need to prove that given $(\mathbf{X}_{\mathcal{T}}^T \mathbf{X}_{\mathcal{S}}, \mathbf{X}_{\mathcal{T}}^T \mathbf{X}_{\mathcal{T}})$, both $\mathbf{X}_{\mathcal{T}}$ and $\tilde{\mathbf{X}}_{\mathcal{T}}$ distributed as

$$\mathbf{X}_{\mathcal{S}} (\mathbf{X}_{\mathcal{S}}^T \mathbf{X}_{\mathcal{S}})^{-1} \mathbf{X}_{\mathcal{S}}^T \mathbf{X}_{\mathcal{T}} + \mathbf{P}_{\mathcal{R}}^T U \mathbf{Q},$$

where $U \sim \mu_{n-s,t}$.

By properties of multivariate normal distributions, $(\mathbf{X}_{\mathcal{T}}^T \mathbf{X}_{\mathcal{S}}, \mathbf{X}_{\mathcal{T}}^T \mathbf{X}_{\mathcal{T}})$ is the sufficient statistic for the conditional distribution of $\mathbf{X}_{\mathcal{T}} \mid \mathbf{X}_{\mathcal{S}}$ and the conditional distribution $\mathbf{X}_{\mathcal{T}} \mid (\mathbf{X}_{\mathcal{S}}, \mathbf{X}_{\mathcal{T}}^T \mathbf{X}_{\mathcal{S}}, \mathbf{X}_{\mathcal{T}}^T \mathbf{X}_{\mathcal{T}})$ is the uniform distribution (proportional to the Haar measure) on the support. Furthermore, the conditional distribution of $\mathbf{P}_{\mathcal{R}} \mathbf{X}_{\mathcal{T}}$ given $(\mathbf{X}_{\mathcal{S}}, \mathbf{X}_{\mathcal{T}}^T \mathbf{X}_{\mathcal{S}}, \mathbf{X}_{\mathcal{T}}^T \mathbf{X}_{\mathcal{T}})$ is the uniform distribution on its support

$$\mathcal{X}_0 = \{\mathbf{x} \in \mathbb{R}^{(n-s) \times t} : \mathbf{x}^T \mathbf{x} = \mathbf{Q}^2\},$$

where we have used the fact that $\mathbf{X}_{\mathcal{T}}^T \mathbf{P}_{\mathcal{R}}^T \mathbf{P}_{\mathcal{R}} \mathbf{X}_{\mathcal{T}} = \mathbf{Q}^2 \in \mathbb{R}^{t \times t}$ and it is of full rank t a.s.

Since \mathbf{Q} is invertible, we define $\psi(\mathbf{x}) = \mathbf{x} \mathbf{Q}^{-1}$ for $\mathbf{x} \in \mathcal{X}_0$. It is easy to see $\psi : \mathcal{X}_0 \mapsto W_{n-s,t}$ and is one-to-one. In particular, define $\mathbf{V} = \mathbf{P}_{\mathcal{R}} \mathbf{X}_{\mathcal{T}}$ and $U_0 = \psi(\mathbf{V})$, which is equivalent to $\mathbf{V} = U_0 \mathbf{Q}$ for $U_0 \in W_{n-s,t}$.

For any fixed $\mathbf{B} \in O(n-s)$, it is routine to show that if \mathbf{V} uniformly distributed on \mathcal{X}_0 then so does $\mathbf{B}\mathbf{V}$. This suggests that when conditional on $(\mathbf{X}_{\mathcal{S}}, \mathbf{X}_{\mathcal{T}}^T \mathbf{X}_{\mathcal{S}}, \mathbf{X}_{\mathcal{T}}^T \mathbf{X}_{\mathcal{T}})$, we have $\psi(\mathbf{V}) \stackrel{d}{=} \psi(\mathbf{B}\mathbf{V})$, which also reads as $U_0 \stackrel{d}{=} \mathbf{B}U_0$. By the uniqueness of (left) the Haar measure on $W_{n-s,t}$, we conclude that $U_0 \sim \mu_{n-s,t}$. Therefore, we prove that $\mathbf{X}_{\mathcal{T}}$ and $\tilde{\mathbf{X}}_{\mathcal{T}}$ have the same conditional distribution when $n-s > t$.

Part 2. When $n-s \leq t$, under (3.3), we have $\mathbf{X}_{\mathcal{T}} \mid \mathbf{X}_{\mathcal{S}} \sim N_{n,t}(\mathbf{X}_{\mathcal{S}} \xi^T, \mathbf{I}_n \otimes \Sigma_{\mathcal{T}|\mathcal{S}})$, so conditional on $\mathbf{X}_{\mathcal{S}}$, $\mathbf{P}_{\mathcal{R}} \mathbf{X}_{\mathcal{T}} \sim N_{n-s,t}(\mathbf{0}_{n \times t}, \mathbf{I}_{n-s} \otimes \Sigma_{\mathcal{T}|\mathcal{S}})$. Note that by definition of \mathbf{Q} , it holds that $\mathbf{P}_{\mathcal{R}} \tilde{\mathbf{X}}_{\mathcal{T}} = U \mathbf{P}_{\mathcal{R}} \mathbf{X}_{\mathcal{T}}$, with U following $\mu_{n-s,n-s}$ on $O(n-s)$ with respect to Haar measure. Therefore, given $\mathbf{X}_{\mathcal{S}}$, we have $\mathbf{X}_{\mathcal{T}} \stackrel{d}{=} \tilde{\mathbf{X}}_{\mathcal{T}}$. This suggests that $(\mathbf{X}_{\mathcal{S}}, \mathbf{X}_{\mathcal{T}}) \stackrel{d}{=} (\mathbf{X}_{\mathcal{S}}, \tilde{\mathbf{X}}_{\mathcal{T}})$. Using the same argument but with $\tilde{\mathbf{X}}_{\mathcal{T}}$ swapped with $\mathbf{X}_{\mathcal{T}}$ and noting that $\mathbf{P}_{\mathcal{R}} \mathbf{X}_{\mathcal{T}} = U^T \mathbf{P}_{\mathcal{R}} \tilde{\mathbf{X}}_{\mathcal{T}}$, we have $(\mathbf{X}_{\mathcal{S}}, \mathbf{X}_{\mathcal{T}}, \tilde{\mathbf{X}}_{\mathcal{T}}) \stackrel{d}{=} (\mathbf{X}_{\mathcal{S}}, \tilde{\mathbf{X}}_{\mathcal{T}}, \mathbf{X}_{\mathcal{T}})$. Therefore, (C.2) has been proved.

C.3 Proof of Theorem 1

To ease the analysis, we first reduce the problem to the “infinite- M ” setting. Denote $T_0 = T(\mathbf{Y}, \mathbf{X}_{\mathcal{T}}, \mathbf{X}_{\mathcal{S}})$ and $T_m = T(\mathbf{Y}, \tilde{\mathbf{X}}_{\mathcal{T}}, \mathbf{X}_{\mathcal{S}})$. For any number q , we can derive

$$\begin{aligned}
& \mathbb{P}(\phi_{T,\alpha} = 1) \\
&= \mathbb{P}\left(\frac{1}{M+1} \left[1 + \sum_{m=1}^M \mathbf{1}\{T_m \geq T_0\}\right] \leq \alpha\right) \\
&\geq \mathbb{P}\left(T_0 > q, \frac{1}{M+1} \left[1 + \sum_{m=1}^M \mathbf{1}\{T_m \geq T_0\}\right] \leq \alpha\right) \\
&= \mathbb{P}(T_0 > q) - \mathbb{P}\left(T_0 > q, \frac{1}{M+1} \left[1 + \sum_{m=1}^M \mathbf{1}\{T_m \geq T_0\}\right] > \alpha\right) \\
&\geq \mathbb{P}(T_0 > q) - \mathbb{P}\left(\frac{1}{M+1} \left[1 + \sum_{m=1}^M \mathbf{1}\{T_m \geq q\}\right] > \alpha\right),
\end{aligned} \tag{C.3}$$

where the last inequality is because if $b > c$ then $\mathbf{1}\{a \geq b\} \leq \mathbf{1}\{a \geq c\}$. Then the theorem is proved if for some q , we have

- $\mathbb{P}(T_0 > q) \geq 1 - (1 - \beta)/2$,
- $\mathbb{P}\left(\frac{1}{M+1} \left[1 + \sum_{m=1}^M \mathbf{1}\{T_m \geq q\}\right] > \alpha\right) \leq (1 - \beta)/2$.

The following lemma is proved in Lin et al. (2025).

Lemma 2. *If $M > 2/\alpha$ and if the probability $\tilde{\alpha} = P(T_m \geq q_n)$ satisfies $2(\tilde{\alpha} + \sqrt{\tilde{\alpha}}) < \alpha$ and $\tilde{\alpha} < 0.5$, then*

$$P\left(\frac{1}{M+1} \left[1 + \sum_{m=1}^M \mathbf{1}\{T_m \geq q_n\}\right] > \alpha\right) \leq e^{-M}.$$

We pick and fix a value of $\tilde{\alpha}$ such that $2(\tilde{\alpha} + \sqrt{\tilde{\alpha}}) < \min(0.5, \alpha)$.

Since $M \geq \max(2\alpha^{-1}, \log(2(1 - \beta)^{-1}))$, we can use Lemma 2 to bound

$$\mathbb{P}\left(\frac{1}{M+1} \left[1 + \sum_{m=1}^M \mathbf{1}\{T_m \geq q_n\}\right] > \alpha\right)$$

from above by $(1 - \beta)/2$ if q_n is chosen such that the probability $P(T_m \geq q_n) \leq \tilde{\alpha}$.

With the above preparation, we will proceed with treating M as infinite, replacing α by $\tilde{\alpha}$, and replacing β by $1 - (1 - \beta)/2$. The rest of the proofs can be summarized as follows:

- Characterize the distribution of $T(\mathbf{Y}, \tilde{\mathbf{X}}_{\mathcal{T}}, \mathbf{X}_{\mathcal{S}})$ for copies $\tilde{\mathbf{X}}_{\mathcal{T}}$ generated by Algorithm 1 and thereby upper bound its $(1 - \alpha)$ -th quantile, which serves as q_n .
- Characterize the distribution of $T(\mathbf{Y}, \mathbf{X}_{\mathcal{T}}, \mathbf{X}_{\mathcal{S}})$ under alternative points and thereby prove that it exceeds q_n with probability larger than β .

C.3.1 Auxiliary Results

The auxiliary results primarily concern concentration tail bounds.

Lemma 3 ((Ledoux, 2001, p.27)). *Suppose $n \geq d$ and $A \sim \mu_{n,d}$, and $f_1(A) = M^T \text{vec}(A)$ for some $M \in \mathbb{R}^{nd \times 1}$. For any $t \geq 0$, we have*

$$\mu_{n,d}(|f_1| \geq t) \leq 2 \exp \left(-\frac{(n-1)t^2}{8 \|M\|_2^2} \right).$$

Lemma 4 ((Götze and Sambale, 2023, Theorem 7.1)). *Suppose $n \geq d$ and $A \sim \mu_{n,d}$, and $f_2(A) = \text{vec}(A)^T M \text{vec}(A)$ for some matrix $M \in \mathbb{R}^{nd \times nd}$. For any $t \geq 0$, we have*

$$\mu_{n,d}(|f_2 - \text{tr}(M)/n| \geq t) \leq 2 \exp \left(-\frac{1}{C} \min \left(\frac{(n-2)^2 t^2}{\|M\|_{\text{HS}}^2}, \frac{(n-2)t}{\|M\|_{\text{op}}} \right) \right),$$

where we may take $C = 128e^2 / \log(2)$.

Lemma 5 (Restated (Birgé, 2001, Lemma 8.1)). *Let X be a noncentral χ^2 variable with D degrees of freedom and noncentrality parameter B . Then for all $x > 0$,*

$$\mathbb{P} \left[X \geq (D+B) + 2\sqrt{(D+2B)x} + 2x \right] \leq \exp(-x), \quad (\text{C.4})$$

and

$$\mathbb{P} \left[X \leq (D+B) - 2\sqrt{(D+2B)x} \right] \leq \exp(-x). \quad (\text{C.5})$$

C.3.2 Power analysis of dense alternatives

Proof. For the copies $\tilde{\mathbf{X}}_{\mathcal{T}} = \mathbf{X}_{\mathcal{S}} (\mathbf{X}_{\mathcal{S}}^T \mathbf{X}_{\mathcal{S}})^{-1} \mathbf{X}_{\mathcal{S}}^T \mathbf{X}_{\mathcal{T}} + \mathbf{P}_{\mathcal{R}}^T U \mathbf{Q}$ generated from Algorithm 1, we have

$$T_{\text{dense}}(\mathbf{Y}, \tilde{\mathbf{X}}_{\mathcal{T}}, \mathbf{X}_{\mathcal{S}}) = \left\| (\mathbf{Y}^T \mathbf{P}_{\mathcal{R}}^T \mathbf{P}_{\mathcal{R}} \mathbf{Y})^{-1/2} \cdot \mathbf{Y}^T \mathbf{P}_{\mathcal{R}}^T U \right\|_2^2 = \text{vec}(U)^T M \text{vec}(U),$$

where U follows $\mu_{n-s,t}$ on $W_{n-s,t}$ and

$$M = (\mathbf{Y}^T \mathbf{P}_{\mathcal{R}}^T \mathbf{P}_{\mathcal{R}} \mathbf{Y})^{-1} \cdot \mathbf{I}_t \otimes \mathbf{P}_{\mathcal{R}} \mathbf{Y} \mathbf{Y}^T \mathbf{P}_{\mathcal{R}}^T.$$

It is easy to see that the eigenvalues of M are 1 (with multiplicity t) and 0, which implies

$$\text{tr}(M) = t, \|M\|_{\text{HS}}^2 = \text{tr}(M^T M) = t, \|M\|_{\text{op}} = 1.$$

It then follows from Lemma 4 that

$$\mu_{n-s,t} \left(\left| T_{\text{dense}}(\mathbf{Y}, \tilde{\mathbf{X}}_{\mathcal{T}}, \mathbf{X}_{\mathcal{S}}) - \frac{t}{n-s} \right| \geq u \right) \leq 2 \exp \left(-\frac{1}{C} \min \left(\frac{(n-s-2)^2 u^2}{t}, (n-s-2)u \right) \right).$$

for constant $C = 128e^2 / \log(2)$.

Let $u_n = C \log(2/\alpha) \sqrt{t}/(n-s)$. When n is large enough, we have

$$\mu_{n-s,t} \left(T_{\text{dense}}(\mathbf{Y}, \tilde{\mathbf{X}}_{\mathcal{T}}, \mathbf{X}_{\mathcal{S}}) \leq \frac{t}{n-s} + u_n \right) \geq 1 - \alpha.$$

So we only need to prove that: there is some constant $c_1 > 0$ such that $\forall \theta \in \Theta_{\text{dense}}(c_1 t^{1/4}/\sqrt{n})$, we have

$$\mathbb{P}_{\theta} \left(T_{\text{dense}}(\mathbf{Y}, \mathbf{X}_{\mathcal{T}}, \mathbf{X}_{\mathcal{S}}) > \frac{t}{n-s} + u_n \right) \geq \beta + o(1).$$

For simplicity, we introduce the following notations:

$$\begin{aligned} S_1 &= \frac{1}{\sigma^2} \|\mathbf{P}_{\mathcal{R}} \mathbf{Y}\|_2^2, \\ S_2 &= \frac{1}{\sigma^2} \mathbf{Y}^T \mathbf{P}_{\mathcal{R}}^T \mathbf{P}_{\mathcal{R}} \mathbf{X}_{\mathcal{T}} (\mathbf{X}_{\mathcal{T}}^T \mathbf{P}_{\mathcal{R}}^T \mathbf{P}_{\mathcal{R}} \mathbf{X}_{\mathcal{T}})^{-1} \mathbf{X}_{\mathcal{T}}^T \mathbf{P}_{\mathcal{R}}^T \mathbf{P}_{\mathcal{R}} \mathbf{Y}, \end{aligned}$$

which allows us to write $T_{\text{dense}} = S_2/S_1$. Let $\epsilon = \mathbf{P}_{\mathcal{R}} (\mathbf{Y} - \mathbf{X}_{\mathcal{T}} \beta_{\mathcal{T}}) \in \mathbb{R}^{n-s}$. We have

$$\epsilon \sim N(\mathbf{0}, \sigma^2 \mathbf{I}_{n-s}), \quad \mathbf{P}_{\mathcal{R}} \mathbf{X}_{\mathcal{T}} \beta_{\mathcal{T}} \sim N(\mathbf{0}, (\beta_{\mathcal{T}}^T \Sigma_{\mathcal{T}|\mathcal{S}} \beta_{\mathcal{T}}) \mathbf{I}_{n-s}), \quad \epsilon \perp \mathbf{P}_{\mathcal{R}} \mathbf{X}.$$

By relationship between normal and Chi-square distributions, we have the following results:

1. $S_1 \mid \mathbf{P}_{\mathcal{R}} \mathbf{X}_{\mathcal{T}} \beta_{\mathcal{T}}$ follows a noncentral χ^2 distribution with $n-s$ degrees of freedom and noncentrality parameter $\|\mathbf{P}_{\mathcal{R}} \mathbf{X}_{\mathcal{T}} \beta_{\mathcal{T}}\|_2^2 / \sigma^2$,
2. $S_2 \mid \mathbf{P}_{\mathcal{R}} \mathbf{X}_{\mathcal{T}} \beta_{\mathcal{T}}$ follows a noncentral χ^2 distribution with t degrees of freedom and noncentrality parameter $\|\mathbf{P}_{\mathcal{R}} \mathbf{X}_{\mathcal{T}} \beta_{\mathcal{T}}\|_2^2 / \sigma^2$, and
3. $\|\mathbf{P}_{\mathcal{R}} \mathbf{X}_{\mathcal{T}} \beta_{\mathcal{T}}\|_2^2 / (\beta_{\mathcal{T}}^T \Sigma_{\mathcal{T}|\mathcal{S}} \beta_{\mathcal{T}})$ follows a central χ^2 distribution with $n-s$ degrees of freedom.

By the assumption on the eigenvalues of Σ , $\Sigma_{\mathcal{T}|\mathcal{S}}$ also has its eigenvalues bounded between M_0^{-1} and M_0 . For $\|\Sigma_{\mathcal{T}|\mathcal{S}} \beta_{\mathcal{T}}\|_2 \geq C_1 t^{1/4}/\sqrt{n}$, we have $\beta_{\mathcal{T}}^T \Sigma_{\mathcal{T}|\mathcal{S}} \beta_{\mathcal{T}} \geq C_1 t^{1/2}/(M_0 n)$. Since $n-s \geq (1-c_1)n$ and $\sigma \leq M_1$, by Lemma 5, we can find some positive constant c_3 depending on (M_0, M_1, M_2, c_1) such that the following holds for sufficiently large n ,

$$P \left(\frac{1}{\sigma^2} \|\mathbf{P}_{\mathcal{R}} \mathbf{X}_{\mathcal{T}} \beta_{\mathcal{T}}\|_2^2 \geq c_3 C_1 \sqrt{t} \right) \geq \frac{1+\beta}{2}. \quad (\text{C.6})$$

For any $c > 0$, define the event

$$\begin{aligned} A(c) &= \{S_1 < n-s + \sigma^{-2} \|\mathbf{P}_{\mathcal{R}} \mathbf{X}_{\mathcal{T}} \beta_{\mathcal{T}}\|_2^2 + c\sqrt{n-s} + c\sigma^{-1} \|\mathbf{P}_{\mathcal{R}} \mathbf{X}_{\mathcal{T}} \beta_{\mathcal{T}}\|_2, \\ &\quad S_2 > t + \sigma^{-2} \|\mathbf{P}_{\mathcal{R}} \mathbf{X}_{\mathcal{T}} \beta_{\mathcal{T}}\|_2^2 - c\sqrt{t} - c\sigma^{-1} \|\mathbf{P}_{\mathcal{R}} \mathbf{X}_{\mathcal{T}} \beta_{\mathcal{T}}\|_2\}. \end{aligned}$$

By Lemma 5, there exists some constant $c_4 > 0$ such that when n is large enough, $P(A(c_4)) \geq 1 + \beta/2$. When the event $A(c_4)$ holds, we have

$$T_{\text{dense}} \geq \frac{t + \sigma^{-2} \|\mathbf{P}_{\mathcal{R}} \mathbf{X}_{\mathcal{T}} \beta_{\mathcal{T}}\|_2^2 - c_4 \sqrt{t} - c_4 \sigma^{-1} \|\mathbf{P}_{\mathcal{R}} \mathbf{X}_{\mathcal{T}} \beta_{\mathcal{T}}\|_2}{n-s + \sigma^{-2} \|\mathbf{P}_{\mathcal{R}} \mathbf{X}_{\mathcal{T}} \beta_{\mathcal{T}}\|_2^2 + c_4 \sqrt{n-s} + c_4 \sigma^{-1} \|\mathbf{P}_{\mathcal{R}} \mathbf{X}_{\mathcal{T}} \beta_{\mathcal{T}}\|_2}.$$

Define the function

$$f_n(z) = \frac{t - c_4\sqrt{t} + z - c_4\sqrt{z}}{n - s + c_4\sqrt{n-s} + z + c_4\sqrt{z}} = 1 - \frac{n - (s+t) + c_4\sqrt{n-s} + c_4\sqrt{t} + 2c_4\sqrt{z}}{n - s + c_4\sqrt{n-s} + z + c_4\sqrt{z}}.$$

Since $c_4 > 0$ and $n - (s+t) > 0$, on $[0, \infty)$, $f_n(z)$ is either increasing or initially decreasing and then increasing. Note that

$$f_n(0) = \frac{t - c_4\sqrt{t}}{n - s + c_4\sqrt{n-s}} \leq \frac{t}{n-s} + u_n,$$

and

$$f_n(c\sqrt{t}) = \frac{t + (c - c_4)\sqrt{t} - c_4c^{1/2}t^{1/4}}{n - s + c_4\sqrt{n-s} + c\sqrt{t} + c_4c^{1/2}t^{1/4}} \geq \frac{t}{n-s} + u_n$$

for sufficiently large c and n , so for some positive constant $c_5 > 0$, we have $f_n(z) \geq t/(n-s) + u_n$ for all $z > c_5\sqrt{t}$. Combining with (C.6), we can choose a positive constant C_1 such that

$$P(T_{\text{dense}} \geq \frac{t}{n-s} + u_n) \geq \beta$$

for sufficiently large n . □

C.3.3 Power analysis of sparse alternatives

Proof. Without loss of generality, we assume $\mathcal{T} = [t]$ and $\mathcal{S} = \{t+1, \dots, t+s\}$. From the construction of the copies, we have $\mathbf{P}_{\mathcal{R}}\tilde{\mathbf{X}}_{\mathcal{T}} = U\mathbf{Q}$, where $U \sim \mu(n-s, r)$ on $W(n-s, r)$. By Lemma 3, we have for any $j \in [t]$,

$$P\left(\left|\frac{\mathbf{Y}^T \mathbf{P}_{\mathcal{R}}^T \mathbf{P}_{\mathcal{R}} \tilde{\mathbf{X}}_j}{\|\mathbf{P}_{\mathcal{R}} \mathbf{Y}\| \|\mathbf{P}_{\mathcal{R}} \tilde{\mathbf{X}}_j\|}\right| \geq u\right) = P\left(\left|\frac{\mathbf{Y}^T \mathbf{P}_{\mathcal{R}}^T \mathbf{P}_{\mathcal{R}} U \mathbf{Q}_j}{\|\mathbf{P}_{\mathcal{R}} \mathbf{Y}\| \|\mathbf{Q}_j\|}\right| \geq u\right) \leq 2 \exp\left(-\frac{(n-s)u^2}{8}\right),$$

where $\tilde{\mathbf{X}}_j$ and \mathbf{Q}_j denote the j -th column of $\tilde{\mathbf{X}}_{\mathcal{T}}$ and \mathbf{Q} . Let $u = c\sqrt{\log(et)/(n-s)}$ for some constant $c > 0$, by the union of events, we have

$$P(T_{\text{sparse}}(\mathbf{Y}, \tilde{\mathbf{X}}_{\mathcal{T}}, \mathbf{X}_{\mathcal{S}}) \geq u) \leq 2t \exp\left(-\frac{c^2 \log(et)}{8}\right).$$

Therefore, there exists some constant $C_{\alpha} > 0$, such that

$$\limsup_{n \rightarrow \infty} P(T_{\text{sparse}}(\mathbf{Y}, \tilde{\mathbf{X}}_{\mathcal{T}}, \mathbf{X}_{\mathcal{S}}) \leq C_{\alpha} \sqrt{\frac{\log(et)}{n}}) \geq 1 - \alpha.$$

Suppose the j_0 -th element of $\Sigma_{\mathcal{T}|\mathcal{S}}\beta_{\mathcal{T}}$, denoted as ν_{j_0} , is larger than $c_2\sqrt{\log(et)/n}$ where $c_2 > 0$ is a constant whose value will be determined in the following derivation.

Let σ_{j_0} be the j_0 -th diagonal entry of $\Sigma_{\mathcal{T}|\mathcal{S}}$, let $\bar{\Sigma}$ be the submatrix of $\Sigma_{\mathcal{T}|\mathcal{S}}$ that excludes the j_0 -th rows and columns, let $\bar{\gamma}$ be the j_0 column of $\Sigma_{\mathcal{T}|\mathcal{S}}$ that excludes the j_0 -th entry. Then we have

$$\mathbf{P}_{\mathcal{R}}\mathbf{X}_{j_0} \sim N(0, \sigma_{j_0}\mathbf{I}_{n-s}),$$

and $\mathbf{P}_{\mathcal{R}}\mathbf{X}_{\mathcal{T}\setminus\{j_0\}} \mid \mathbf{P}_{\mathcal{R}}\mathbf{X}_{j_0} \sim N\left(\mathbf{P}_{\mathcal{R}}\mathbf{X}_{j_0}\frac{\bar{\gamma}^T}{\sigma_{j_0}^2}, \mathbf{I}_{n-s} \otimes (\bar{\Sigma} - \bar{\gamma}\bar{\gamma}^T/\sigma_{j_0})\right),$

Let $\bar{\beta}$ be the subvector of $\beta_{\mathcal{T}}$ that excludes the j_0 -th entry. Using the relationship that $\nu_{j_0} = \bar{\gamma}^T\bar{\beta} + \sigma_{j_0}\beta_{j_0}$, we can show

$$\mathbf{P}_{\mathcal{R}}\mathbf{Y} \mid \mathbf{P}_{\mathcal{R}}\mathbf{X}_{j_0} \sim N\left(\frac{\nu_{j_0}}{\sigma_{j_0}}\mathbf{P}_{\mathcal{R}}\mathbf{X}_{j_0}, \bar{\sigma}^2\mathbf{I}_{n-s}\right),$$

where $\bar{\sigma}^2 = (\sigma^2 + \beta^T\Sigma_{\mathcal{T}|\mathcal{S}}\beta - \nu_{j_0}^2)$. By assumption that $\|\beta\|_2^2$ is bounded and $\Sigma_{\mathcal{T}|\mathcal{S}}$ has bounded eigenvalues, $\bar{\sigma}^2$ is also bounded.

Furthermore, since $\|\Sigma\| \leq M_0$, the marginal distribution of $\|\mathbf{P}_{\mathcal{R}}\mathbf{Y}\|$ is scaled χ^2 with a bounded scale. Therefore, we can find some positive constant c_3 depending on (M_0, M_1, M_2, β) such that the following holds for sufficiently large n :

$$P\left(\|\mathbf{P}_{\mathcal{R}}\mathbf{X}_{j_0}\|_2^2 \in \left(\frac{\sigma_{j_0}}{2}(n-s), 2\sigma_{j_0}(n-s)\right), \|\mathbf{P}_{\mathcal{R}}\mathbf{Y}\|_2^2 \leq c_3(n-s)\right) \geq \frac{1+\beta}{2}. \quad (\text{C.7})$$

Furthermore, $\mathbf{Y}^T\mathbf{P}_{\mathcal{R}}^T\mathbf{P}_{\mathcal{R}}\mathbf{X}_{j_0} \stackrel{d}{=} \frac{\nu_{j_0}}{\sigma_{j_0}}\|\mathbf{P}_{\mathcal{R}}\mathbf{X}_{j_0}\|^2 + \bar{\sigma}\|\mathbf{P}_{\mathcal{R}}\mathbf{X}_{j_0}\|Z$, where Z is an independent standard normal r.v. We obtain

$$\begin{aligned} & P\left(\mathbf{Y}^T\mathbf{P}_{\mathcal{R}}^T\mathbf{P}_{\mathcal{R}}\mathbf{X}_{j_0} \leq \frac{\nu_{j_0}}{2\sigma_{j_0}}\|\mathbf{P}_{\mathcal{R}}\mathbf{X}_{j_0}\|^2\right) \\ &= P\left(\frac{\nu_{j_0}}{2\sigma_{j_0}}\|\mathbf{P}_{\mathcal{R}}\mathbf{X}_{j_0}\| + \bar{\sigma}Z < 0\right) \\ &\leq \mathbb{E}\exp\left(-\frac{\nu_{j_0}^2}{8\sigma_{j_0}^2\bar{\sigma}^2}\|\mathbf{P}_{\mathcal{R}}\mathbf{X}_{j_0}\|^2\right) \\ &= \mathbb{E}\exp\left(-\frac{\nu_{j_0}^2}{8\bar{\sigma}^2}\xi_{n-s}\right) \\ &= \left(1 + \frac{\nu_{j_0}^2}{4\bar{\sigma}^2}\right)^{-(n-s)/2} \\ &\leq \left(1 + \frac{c_2^2\log(et)/n}{4\bar{\sigma}^2}\right)^{-(1-c_1)n/2} \\ &\leq \left(1 + \frac{c_2^2(1-c_1)\log(et)}{8\bar{\sigma}^2}\right)^{-1}, \end{aligned} \quad (\text{C.8})$$

where ξ_{n-s} denotes a χ_{n-s}^2 r.v. and the second last inequality is due to $s < c_1n$ and $\nu_{j_0} \geq c_2\sqrt{\log(et)/n}$. Therefore, we can pick a constant c_2 depending on $(c_1, M_0, M_1, M_2, C_\alpha, c_3)$ so

that $c_2 \geq C_\alpha \sqrt{2\sigma_{j_0} c_3}$ and the right hand side of (C.8) is smaller than $(1 - \beta)/2$. We then have

$$P \left(\mathbf{Y}^T \mathbf{P}_{\mathcal{R}}^T \mathbf{P}_{\mathcal{R}} \mathbf{X}_{j_0} \geq \frac{\nu_{j_0}}{2\sigma_{j_0}} \|\mathbf{P}_{\mathcal{R}} \mathbf{X}_{j_0}\|^2 \right) \geq \frac{1 + \beta}{2}.$$

Combining the last inequality with (C.7), we have

$$P \left(\left| \frac{\mathbf{Y}^T \mathbf{P}_{\mathcal{R}}^T \mathbf{P}_{\mathcal{R}} \mathbf{X}_{j_0}}{\|\mathbf{P}_{\mathcal{R}} \mathbf{Y}\| \|\mathbf{P}_{\mathcal{R}} \mathbf{X}_{j_0}\|} \right| \geq C_\alpha \sqrt{\frac{\log(et)}{n}} \right) \geq \beta.$$

□

C.4 Proof of Theorem 2

When $t = 1$, (Bradic et al., 2022, Theorem 3) establishes that the parametric rate $1/\sqrt{n}$ is a fundamental boundary for inference. This implies that when t is bounded, Theorem 2 holds. To complete the proof, we focus on the case where t diverges along with n .

Following a similar approach to that of Cai and Guo (2017); Bradic et al. (2022), the proof of Theorem 2 can be summarized as follows: Fix some interior point $\theta_* = (\mathbf{0}, \beta_{\mathcal{S}}^*, \mathbf{I}_d, \sigma_*)$ satisfying $\sigma_* > \kappa$ and $\|\beta_{\mathcal{S}}^*\|_2^2 \leq \xi M_2$ for some constants $\kappa \in (0, \sigma_*)$ and $\xi \in (0, 1)$. We need to construct a large collection of points in the alternative space, each of which has a corresponding population that is close to the population of θ_* in terms of some statistical distance for sufficiently large t .

C.4.1 Auxiliary Results

The auxiliary results presented here have mostly been established in Cai and Guo (2017); Bradic et al. (2022). However, for the sake of completeness, we provide detailed proofs for each of them.

Lemma 6. *For any test ψ_* and point $\theta_*, \theta_1, \dots, \theta_N$, we have*

$$\left| N^{-1} \sum_{j=1}^N \mathbb{E}_{\theta_j} \psi_* - \mathbb{E}_{\theta_*} \psi_* \right| \leq \left[\mathbb{E}_{\theta_*} \left(N^{-1} \sum_{j=1}^N \frac{d\mathbb{P}_{\theta_j}}{d\mathbb{P}_{\theta_*}} - 1 \right)^2 \right]^{1/2}$$

Proof.

$$\begin{aligned} \left| N^{-1} \sum_{j=1}^N \mathbb{E}_{\theta_j} \psi_* - \mathbb{E}_{\theta_*} \psi_* \right| &= \left| N^{-1} \sum_{j=1}^N \left(\mathbb{E}_{\theta_*} \psi_* \frac{d\mathbb{P}_{\theta_j}}{d\mathbb{P}_{\theta_*}} - \mathbb{E}_{\theta_*} \psi_* \right) \right| = \mathbb{E}_{\theta_*} \psi_* \left| N^{-1} \sum_{j=1}^N \frac{d\mathbb{P}_{\theta_j}}{d\mathbb{P}_{\theta_*}} - 1 \right| \\ &\stackrel{(i)}{\leq} \mathbb{E}_{\theta_*} \left| N^{-1} \sum_{j=1}^N \frac{d\mathbb{P}_{\theta_j}}{d\mathbb{P}_{\theta_*}} - 1 \right| \stackrel{(ii)}{\leq} \left[\mathbb{E}_{\theta_*} \left(N^{-1} \sum_{j=1}^N \frac{d\mathbb{P}_{\theta_j}}{d\mathbb{P}_{\theta_*}} - 1 \right)^2 \right]^{1/2}, \end{aligned}$$

where (i) holds by $|\psi_*| \leq 1$ almost surely and (ii) holds by Lyapunov's inequality. □

For any integer k , let $\mathcal{M}_{k,t}$ be the set of all k -sparse vectors in $\{0, 1\}^t$, and express it as

$$\mathcal{M}_{k,t} = \{\delta \in \{0, 1\}^t : \|\delta\|_0 = k\} = \left\{ \delta_{k,t}^{(1)}, \dots, \delta_{k,t}^{(N_{k,t})} \right\}, \quad (\text{C.9})$$

where $N_{k,t} = \binom{t}{k}$ is denote the cardinality of $\mathcal{M}_{k,t}$.

Lemma 7. Consider $\theta_* = (\mathbf{0}, \beta_S^*, \mathbf{I}_d, \sigma_*)$ and a fixed sequence of $\{\delta_j \in \mathbb{R}^t\}_{j=1}^N$ satisfying that $\|\delta_j\| = r$ for some $r > 0$. Define alternative points θ_j as

$$\theta_j = \left(\rho \delta_j, \beta_S^*, \mathbf{I}_d, \sqrt{\sigma_*^2 - \rho^2 r^2} \right)$$

for some $\rho \in (0, \sigma_*/r)$. Then we have

$$\mathbb{E}_{\theta_*} \left(N^{-1} \sum_{j=1}^N \frac{d\mathbb{P}_{\theta_j}}{d\mathbb{P}_{\theta_*}} - 1 \right)^2 = N^{-2} \sum_{j_1=1}^N \sum_{j_2=1}^N \left[1 - \frac{\rho^2}{\sigma_*^2} \delta_{j_1}^T \delta_{j_2} \right]^{-n} - 1.$$

Specially, for some integer $1 \leq k \leq t$ such that $0 < k\rho^2/\sigma_*^2 \leq 1/2$, if $N = N_{k,t}$ and $\delta_j = \delta_{k,t}^{(j)}, j = 1, \dots, N$ as defined in (C.9), then we have

$$\mathbb{E}_{\theta_*} \left(N^{-1} \sum_{j=1}^N \frac{d\mathbb{P}_{\theta_j}}{d\mathbb{P}_{\theta_*}} - 1 \right)^2 \leq e^{\frac{k^2}{t-k}} \left(1 - \frac{k}{t} + \frac{k}{t} \exp \left(\frac{2n\rho^2}{\sigma_*^2} \right) \right)^k - 1.$$

Proof. Let $\tilde{\Sigma}$ and $\tilde{\Sigma}_j, j = 1, \dots, N$, denote the covariance matrices of $(Y, X_{\mathcal{T}}, Z_S)$ corresponding to the parameters θ_* and θ_j , respectively. These matrices are computed as follows:

$$\tilde{\Sigma} = \begin{pmatrix} \|\beta_S^*\|^2 + \sigma_*^2 & \mathbf{0}_{1 \times t} & (\beta_S^*)^T \\ \mathbf{0}_{t \times 1} & \mathbf{I}_{t \times t} & \mathbf{0}_{t \times s} \\ \beta_S^* & \mathbf{0}_{s \times t} & \mathbf{I}_{s \times s} \end{pmatrix}, \quad \tilde{\Sigma}_j = \begin{pmatrix} \|\beta_S^*\|^2 + \sigma_*^2 & \rho \delta_j^T & (\beta_S^*)^T \\ \rho \delta_j & \mathbf{I}_{t \times t} & \mathbf{0}_{t \times s} \\ \beta_S^* & \mathbf{0}_{s \times t} & \mathbf{I}_{s \times s} \end{pmatrix}.$$

By Lemma 11 in Cai and Guo (2017), we have

$$\mathbb{E}_{\theta_*} \left(\frac{d\mathbb{P}_{\theta_{j_1}}}{d\mathbb{P}_{\theta_*}} \times \frac{d\mathbb{P}_{\theta_{j_2}}}{d\mathbb{P}_{\theta_*}} \right) = \left(\det \left(\mathbf{I} - \tilde{\Sigma}^{-1} \left(\tilde{\Sigma}_{j_1} - \tilde{\Sigma} \right) \tilde{\Sigma}^{-1} \left(\tilde{\Sigma}_{j_2} - \tilde{\Sigma} \right) \right) \right)^{-n/2}. \quad (\text{C.10})$$

Note that

$$\tilde{\Sigma}^{-1} = \begin{pmatrix} \frac{1}{\sigma_*^2} & \mathbf{0}_{1 \times t} & -\frac{1}{\sigma_*^2} (\beta_S^*)^T \\ \mathbf{0}_{t \times 1} & \mathbf{I}_{t \times t} & \mathbf{0}_{t \times s} \\ -\frac{1}{\sigma_*^2} \beta_S^* & \mathbf{0}_{s \times t} & \mathbf{I}_{s \times s} + \frac{1}{\sigma_*^2} \beta_S^* (\beta_S^*)^T \end{pmatrix}$$

and

$$\tilde{\Sigma}^{-1} \left(\tilde{\Sigma}_j - \tilde{\Sigma} \right) = \begin{pmatrix} 0 & \frac{\rho}{\sigma_*^2} \delta_j^T & \mathbf{0}_{1 \times s} \\ \rho \delta_j & \mathbf{0}_{t \times t} & \mathbf{0}_{t \times s} \\ \mathbf{0}_{s \times 1} & -\frac{\rho}{\sigma_*^2} \beta_S^* \delta_j^T & \mathbf{0}_{s \times s} \end{pmatrix}.$$

Hence, we have

$$\tilde{\Sigma}^{-1} \left(\tilde{\Sigma}_{j_1} - \tilde{\Sigma} \right) \tilde{\Sigma}^{-1} \left(\tilde{\Sigma}_{j_2} - \tilde{\Sigma} \right) = \begin{pmatrix} \frac{\rho^2}{\sigma_*^2} \delta_{j_1}^T \delta_{j_2} & \mathbf{0}_{1 \times t} & \mathbf{0}_{1 \times s} \\ \mathbf{0}_{t \times 1} & \frac{\rho^2}{\sigma_*^2} \delta_{j_1} \delta_{j_2}^T & \mathbf{0}_{t \times s} \\ -\frac{\rho^2}{\sigma_*^2} \beta_S^* \delta_{j_1}^T \delta_{j_2} & \mathbf{0}_{s \times t} & \mathbf{0}_{s \times s} \end{pmatrix}.$$

Since the matrix $\tilde{\Sigma}^{-1} \left(\tilde{\Sigma}_{j_1} - \tilde{\Sigma} \right) \tilde{\Sigma}^{-1} \left(\tilde{\Sigma}_{j_2} - \tilde{\Sigma} \right)$ is of two equal eigenvalues $\frac{\rho^2}{\sigma_*^2} \delta_{j_1}^T \delta_{j_2}$, it follows from (C.10) that

$$\mathbb{E}_{\theta_*} \left(\frac{d \mathbb{P}_{\theta_{j_1}}}{d \mathbb{P}_{\theta_*}} \times \frac{d \mathbb{P}_{\theta_{j_2}}}{d \mathbb{P}_{\theta_*}} \right) = \left(1 - \frac{\rho^2}{\sigma_*^2} \delta_{j_1}^T \delta_{j_2} \right)^{-n}.$$

Therefore,

$$\begin{aligned} \mathbb{E}_{\theta_*} \left(N^{-1} \sum_{j=1}^N \frac{d \mathbb{P}_{\theta_j}}{d \mathbb{P}_{\theta_*}} - 1 \right)^2 &= N^{-2} \sum_{j_1=1}^N \sum_{j_2=1}^N \mathbb{E}_{\theta_*} \left(\frac{d \mathbb{P}_{\theta_{j_1}}}{d \mathbb{P}_{\theta_*}} \times \frac{d \mathbb{P}_{\theta_{j_2}}}{d \mathbb{P}_{\theta_*}} \right) - 1 \\ &= N^{-2} \sum_{j_1=1}^N \sum_{j_2=1}^N \left[1 - \frac{\rho^2}{\sigma_*^2} \delta_{j_1}^T \delta_{j_2} \right]^{-n} - 1. \end{aligned}$$

This proved the first part of the lemma.

Now consider the special case where $N = N_{k,t}$ and $\delta_j = \delta_{k,t}^{(j)}$ for $j = 1, \dots, N_{k,t}$ as defined in (C.9). For any fixed j_1 , if j_2 is uniformly sampled from $\{1, 2, \dots, N_{k,t}\}$, then $\delta_{j_1}^T \delta_{j_2} \stackrel{d}{=} J$, where J follows a Hypergeometric (t, k, k) distribution. Note that $1/(1-x) \leq \exp(2x)$ for $x \in [0, 1/2]$ and $\frac{\rho^2}{\sigma_*^2} \delta_{j_1}^T \delta_{j_2} \leq k\rho^2/\sigma_*^2 \leq 1/2$, then

$$\begin{aligned} \mathbb{E}_{\theta_*} \left(N^{-1} \sum_{j=1}^N \frac{d \mathbb{P}_{\theta_j}}{d \mathbb{P}_{\theta_*}} - 1 \right)^2 &= N^{-2} \sum_{j_1=1}^N \sum_{j_2=1}^N \left[1 - \frac{\rho^2}{\sigma_*^2} \delta_{(j_1)}^T \delta_{(j_2)} \right]^{-n} - 1 \\ &\leq \mathbb{E} \exp \left(\frac{2n\rho^2}{\sigma_*^2} J \right) - 1 \\ &\stackrel{(*)}{\leq} e^{\frac{k^2}{t-k}} \left(1 - \frac{k}{t} + \frac{k}{t} \exp \left(\frac{2n\rho^2}{\sigma_*^2} \right) \right)^k - 1, \end{aligned}$$

where inequality $(*)$ holds following Lemma 3 in Cai and Guo (2017). □

C.4.2 Proof of Theorem 2

Proof. The proof can be divided into two parts:

ℓ_2 norm with dense alternatives: Let constant $r \in (0, 1)$ with $r/(1 - \sqrt{r}) \leq \ln(1 + (\beta - \alpha)^2)/2$ and $k = \lceil \sqrt{rt} \rceil$. For $\theta_* = (\mathbf{0}, \beta_S^*, \mathbf{I}_d, \sigma_*) \in \Theta_0$, satisfying $\sigma_* > \kappa$, $\|\beta_S^*\|_2^2 \leq \xi M_2$ for some constants $\kappa \in (0, \sigma_*)$ and $\xi \in (0, 1)$. Recall the definition of $\mathcal{M}_{k,t}$ in (C.9) and define alternative points $\theta_j = (\beta_{\mathcal{T}}^{(j)}, \beta_S^*, \mathbf{I}_d, \sigma_1)$, $j \in \{1, \dots, N_{k,t}\}$ with

$$\beta_{\mathcal{T}}^{(j)} = \rho_1 \delta_{k,t}^{(j)} / \sqrt{n}, \quad \text{and} \quad \sigma_1 = \sqrt{\sigma_*^2 - k\rho_1^2/n},$$

where

$$\rho_1 = \frac{1}{C_1^{1/4}} \min \left\{ \kappa, \sqrt{(1 - \xi)M_2}, \min \left\{ 1, C_1^{1/4} \right\} \sigma_* \sqrt{\frac{\log 2}{2}} \right\}.$$

Recall that $t \leq C_1 n^2$. We have

$$\|\beta_S^*\|^2 + \|\beta_{\mathcal{T}}^{(j)}\|^2 \leq \xi M_2 + \frac{(1 - \xi)M_2}{\sqrt{C_1}} \frac{\sqrt{t}}{n} \leq M_2, \quad \sigma_*^2 \geq \kappa^2 \geq k\rho_1^2/n, \quad \|\beta_{\mathcal{T}}^{(j)}\|_2 = \rho_1 \frac{\sqrt{k}}{\sqrt{n}} \geq c \frac{t^{1/4}}{\sqrt{n}}$$

for some constant $c > 0$. Therefore, we have verified that $\theta_j \in \Theta_{\text{dense}}(c \frac{t^{1/4}}{\sqrt{n}})$.

By Lemma 6, we only need to show that:

$$\limsup_{n \rightarrow \infty} \mathbb{E}_{\theta_*} \left(N^{-1} \sum_{j=1}^N \frac{d\mathbb{P}_{\theta_j}}{d\mathbb{P}_{\theta_*}} - 1 \right)^2 \leq (\beta - \alpha)^2 \quad (\text{C.11})$$

Note that $\frac{k\rho_1^2}{n\sigma_*^2} \leq \frac{\sqrt{t}\rho_1^2}{n\sigma_*^2} \leq \frac{1}{2}$, following Lemma 7, we have

$$\mathbb{E}_{\theta_*} \left(N^{-1} \sum_{j=1}^N \frac{d\mathbb{P}_{\theta_j}}{d\mathbb{P}_{\theta_*}} - 1 \right)^2 \leq e^{\frac{k^2}{t-k}} \left(1 - \frac{k}{t} + \frac{k}{t} \exp \left(\frac{2\rho_1^2}{\sigma_*^2} \right) \right)^k - 1, \quad$$

where

$$e^{\frac{k^2}{t-k}} \leq e^{\frac{rt}{t - \lceil \sqrt{rt} \rceil}} \leq e^{r/(1 - \sqrt{r})} \leq \sqrt{1 + (\beta - \alpha)^2}$$

and

$$\begin{aligned} \left(1 - \frac{k}{t} + \frac{k}{t} \exp \left(\frac{2n\rho^2}{\sigma_*^2} \right) \right)^k &\stackrel{(i)}{\leq} \exp \left\{ \frac{k^2}{t} \left[\exp \left(\frac{2\rho_1^2}{\sigma_*^2} \right) - 1 \right] \right\}, \\ &\leq e^r \leq \sqrt{1 + (\beta - \alpha)^2} \end{aligned}$$

where (i) holds since $(1 + a)^{1/a} \leq e$, $\forall a > 0$ and the second inequality is due to the definition of ρ_1 . Therefore, we have proved (C.11).

ℓ_∞ norm with sparse alternatives: For $\theta_* = (\mathbf{0}, \beta_S^*, \mathbf{I}_d, \sigma_*) \in \Theta_0$, satisfying $\sigma_* > \kappa$, $\|\beta_S^*\|_2^2 \leq \xi M_2$ for some constants $\kappa \in (0, \sigma_*)$ and $\xi \in (0, 1)$. Recall the definition of $\mathcal{M}_{1,t}$ in (C.9) and define alternative points $\theta_j = (\beta_{\mathcal{T}}^{(j)}, \beta_S^*, \mathbf{I}_d, \sigma_1)$, $j = 1, \dots, N_{1,t}$ with

$$\beta_{\mathcal{T}}^{(j)} = \delta_{1,t}^{(j)} \rho_2 \sqrt{\log t/n}, \quad \sigma_1 = \sqrt{\sigma_*^2 - \rho_2^2 \log t/n},$$

$$\text{where } \rho_2 = \frac{1}{\sqrt{C_2}} \min \left\{ \kappa, \sqrt{(1 - \xi)M_2}, \sigma_* \sqrt{\frac{\log 2}{2}}, \sqrt{\frac{C_2}{2}} \sigma_* \ln(1 + (\beta - \alpha)^2) \right\}.$$

Recall that $\log t \leq C_2 n$. By definition of ρ_2 , we have

$$\|\beta_S^*\|^2 + \|\beta_{\mathcal{T}}^{(j)}\|^2 \leq \xi M_2 + \frac{(1-\xi)M_2 \log t}{C_2 n} \leq M_2, \quad \sigma_*^2 \geq \kappa^2 \geq \rho_2^2 \frac{\log t}{n}, \quad \|\beta_{\mathcal{T}}^{(j)}\|_\infty = \rho_2 \sqrt{\frac{\log t}{n}}.$$

we have $\theta_j \in \Theta_{\text{sparse}}(c \frac{1}{\sqrt{n}})$ for some constant $c > 0$.

By Lemma 6, we only need to show that:

$$\limsup_{n \rightarrow \infty} \mathbb{E}_{\theta_*} \left(N^{-1} \sum_{j=1}^N \frac{d\mathbb{P}_{\theta_j}}{d\mathbb{P}_{\theta_*}} - 1 \right)^2 \leq (\beta - \alpha)^2.$$

Note that $\frac{\rho_2^2 \log t}{\sigma_*^2} \leq \frac{\log 2}{2}$, following Lemma 7 with $k = 1$, we have

$$\begin{aligned} \mathbb{E}_{\theta_*} \left(N^{-1} \sum_{j=1}^N \frac{d\mathbb{P}_{\theta_j}}{d\mathbb{P}_{\theta_*}} - 1 \right)^2 &\leq e^{\frac{1}{t-1}} \left(1 - \frac{1}{t} + \frac{1}{t} \exp \left(\frac{2\rho_2^2 \log t}{\sigma_*^2} \right) \right) - 1 \\ &= e^{\frac{1}{t-1}} \left(1 + \exp \left[\left(\frac{2\rho_2^2}{\sigma_*^2} - 1 \right) \log t \right] - \frac{1}{t} \right) - 1. \end{aligned}$$

Therefore, we have

$$\mathbb{E}_{\theta_*} \left(N^{-1} \sum_{j=1}^N \frac{d\mathbb{P}_{\theta_j}}{d\mathbb{P}_{\theta_*}} - 1 \right)^2 \leq e^{\frac{1}{t-1}} \left(1 - \frac{1}{t} \right) - 1 \leq (\beta - \alpha)^2$$

for sufficiently large t . □

D Details of Simulation Studies

In this section, we provide details for the simulation studies in Section 6 in the main text. For completeness and clarity, figures are reproduced to allow detailed discussion without cross-referencing. Throughout this section, we fix the procedure parameters $M = 100$ and $L = 3$ for conducting Algorithm 2.

We evaluate the power of the G -CRT for GGMs with the statistic functions discussed in Section 2.4 for testing multivariate conditional independence. We consider a range of regression models for $\mathcal{L}(Y | X)$, including linear regression, nonlinear regression, logistic regression, and nonlinear binary regression. For each regression model, we consider a low-dimension setting ($p = 20$ and $n = 50$) and a high-dimension setting ($p = 120$ and $n = 80$), and we compare our tests with several existing testing methods.

In each experiment, we randomly permute the nodes of a band graph (along with the coordinates of its precision matrix) with precision matrix $\mathbf{\Omega}$ satisfies that for $i, j \in \{1, \dots, p\}$:

$$\omega_{i,j} = \begin{cases} 1 & \text{if } i = j, \\ s & \text{if } 1 \leq |i - j| \leq K, \\ 0 & \text{if } |i - j| > K, \end{cases}$$

where $K = 6$ is the bandwidth and $s = 0.2$ is the signal magnitude.

Without loss of generality, we assume $\mathbf{\Omega}$ has been standardized so that the diagonal elements of $\mathbf{\Omega}^{-1}$ all equal to 1. The covariate vectors are i.i.d. samples drawn from $\mathbf{N}_p(\mathbf{0}, \mathbf{\Omega}^{-1})$. The response variable Y , depending on the simulation setting, will be generated under linear or non-linear models, where a constant factor θ is used to control the magnitude of the dependence of Y on X .

We consider testing the null hypothesis $H_0 : Y \perp\!\!\!\perp X_{\mathcal{T}} \mid X_{-\mathcal{T}}$ for $\mathcal{T} = \{1, 2, \dots, 8\}$. Note that choosing \mathcal{T} to consist of the first 8 indices is not particular to the band graph structure because the nodes of G have been permuted. Our G -CRT procedure will make use of the graph G but will know neither $\mathbf{\Omega}$ nor the mean parameters. For any testing procedure that computes a p-value for individual hypothesis $H_{0,i} : Y \perp\!\!\!\perp X_i \mid X_{-i}$, we adapt the Bonferroni correction to obtain a valid p-value. We repeat each experiment at least 400 times and estimate the power of a method by calculating the fraction of times that it rejects the null hypothesis at the significance level $\alpha = 0.05$. In each figure of this subsection, each error bar corresponds to one standard error.

D.1 Gaussian linear regression

In the first experiment, the response variable Y given the covariates $X \in \mathbb{R}^p$ is generated under a Gaussian linear model such that $Y = X^\top \beta + \varepsilon$ with some independent noise $\varepsilon \sim \mathbf{N}(0, 1)$. The regression coefficient β is determined randomly at the beginning of each replication, whose first 20 coefficients are independently drawn from a uniform distribution on the interval $(1/\sqrt{20}, 2/\sqrt{20})$ and all remaining coefficients are set to zero. The first 8 coordinates of β corresponding to $X_{\mathcal{T}}$ (recall that $\mathcal{T} = \{1, 2, \dots, 8\}$) are then scaled by a factor θ , which controls the signal strength for the conditional independence testing problem.

For a Gaussian linear model, the testing problem is equivalent to testing

$$H_0 : \beta_{\mathcal{T}} = 0 \quad \text{versus} \quad H_1 : \beta_{\mathcal{T}} \neq 0. \quad (\text{D.1})$$

It is known that if $p < n$ and $|\mathcal{T}| > 1$, a uniformly most powerful unbiased test does not exist yet the F-test is a uniformly most power invariant (UMPI) test under a certain group of transformation; see Shao (2003, Chapter 6.3.2). Therefore, we will use F-test as a baseline for comparison in our low-dimensional experiments.

In a high-dimensional setting, Verzelen and Villers (2010) consider the same hypothesis as in (D.1) with Gaussian random designs, but their procedure is feasible only if the size of \mathcal{T}^c (i.e., $p - |\mathcal{T}|$) is smaller than n , which is not satisfied in our high-dimensional simulations. To choose a baseline method for comparison in high-dimensional settings, we consider the debiasing Lasso or de-sparsifying Lasso technique, which is developed for constructing confidence intervals for low-dimensional projections of β (Zhang and Zhang, 2014; van de Geer et al., 2014; Javanmard and Montanari, 2014b). Although this technique can be used to construct hypothesis tests (Bühlmann, 2013), the asymptotic validity requires a sparsity condition that the number of the true nonzero coefficients is of order $o(\sqrt{n})$, which is not met in our simulation settings. Therefore, in our high dimensional experiments, only methods based on the CRT are theoretically guaranteed to control the Type I error.

Figure 6a presents the power curves for several testing methods in the low-dimensional experiment with $p = 20$ and $n = 50$, where power is plotted against varying values of θ . We

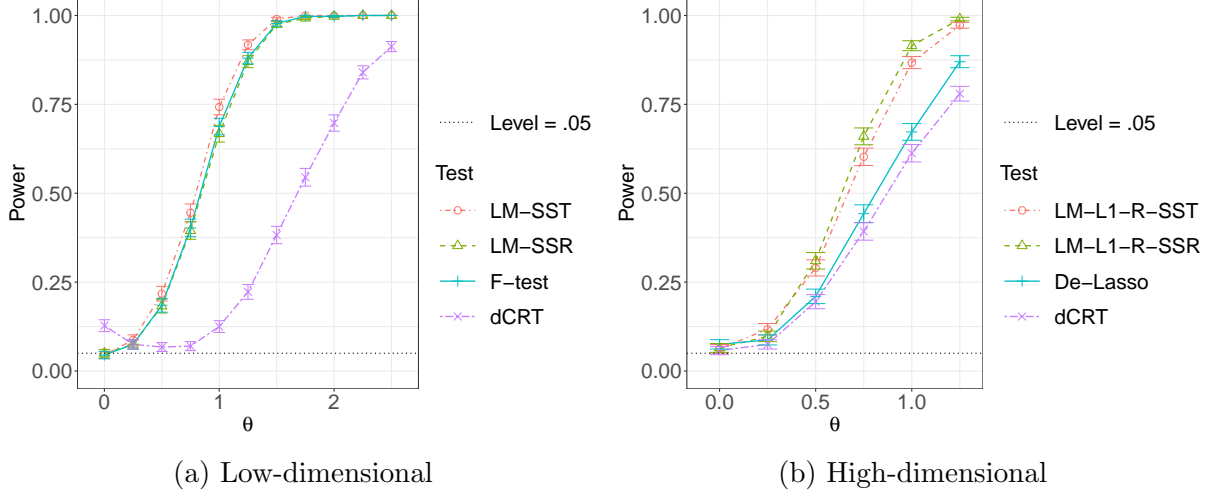


Figure 6: Power comparison for testing conditional independence in linear regression.

examine our G -CRT procedure with the statistics LM-SST and LM-SSR by comparison to the classical F-test for testing (D.1) and the Bonferroni-adjusted dCRT using Gaussian Lasso models. The dCRT is implemented using the first author’s source code with a properly chosen model and other default arguments. We note that while our G -CRTs and F-test control the Type I error at the nominal level, the dCRT does not, as its estimated power significantly exceeds the nominal level $\alpha = 0.05$. This exceedance is likely due to the error of estimating $\mathcal{L}(X_i | X_{-i})$ by the default procedure of dCRT. The dCRT also suffers from a loss of power relative to the other methods. In addition, the G -CRTs with LM-SSR and LM-SST perform comparably and achieve high power on par with the F-test. As θ increases, the power of both G -CRTs converges to 1, demonstrating superior performance.

Figure 6b presents the power curves in the high-dimensional experiment with $p = 120$ and $n = 80$. We consider the test statistics L1-R-SST and L1-R-SSR for the G -CRT. In addition to the dCRT, we also consider the Bonferroni-adjusted de-sparsified Lasso (van de Geer et al., 2014), labelled as De-Lasso, which can be implemented using the function `lasso.proj()` in the R package `hdi`. Figure 6b shows that all methods control the Type I error at the nominal level, and their power increases as θ grows. Our G -CRT with both statistic functions can achieve nearly power 1 when $\theta = 1.25$, but L1-R-SSR seems to gain a slight edge. The superior power of our approach over the other two Bonferroni-adjusted tests demonstrates the effectiveness of G -CRT in capturing the joint signal for testing conditional independence in high dimensions.

D.2 Nonlinear regression

In this subsection, we consider a non-linear dependence between the response and the covariates. Specifically, we perform a basis expansion of X incorporating non-linear transformations (such as squares, reciprocals, trigonometric functions, and interactions) and Y is generated as a linear combination of these basis functions with added standard Gaussian

noise. Specifically, the expanded basis $\mathbf{B}(\mathbf{x})$ for a given $\mathbf{x} = (x_1, \dots, x_p)$ is defined as

$$\mathbf{B}(\mathbf{x}) = \left[\underbrace{\frac{x_1^2}{2}, \frac{1}{1+x_2^2}, \cos(\pi x_3), \sin(\pi x_4), x_5 x_6, \sin(x_7 x_8), \frac{\sin(\pi x_9)}{4+x_{10}^2}}_{\text{I: 7 terms of nonlinear functions}}, \underbrace{\frac{x_{11}^2}{2}, \dots, \frac{\sin(\pi x_{19})}{4+x_{20}^2}}_{\text{II: 7 terms in the same form as I}} \right]. \quad (\text{D.2})$$

Let β be a coefficient vector of dimension 20 so that its first 7 entries (corresponding to the functions involving x_1, \dots, x_{10}) are all equal to θ and its next 7 entries (corresponding to the functions involving x_{11}, \dots, x_{20}) are all equal to 1. The signal strength of $X_{\mathcal{T}}$ will be controlled by the factor θ . Then the response is defined as

$$Y = \mathbf{B}(X)\beta + \varepsilon \quad (\text{D.3})$$

with some independent noise $\varepsilon \sim \mathbf{N}(0, 1)$. For this nonlinear regression model, the tests based on Gaussian linear models in Section D.1 may not be powerful any more because the linear dependence between the response and the covariates can be very weak if not void. To capture the nonlinear dependence, we consider the G -CRT with the statistic RF and its two-step variants, RF-D and RF-RR. For comparison, we consider the same baseline tests as in Section D.1 but change the models in the dCRT to random forests.

Figures 7a and 7b represent the results in low-dimensional and high-dimensional settings, respectively. In both settings, our G -CRT with either of the two-step statistics (RF-D and RF-RR) exhibits superior performance. The advantages of these statistics against the direct RF statistic are significant in the high-dimensional setting, which demonstrates the potential of the distillation strategy in boosting power.

Besides, the F-test, which is UMPI in low-dimensional Gaussian linear regression, has slight Type I error inflation, and it does not have competitive power. Furthermore, the Bonferroni-adjusted methods, including the dCRT using random forests and the de-sparsified Lasso, fail to reach the same power as the G -CRTs. These comparisons highlight the need for incorporating flexible machine learning methods to detect joint signals in conditional independence testing problems.

D.3 Logistic regression

We employ the same generation of random regression coefficients β as in Section D.1, but the response is sampled from the Bernoulli distribution with probability $\sigma(X^\top \beta)$, where $\sigma(t) = e^t / (1 + e^t)$ is the sigmoid function (i.e. the inverse of the logit function).

In the low-dimensional setting with $p = 20$ and $n = 50$, we evaluate the power of our G -CRT with the statistics GLM-Dev and RF. For comparison, we also consider the Bonferroni-adjusted dCRT using logistic Lasso models and the classical Chi-squared test based on the deviance of nested models (see McCullagh and Nelder (1989, Chapter 4.3.4) and Hastie and Pregibon (2017) for more details).

Figure 8a presents the power curves of these tests for the low-dimensional logistic regression experiment. The Chi-squared test fails to control the Type I error at the nominal level in this experiment, which is because its asymptotic validity does not hold with the limited sample size n . Therefore, we should omit the Chi-squared test in the power comparison. The

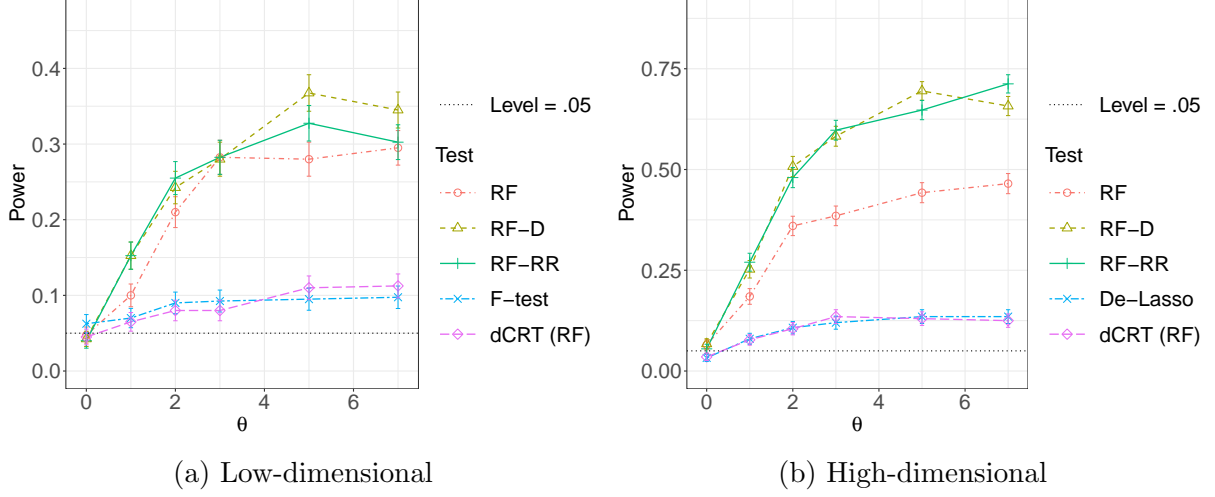


Figure 7: Power comparison for testing conditional independence in nonlinear regression

other three tests control the Type I error at the nominal level and have power increasing as θ increases. Both the dCRT and the G -CRT with the RF statistics have low power when $\theta = 1$, but as θ increases, the power of the dCRT increases faster. This suggests that using the sum of importance scores from random forests may be inefficient in detecting signals in logistic regression. Notably, our G -CRT with the GLM-Dev statistic consistently achieves the highest power among the three tests.

In the high-dimensional setting with $p = 120$ and $n = 80$, we evaluate the G -CRT using two additional statistics besides RF: GLM-L1-D and GLM-L1-R-SST. For comparison, we also consider a bias-correction method for high-dimensional logistic Lasso regression proposed by Cai et al. (2023), which can be implemented using the **LF()** function in the R package **SIHR**. The Bonferroni-adjusted test based on the asymptotic normality of this bias-corrected estimator will be referred to as the CGM test.

Figure 8b shows the power curves for the high-dimensional logistic regression experiment. All considered tests control the Type I error at the nominal level and their power increases as θ increases. It seems that the CGM test is too conservative and powerless for $\theta \in (0, 1)$. The comparison between the dCRT and the G -CRT with the statistic RF is similar to that in the low-dimensional setting. The two G -CRTs with statistic functions GLM-L1-D and GLM-L1-R-SST perform the best, yet GLM-L1-R-SST seems to be the most powerful. This is surprising because the second step of the computation of GLM-L1-R-SST does not make use of the original response or the likelihood function of the logistic regression. This observation highlights the potential to boost power when using a flexible test statistic function in a CRT method.

D.4 Nonlinear binary regression

In this subsection, we consider a binary response variable that depends on the covariates through a nonlinear link function. Specifically, we transform the first 20 coordinates of any

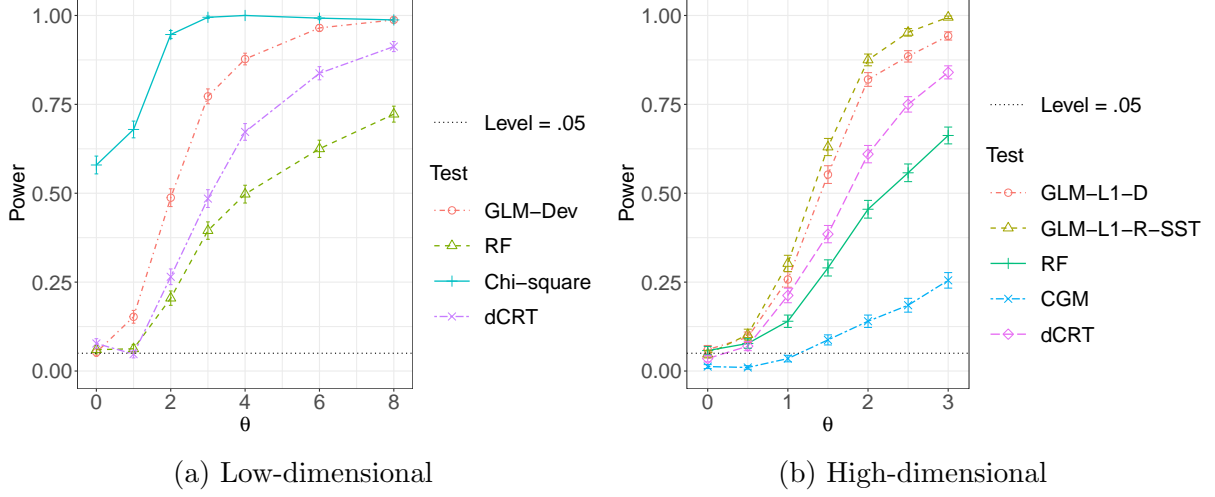


Figure 8: Power comparison for testing conditional independence in logistic regression.

covariate vector X component-wise through a step function

$$\mathbf{b}(x) = (1_{\{x < l\}} - 2 \cdot 1_{\{l \leq x \leq u\}} + 1_{\{x > u\}}) / 4,$$

where l and u are the $1/3$ and $2/3$ quantiles of the standard normal distribution, and obtain a vector $Z = \mathbf{b}(X_{[20]})$. We then sample Y from the Bernoulli distribution with probability $\sigma(Z^\top \beta)$, where the first 10 coordinates of β are equal to θ and the rest are equal to 1. The signal strength of $X_{\mathcal{T}}$ will be controlled by the factor θ . In each experiment, we will evaluate our G -CRT procedure with the statistic RF and its variants, RF-D and RF-RR. Note that the statistic RF-RR is based on regression models that treat the response variable as continuous, but it is compatible with the CRT framework. For comparison, we consider the same baseline tests as in Section D.3 but change the models in the dCRT to random forests. Due to the high variability in estimating power in the context of nonlinear binary regression, we increase the number of replications for each experiment from 400 to 800.

Figure 9a presents the power curves for low-dimensional nonlinear binary regression. The Chi-square test again fails to control the Type I error at the nominal level when $\theta = 0$ and thus it should not be considered in the comparison. In addition, the Bonferroni-adjusted dCRT using random forests is powerless even when θ is as large as 5. Our G -CRTs using all three test statistic functions, RF, RF-D, and RF-RR, perform reasonably well, with power increasing in θ .

Figure 9b shows the results for high-dimensional nonlinear binary regressions. Similar to the results in Figure 8b, the CGM test is too conservative and lacks power across the considered range of θ . In addition, the Bonferroni-adjusted dCRT falls short of achieving high power. Notably, for the G -CRT with any of the three statistics, there is an increasing trend in power as θ increases. However, the statistics RF-D and RF-RR exhibit significantly better performance than the direct RF statistic. This discrepancy in performance corroborates the finding from Figure 7b that the distillation strategy can boost the power of the G -CRT, especially in high-dimensional problems.

Overall, the experimental results demonstrate that our proposed G -CRT is effective in both low and high-dimensional settings. By incorporating either parametric models or ma-

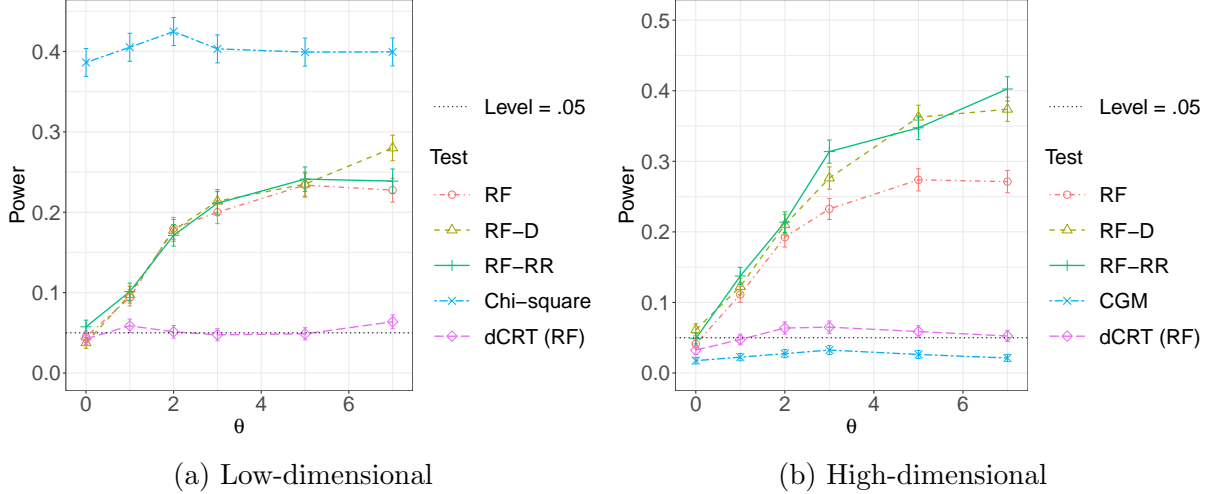


Figure 9: Power comparison for testing MCI in nonlinear binary regressions. The first three tests are the G -CRT with different statistics, and the other two are existing methods.

chine learning algorithms, G -CRT can adapt to detect complex dependence between a response variable and multivariate covariates, whether linear or nonlinear, categorical or continuous. The G -CRT is not only on par with the UMPI test in low-dimensional linear regression but also outperforms the Bonferroni-adjusted competitors in more complex scenarios.

E Additional Simulations

This section provides additional simulation studies to examine several aspects of the G -CRT. These aspects are (1) using expanded supergraphs, (2) testing univariate X_7 , and (3) robustness to violation of the normality assumption.

E.1 Supergraph in G -CRT

The G -CRT only requires a supergraph of the true graph (the faithful graph). However, when using a supergraph containing numerous additional edges, the conditional distribution given the sufficient statistic becomes restricted, which may potentially result in reduced statistical power. Therefore, it is interesting to investigate how the power of the G -CRT is affected when using the true graph versus various supergraphs.

To examine this, we extend the high-dimensional linear regression experiment from Section 6.1 by implementing the G -CRT with graphs that include more edges than the true graph. The true graph G_0 for the covariate is a banded graph with bandwidth $K = 6$. Specifically, the true graph G_0 for the covariates is a banded graph with bandwidth $K = 6$. We consider two larger, nested banded graphs: G_1 with $K = 12$ and G_2 with $K = 18$. For simplicity, we focus on the statistic **LM-L1-R-SSR**.

The results of this extended experiment are shown in Figure 10. We observe that while there is indeed a decline in power when using supergraphs with additional edges, this reduction is relatively mild. Notably, the oversized graph G_2 is significantly larger than the true

graph G_0 : most nodes in G_2 have up to 36 neighbors, whereas in G_0 , nodes have at most 12 neighbors. Despite this substantial increase in graph density, the power of the G -CRT using G_2 remains close to that achieved with G_0 . We note that the degree of G_2 is not too large compared to the sample size $n = 80$, so the G -CRT remains applicable.

Overall, these findings suggest that moderate expansions of the true graph cause only slight power losses, and the G -CRT with a supergraph not too large compared to the sample size continues to exhibit performance close to that achieved when using the true graph.

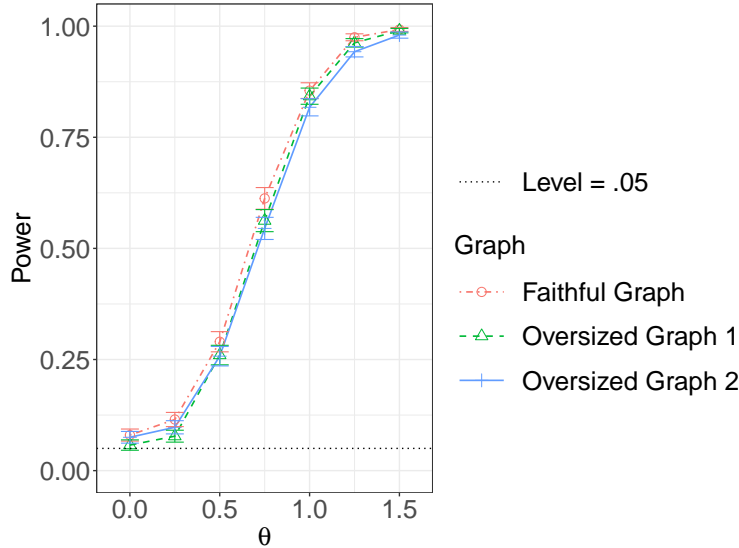


Figure 10: Power of G -CRT with supergraphs in linear regression with $n = 80$ and $p = 120$. The faithful graph has bandwidth $K = 6$, G_1 has $K = 12$, and G_2 has $K = 18$.

E.2 Univariate CRT

As discussed in Section 2.3, our method improves over the Bonferroni-adjusted univariate CRT by sampling $X_{\mathcal{T}}$ jointly from the conditional distribution given the sufficient statistic. A natural concern is whether this joint sampling leads to a loss of power when \mathcal{T} contains only a single variable. To examine this question, we revisit the experiment on linear regression in Section 6.1 but consider only testing $\mathcal{T} = \{1\}$. The results are shown in Figure 11.

In the low-dimensional setting, our methods perform comparably to the classical F -test. In the high-dimensional setting, our methods achieve similar power to the debiased Lasso and are only slightly less powerful than the dCRT. These results suggest that the joint conditional sampling strategy used by our method does not hinder performance in the univariate case and remains competitive across both low- and high-dimensional regimes.

E.3 G -CRT with Violation of the Gaussian Assumption

While the G -CRT method is developed under the assumption that the covariates follow a multivariate Gaussian distribution, it is of practical interest to understand how the method behaves when this assumption is violated.

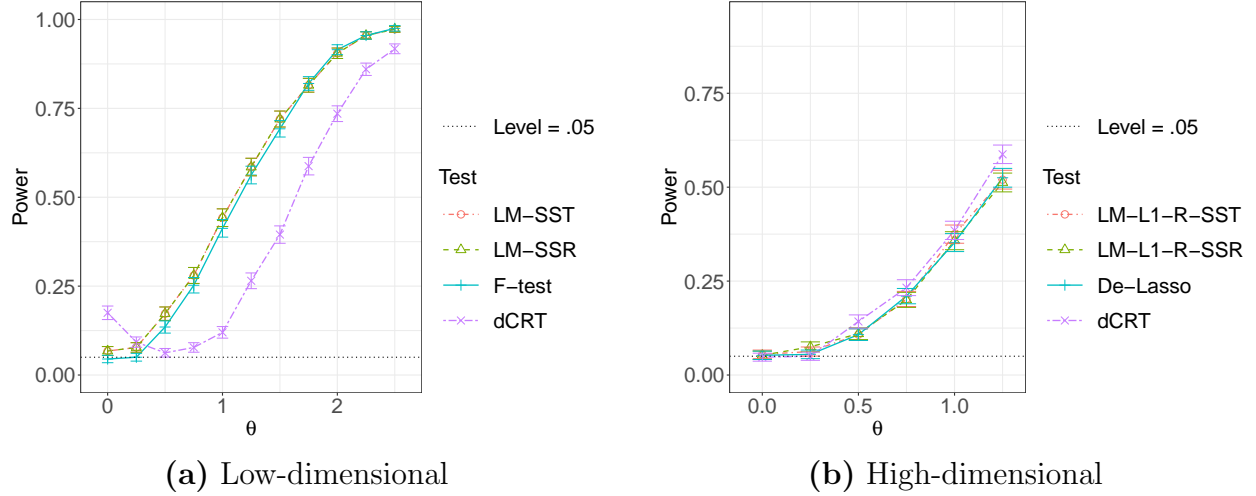


Figure 11: Power comparison for testing univariate conditional independence in linear regression.

To assess the robustness of the proposed G -CRT under non-Gaussian designs, we revisit the linear regression experiment from Section 6.1 and modify the distribution used to generate the covariates. Specifically, we implement the following sampling procedure:

1. We begin with sampling an initial design matrix $\mathbf{X}^{(0)}$ from an AR(6) model. The first column $\mathbf{X}_{:,1}^{(0)}$ is sampled i.i.d. from the standard t -distribution with 3 degrees of freedom (denoted as t_3). For each subsequent column $j = 2, \dots, p$, we define

$$\mathbf{X}_{:,j}^{(0)} = \sum_{\ell=1}^{k_j} \gamma_{\ell} \mathbf{X}_{:,j-\ell}^{(0)} + \sigma_{\epsilon} \boldsymbol{\epsilon}_j,$$

where $k_j = \min(j-1, k)$, and $\boldsymbol{\epsilon}_j$ is an n -dimensional noise vector with i.i.d. entries drawn from t_3 . The constants are fixed as follows: $k = 6$, $\sigma_{\epsilon} = 0.7$, and $\boldsymbol{\gamma} = (1, 1, -1, -1, 1, 1)/5$.

2. Define a graph G_0 such that the pair (i, j) is connected if and only if $|i - j| \leq 6$. We then randomly permute the columns of $\mathbf{X}^{(0)}$ and the nodes of G_0 to obtain the final covariate matrix \mathbf{X} and graph G to be used in testing.

This procedure ensures that \mathbf{X} satisfies the Markov property with respect to G , while the marginal distributions are heavy-tailed due to the use of t_3 noise. In this experiment, the graphical assumption still holds, but the Gaussian assumption is violated because the distribution of the covariate variables is now heavy-tailed.

The results of this experiment are shown in Figure 12. We observe that the G -CRT remains valid in both low- and high-dimensional settings, maintaining proper Type I error control.

In the low-dimensional case, the power of the G -CRT using the LM-SSR statistic is comparable to that of the F -test, which is the UMPI test in the low-dimensional linear regression model. In the high-dimensional case, the G -CRT using the LM-L1-R-SSR statistic

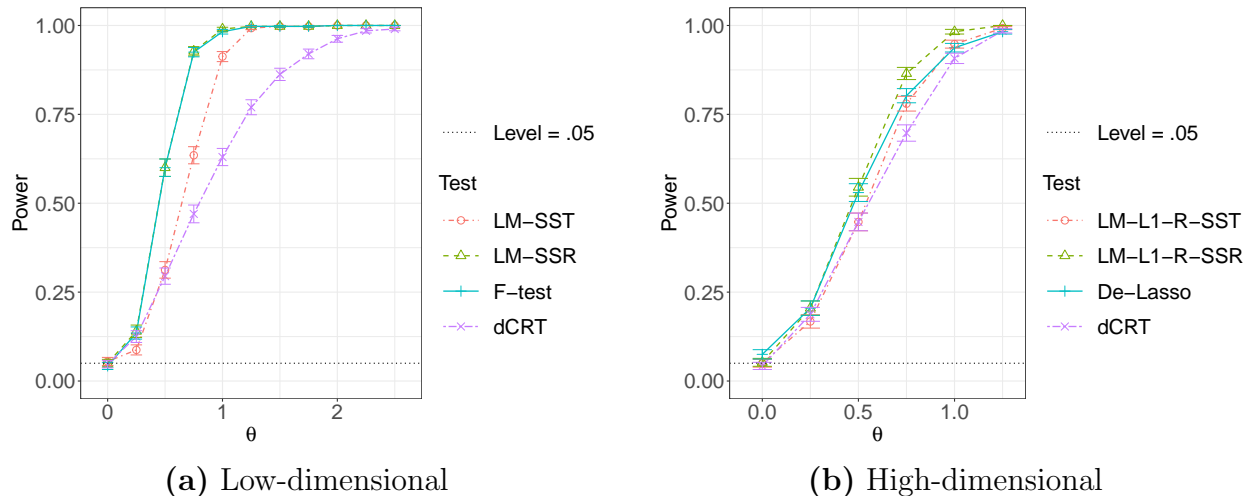


Figure 12: Power comparison for testing conditional independence in linear regression with non-Gaussian covariates.

achieves substantially higher power than both the Bonferroni-adjusted debiased Lasso and the dCRT when the signal is moderately large ($\theta \geq 0.75$).

We conclude that the G -CRT remains robust to moderate violations of the Gaussian assumption: it continues to control the Type I error numerically and retains high power even under heavy-tailed covariate distributions.

F Details of Real-World Examples

In this section, we provide detailed information about the applications of our testing methods to real-world datasets in Section 7 in the main paper.

F.1 Dependence of fund return

F.1.1 Information on the dataset

An exchange-traded fund (ETF) is a basket of securities that tracks a specific index. The SPDR Dow Jones Industrial Average ETF Trust (DIA) was introduced in January 1998 and has been proven popular in the market (Hegde and McDermott, 2004). DIA tracks the performance of the Dow Jones Industrial Average (DJIA, also known as Dow 30). It is a famous stock market index that measures the stock performance of 30 well-established companies listed on stock exchanges in the United States. Created by Charles Dow and first calculated in 1896, the DJIA has been one of the most informative indexes for investors who are interested in stable returns based on well-established blue-chip stocks. This index is maintained and reviewed by a committee and the composition of the index has changed over time to reflect the evolving U.S. economy. For this problem, we consider the period from September 1st, 2020 to Jun 30th, 2022, and consider the stock prices of 103 large-cap U.S. stocks, including all the stocks either from the Standard & Poor's 100 Index or from DJIA. These stocks are assumed to be influential on the DIA. We obtain the daily adjusted

closing prices of each stock from Yahoo Finance (finance.yahoo.com) and compute the 5-day (weekly) average of its returns. The return is defined as $(P_t - P_{t-1})/P_{t-1}$, where P_t and P_{t-1} are the adjusted closing prices of the current day and the last trading day on the stock market, respectively.

The Standard and Poor's 100 Index (SP100) includes 101 stocks (there are two classes of stock corresponding to one of the component companies). The holdings of the SP100 can be found on the homepage of the index-linked product iShares S&P 100 ETF (<https://www.ishares.com/us/products/239723/ishares-sp-100-etf>). We used the version of the holdings on September 29, 2023 for our analysis. We define sectors of these stocks almost the same as shown on the webpage but put the three stocks MA, PYPL, and V of payment technology companies in the sector of Information Technology rather than Financial, and put TGT in Consumer Discretionary rather than Consumer Staples. In our analysis, we have also included the two stocks TRV and WBA that are included by DJIA but not by the SP100. In total, we consider 103 stocks and they are divided into 11 sectors:

1. Communication Services (10): CHTR, CMCSA, DIS, GOOG, GOOGL, META, NFLX, T, TMUS, VZ
2. Consumer Discretionary (12): AMZN, BKNG, F, GM, HD, LOW, MCD, NKE, SBUX, TGT, TRV, TSLA
3. Consumer Staples (10): CL, COST, KHC, KO, MDLZ, MO, PEP, PG, PM, WMT
4. Energy (3): COP, CVX, XOM
5. Financials (15): AIG, AXP, BAC, BK, BLK, BRK-B, C, COF, GS, JPM, MET, MS, SCHW, USB, WFC
6. Health Care (15): ABBV, ABT, AMGN, BMY, CVS, DHR, GILD, JNJ, LLY, MDT, MRK, PFE, TMO, UNH, WBA
7. Industrials (13): BA, CAT, DE, EMR, FDX, GD, GE, HON, LMT, MMM, RTX, UNP, UPS
8. Information Technology (17): AAPL, ACN, ADBE, AMD, AVGO, CRM, CSCO, IBM, INTC, MA, MSFT, NVDA, ORCL, PYPL, QCOM, TXN, V
9. Materials (2): DOW, LIN
10. Real Estate (2): AMT, SPG
11. Utilities (4): DUK, EXC, NEE, SO

For any stock, denoted by Z_i 's the 5-day averages of returns. To enhance the normality shown in the data, we then consider transformation using a piece-wise function

$$\psi(z) = \begin{cases} \text{sign}(z) \cdot |z|^\lambda, & \text{if } |z| < c, \\ \text{sign}(z) \cdot (a + 0.01 \cdot \log(|z|)), & \text{otherwise,} \end{cases} \quad (\text{F.1})$$

Table 2: Results of GoF tests for modeling the stock returns by the GGM with the estimated graph.

	Method		
	M^1P_1	Bonf	F_Σ
p-value	1.000	0.352	0.321

where $a = c^\lambda - 0.01 \cdot \log(c)$. The parameter λ is tuned over a grid from 0.1 to 2, and the parameter c is tuned over a grid between the 80% quantile and the maximum of the observed values of Z_i . The criteria to be maximized is the p-value of the Shapiro–Wilk test on the transformed data. After this transformation, only two stocks have p-values from the Shapiro–Wilk tests smaller than 0.05, and we alternatively use the Box-Cox transformation:

$$\varphi(z) = \begin{cases} \frac{z^\lambda - 1}{\lambda}, & \text{if } \lambda \neq 0, \\ \ln(z), & \text{if } \lambda = 0, \end{cases} \quad (\text{F.2})$$

where the parameter λ is tuned by using the `boxcox()` function in the **R** package **MASS**.

F.1.2 Preliminary analysis

Our analysis begins with a graphical modeling for the stock returns X . Suppose the observations of X are i.i.d. sampled from a normal distribution, and we want to find a graph G so that the distribution belongs to a GGM w.r.t. G . As discussed in Section 4.3, all we need to implement the G -CRT is one particular supergraph of the true graph. To facilitate the selection of such a super-graph, we incorporate the prior knowledge of the stock sectors (based on their industries). We estimate G using GLasso with regularization parameter $\lambda = 0.15$ and with no penalty on edges between stocks in the same sector. This approach yields a graph \hat{G} , whose maximal degree is 30, the median degree is 19, and around 18.4% pairs of nodes are connected. The graph \hat{G} we estimated using GLasso is shown in Figure 13, where nodes are colored according to their sectors.

We apply the MC-GoF test in Appendix B.1 with statistics F_Σ as well as the two existing benchmarks M^1P_1 and Bonf to test the goodness-of-fit of the GGM with \hat{G} . The p-values are listed in Table 2 and are all above 0.3, indicating the GGM with \hat{G} is sufficient for modeling the stock data.

The relationship between Y and X can be modeled either by a linear model or by a nonparametric regression model. In addition, the dimension of data ($p = 103$) is larger than the number of observations ($n = 92$). Therefore, we should consider the testing methods that have been numerically studied in Sections D.1 and D.2. For the G -CRT, we choose the winning statistic functions L1-R-SSR in high-dimensional linear regression and RF-RR in high-dimensional nonlinear regression. We also consider the Bonferroni-adjusted methods including the de-sparsified Lasso and the dCRT with either Gaussian Lasso models (L1) or random forests (RF). Before we apply these tests, we conduct a simulation study to assess the Type I error control of various statistical tests to test the conditional independence of $Y \perp\!\!\!\perp X_{\mathcal{T}} \mid X_{\mathcal{S}}$. First, we fit a lasso linear regression model of Y on $X_{\mathcal{S}}$, with penalty parameter tuned by 10-fold cross-validation. Subsequently, in each replication of the simulation, a new

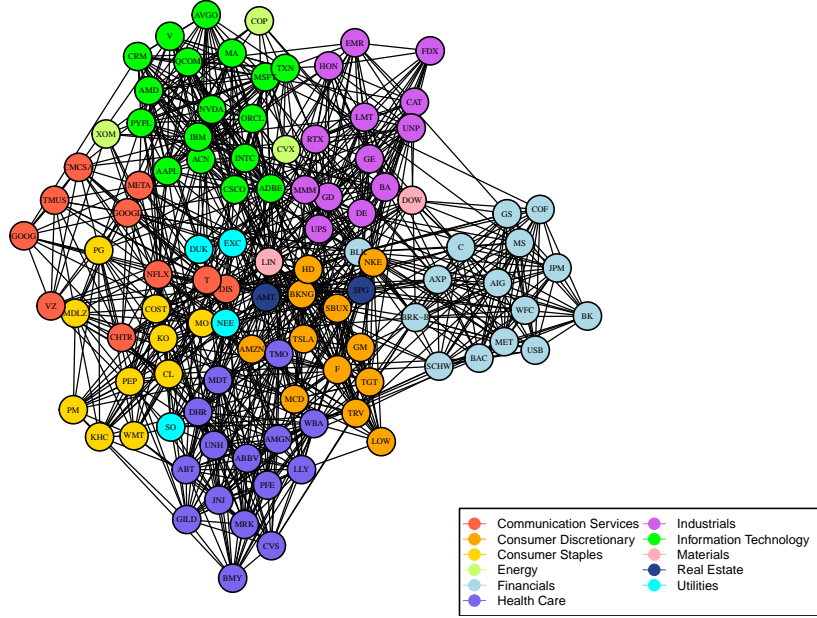


Figure 13: Estimated Graph with Color for Sector

covariate matrix $\tilde{\mathbf{X}}$ is generated via running Algorithm 2 with $\mathcal{I} = [p]$, $M = 1$, and $L = 20$. This guarantees that if the distribution of the input \mathbf{X} is in \mathcal{M}_G , so is the distribution of $\tilde{\mathbf{X}}$. $L = 20$ is large enough to reduce the correlation between the output $\tilde{\mathbf{X}}$ and the input \mathbf{X} . Then, a new response vector $\tilde{\mathbf{Y}}$ is generated using the fitted lasso linear regression model with the generated covariate matrix $\tilde{\mathbf{X}}$. The p-values of the tests for conditional independence are then computed based on the simulated $\tilde{\mathbf{X}}$ and $\tilde{\mathbf{Y}}$.

We repeat the experiment 400 times and report the rejection proportions of these tests at the significance level $\alpha = 0.05$ in Table 3. Only the estimated size of the de-sparsified Lasso exceeds the nominal level $\alpha = 0.05$.

F.1.3 Analysis on the fund dependence

We focus on the tests that control the Type I error and the p-values are reported in Table 1 in the main text.

For \mathcal{T}_1 , both G -CRTs reject the null hypothesis at the significance level $\alpha = 0.05$. In contrast, the dCRTs accept the null hypothesis, which may be because each of the stocks in \mathcal{T}_1 has a relatively small influence on the fund return and none of them can be detected by the dCRTs, after adjusting for multiple comparisons. Nonetheless, the five stocks in \mathcal{T}_1

Table 3: Estimated sizes of various conditional independence tests on simulated returns ($\alpha = 0.05$).

\mathcal{T}	Method				
	LM-L1-R-SSR	RF-RR	De-Lasso	dCRT (L1)	dCRT (RF)
\mathcal{T}_1	0.045 (0.014)	0.065 (0.015)	0.265 (0.020)	0.060 (0.018)	0.022 (0.017)
\mathcal{T}_2	0.052 (0.015)	0.048 (0.015)	0.158 (0.020)	0.080 (0.018)	0.003 (0.015)

together as a whole are influential on the fund return, and our G -CRTs successfully detect this signal.

For \mathcal{T}_2 , all the considered tests reject the null hypothesis with small p-values. This suggests that the stocks in \mathcal{T}_2 are influential on the fund return. We subsequently consider a situation where the response variables are contaminated by additive noises and thus the “signal-to-noise” ratio becomes smaller. We want to investigate whether the rejection decision of these tests would remain unchanged as the noise level increases. Specifically, we repeatedly set $\tilde{Y} = Y + \sigma\epsilon$, where ϵ is a standard normal random variable and σ is a parameter to be controlled, and apply all the testing methods to the dataset with \tilde{Y} .

The rejection rates of the tests across different values of σ are presented in Figure 14. We can see that the rejection rate of each method decreases as the noise level σ increases. This is expected because as the “signal-to-noise” ratio becomes smaller, it becomes harder for any test to detect the conditional dependence of \tilde{Y} on $X_{\mathcal{T}_2}$. The two tests based on random forests, i.e., the G -CRT with the statistic RF-RR and the dCRT with random forests, have lower rejection rates than the other two tests that are based on linear models. This is not surprising because test statistic functions based on random forests are more effective in nonlinear regression, and are not as efficient as model-based statistic functions in this problem, where the linear model provides a rather good fit to the data. Among the two tests based on linear models, the rejection rate of the dCRT with Gaussian Lasso models drops down to 71% as the noise level increases to 0.1, while the G -CRT with the LM-L1-R-SSR statistic still maintains its rejection decision more often than 94%. Overall, the G -CRT with the LM-L1-R-SSR statistic has uniformly higher rejection rates, exhibiting robustness to additive noises.

In conclusion, the G -CRT is shown powerful in detecting the dependence of the DIA return on some specific sets of stocks. When the dependence on each stock is weak, as in \mathcal{T}_1 , the G -CRT can efficiently detect joint dependence while others can not. When the response is contaminated by additive noises and the dependence on the stocks in \mathcal{T}_2 is weakened, the G -CRT with the LM-L1-R-SSR statistic maintains relatively high rejection rates. In both cases, the G -CRT outperforms the Bonferroni-adjusted dCRT in terms of making the correct rejection decision, which demonstrates its potential for unveiling undisclosed holdings of funds.

F.2 Breast Cancer Relapse

This example illustrates the application of the G -CRT in a situation where the classical likelihood ratio test is not applicable.

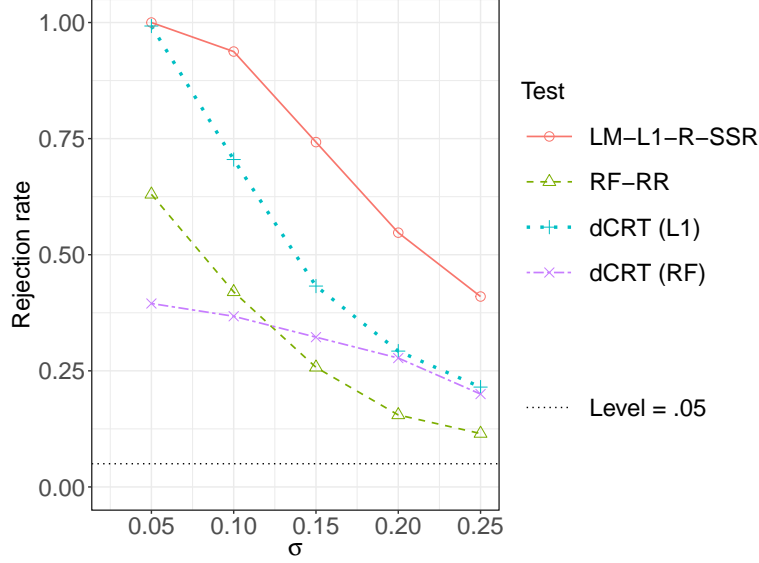


Figure 14: Rejection rates of various conditional independence tests for \mathcal{T}_2 based on noisy observations of the DIA return. σ is the standard deviation of the additive noises.

F.2.1 Information on the dataset

The breast cancer relapse (BCR) dataset was collected by Wang et al. (2005), which aimed to improve risk assessment in patients with lymph-node-negative breast cancer by identifying genome-wide measures of gene expression associated with developments of distant metastases.

We obtain the breast cancer relapse (BCR) dataset from the NCBI GEO database with accession GSE2034 (Barrett et al., 2012) at (<https://www.ncbi.nlm.nih.gov/geo/query/acc.cgi?acc=gse2034>). The original dataset contains the expression of 22,000 transcripts from the total RNA of frozen tumour samples from 180 lymph-node negative relapse-free patients and 106 lymph-node negative patients that developed distant metastasis (Wang et al., 2005). The dataset comes along with patients' clinical information, including ER status, time to relapse or last follow-up (months), relapse status, and Brain relapse status. Patients were divided into two groups based on oestrogen receptor (ER) levels: those with more than 10 fmol per mg protein (ER-positive) and those with less. We focus on the ER-positive group comprising 209 patients and illustrate the application of the G -CRT in the determination of important genes associated with distant metastases. The list of 76 identified genes can be found in Wang et al. (2005, Table 3), among which we focus on the 60 genes associated with the ER-positive group.

The variable Y can be derived from the clinical information. The covariates are the gene expression levels, after applying the rank-based Inverse Normal Transformation (INT) (Fisher and Yates, 1953). The INT transform of a n -vector of observations Z_i is defined as follows:

$$Z_i^{(\text{INT})} = \Phi^{-1} \left(\frac{r_i - 0.5}{n} \right),$$

where r_i is the rank of Z_i and Φ^{-1} is the inverse CDF of the standard normal distribution.

See Beasley et al. (2009); McCaw et al. (2020) for more details about INT.

F.2.2 Preliminary analysis

Now we consider modeling $\mathcal{L}(Y | X)$ by a K -class symmetric multinomial logistic regression with a lasso penalty (Friedman et al., 2010). This model assumes that

$$\mathbf{P}(Y = k | X = x) = \frac{\exp(\beta_{0,k} + x^\top \beta_k)}{\sum_{l=1}^K \exp(\beta_{0,l} + x^\top \beta_l)}, \quad k = 1, \dots, K, \quad (\text{F.3})$$

where $K = 3$ for the current example, and $\beta_{0,k} \in \mathbb{R}$ and $\beta_k \in \mathbb{R}^p$ are unknown regression parameters.

The lasso estimator is the maximizer of the following penalized log-likelihood

$$\max_{\{\beta_{0,k}, \beta_k\}_{k=1}^K \in \mathbb{R}^{K(p+1)}} \left[\frac{1}{N} \sum_{i=1}^N \log \mathbf{P}(Y = Y_i | X = X_i) - \lambda \sum_{k=1}^K \|\beta_k\|_1 \right], \quad (\text{F.4})$$

where λ is a tuning parameter. If for any $k \leq K$, the j th entry of the estimated β_k is nonzero, then the j th covariate is viewed as important and will be selected. With different values of the tuning parameter λ , we may select different sets of important variables. See Hastie et al. (2009) for a general introduction to cross-validation for selecting tuning parameters.

We conduct the lasso-multinomial logistic regression with cross-validation using the function `cv.glmnet()` in the celebrated **R** package `glmnet` with the argument `family` set to `multinomial`. For the BCR dataset, if we apply 5-fold cross-validation and compute the mean deviance on the left-out data, the minimizer $\hat{\lambda}_{\min}$ of the cross-validation error suggests selecting 13 genes. The minimizer $\hat{\lambda}_{\min}$ is expected to select the model with a good prediction performance. On the other hand, the so-called “one-standard-error” rule – selecting the largest value of λ such that the cross-validation error is within one standard error of the minimum – is often applied when selecting the best model to achieve model parsimony.

The two genes selected by the “one-standard-error” rule are 209835_x_at and 218478_s_at; they form the set \mathcal{S} . Furthermore, \mathcal{T} is defined to be the 11 genes selected by $\hat{\lambda}_{\min}$ but not by the “one-standard-error” rule, which includes 201091_s_at, 204540_at, 205034_at, 207118_s_at, 209524_at, 209835_x_at, 210028_s_at, 214919_s_at, 215633_x_at, 217471_at, 218430_s_at, 218478_s_at, 218533_s_at.

It is then of interest to determine whether the genes selected by the model tuned by the “one-standard-error” rule sufficiently determine the response variable. The inference problem is to test

$$H_0 : Y \perp\!\!\!\perp X_{\mathcal{T}} | X_{\mathcal{S}}. \quad (\text{F.5})$$

A natural idea for testing (F.5) would be to fit two nested (ordinary) multinomial logistic models, one with $X_{\mathcal{S}}$ only and the other with both $X_{\mathcal{S}}$ and $X_{\mathcal{T}}$, and perform the likelihood ratio test. The test statistic may then be converted to an asymptotic p-value by comparing it with a Chi-squared distribution. This approach results in a p-value of 5×10^{-5} , suggesting that H_0 should be rejected. However, the theoretical guarantee of this asymptotic p-value requires the sample size n to diverge while the models are fixed. In the current problem, n is not large enough for the approximate validity of this p-value. Instead, we turn to the G -CRT

Table 4: Sizes of various conditional independence tests on simulated BCR data based on 400 replications (significance level $\alpha = 0.05$). Standard errors are placed in parentheses

Method			
LRT	G -CRT (RF)	dCRT (L1)	dCRT (RF)
0.189 (0.016)	0.055 (0.015)	0.048 (0.018)	0.050 (0.018)

for its wide applicability instead. When implementing the G -CRT, we use a complete graph for G because the dimension of covariates $X_{\mathcal{T} \cup \mathcal{S}}$ is 13, much smaller than the sample size n . Consequently, the modeling assumption is that $X_{\mathcal{T} \cup \mathcal{S}}$ follows a multivariate Gaussian distribution. Given that Y is a multi-class response, we can conduct the G -CRT with the RF statistic. For comparison, we also conduct the Bonferroni-adjusted dCRT with either Gaussian Lasso models or random forests by treating the response as a continuous variable.

F.2.3 Verifying Type I error control

To check the Type I error control of all considered tests, we perform a simulation study to check the Type I error control of the considered tests. Specifically, we first fit the lasso-multinomial logistic regression of Y on $X_{\mathcal{S}}$ with the penalty parameter tuned by 5-fold cross-validation. This results in the regression coefficient estimates $\hat{\beta}_{\mathcal{S},k}$ for $k = 1, \dots, K$ (recall that $K = 3$ for this model). In the experiment, we repeatedly sample new covariates $\tilde{X}_{\mathcal{T} \cup \mathcal{S}}$ from a multivariate normal distribution using the sample mean and the sample covariance matrix of the observed $X_{\mathcal{T} \cup \mathcal{S}}$, and subsequently generate a new response \tilde{Y} from the multinomial logistic regression model using $\tilde{X}_{\mathcal{S}}$ and the estimated regression coefficients $\hat{\beta}_{\mathcal{S},k}$ ($k = 1, \dots, K$). We then compute the p-values of the considered tests, including the asymptotic Chi-square p-value of the likelihood ratio test (LRT), the graphical conditional randomization test (G -CRT) with the **RF** statistic, and the two variants of the dCRT that treat the response variable as a continuous variable.

We repeat the experiment 400 times, and report the rejection proportions of these tests at the significance level $\alpha = 0.05$ in Table 4. It shows that the asymptotic likelihood ratio test is not valid and will lead to an inflated Type I error. This is further illustrated by the histogram in Figure 15, which shows that the asymptotic p-value of the LRT is far from being uniformly distributed. On the other hand, the G -CRT and the two dCRTs control the Type I error, as predicted by the theory.

F.2.4 Results of tests

While the applicability of the likelihood ratio test is refuted for the BCR dataset, the G -CRT results in a p-value of 0.002. In contrast, the dCRT with Gaussian Lasso models yields a p-value of 0.225, and the dCRT with random forests yields 0.242.

In conclusion, the G -CRT rejects H_0 at the significance level $\alpha = 0.05$, whereas the two dCRTs do not. The rejection decision from the G -CRT is more reliable than that from the asymptotic likelihood ratio test, since the latter does not control the Type I error given the sample size and models in the current context. Furthermore, the Bonferroni-adjusted dCRTs fail to detect the conditional dependence of the response Y on the covariates $X_{\mathcal{T}}$, while the

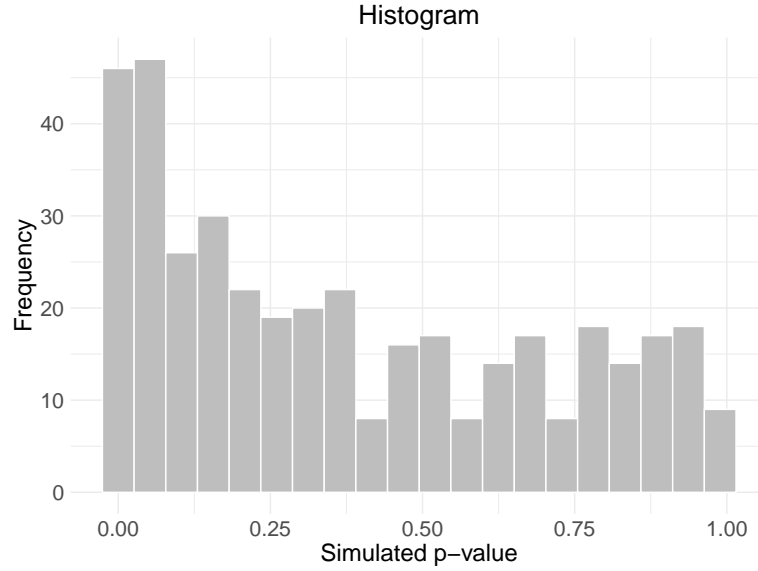


Figure 15: Histogram of the p-value of the asymptotic likelihood ratio test on simulated BCR data

G -CRT effectively captures the joint signal. This example illustrates the efficiency and the broad applicability of our proposed method in detecting joint signals for testing conditional independence.